Project Number: ME-AHH-0702

Testing and Analysis of Low Cost Prosthetic Feet

A Major Qualifying Project Report

Submitted to the Faculty

of the

WORCESTER POLYTECHNIC INSTITUTE

in partial fulfillment of the requirements for the

Degree of Bachelor of Science

in Mechanical Engineering

by

Morgan Carpenter

Carolyn Hunter

Dean Rheaume

Date: April 24, 2008

Approved:

_____

Prof. Allen H. Hoffman, Major Advisor

_____

Prof. Holly K. Ault, Co-Advisor

Keywords
1. prosthetics
2. assistive technology
3. finite element analysis

Abstract

The Center for International Rehabilitation (CIR) is a non-profit organization working in developing countries to rehabilitate those who have lost their mobility after an amputation. CIR has developed a lower limb prosthetic (monolimb) for transtibial amputees, which is then rigidly attached to a prosthetic foot. CIR requested a study of the effect of coupling their monolimb with two existing prosthetic foot designs; the International Committee of the Red Cross's SACH foot and Northwestern's Shape and Roll (SR) prosthetic foot.

The combination of the prosthetic feet and monolimb were modeled and studied using finite element analysis (FEA). The FEA results were then compared to the physical testing of the prosthetics under various static loading conditions seen during walking. These results suggest that the SR foot does not perform as well as the SACH foot under high loading conditions and could result in premature wear of the prosthetic combination. The results of this work will aid CIR in their efforts to provide appropriate prostheses to populations in developing countries.

Table of Contents

List of Figures x

List of Tables xiii

Executive Summary 1

1. Introduction 5

2. Background 7

2.1. Prosthetics in Developing Nations 7

2.2. Center for International Rehabilitation 8

2.3. CIR's Monolimb 8

2.4. The Gait Cycle 12

2.4.1. Stance Period 13

2.4.2. Swing Period 15

2.4.3. Biomechanics of the Foot and Ankle 16

2.5. Prosthetic Feet 17

2.5.1. Roll-Over Shape 18

2.5.2. Energy Storage and Return 18

2.5.3. Mechanical Properties 19

2.5.4. SACH Foot 19

2.5.5. Shape and Roll Foot 21

2.5.6. Additional Prosthetics for Developing Countries 26

2.6. Ground Reaction Forces during Gait 28

2.7. Strain Gauges 29

2.8. ISO Standards 30

3. Methods 32

3.1. Determination of Axes for Prosthetic Components 32

3.1.1. Prosthetic Feet 32
3.1.2. Monolimb 33
3.2. CAD Modeling 34
3.2.1. SR Foot 34
3.2.2. SACH Foot 36
3.2.3. Monolimb 40
3.3. Coefficient of Friction 41
3.4. Finite Element Analysis 42
3.4.1. Simple Test Case 42
3.4.2. Meshing of SR Foot 44
3.4.3. Meshing of SACH Foot 47
3.4.4. Model Constraints 49
3.5. Physical Testing 49
3.5.1. Alignment 49
3.5.2. Foot Orientations 51
3.5.3. Strain Gauges 52
3.5.4. BlueHill Software 53
3.5.5. Compression Testing Machine 53
3.5.6. Force Application 54
3.5.7. Data Collection 55
3.5.8. Data Analysis 56
4. Results 57
4.1. Physical Results 57
4.1.1. Heel-strike 57
4.1.2. Midstance 59

4.1.3. Toe-off 60
4.1.4. Compression Results 62
4.2. FEA Results 63
5. Analysis 65
5.1. Strains on the Monolimb 65
5.2. Stiffness of Prosthetics 67
5.3. Stresses On Monolimb 68
5.4. Deformation of SR Heel 70
6. Discussion 72
6.1. Comparison of FEA and Physical Testing 72
5.2. Potential Errors in Study 73
6.3. Feet Acceptability 74
6.4. Recommendations 74
7. Conclusion 75
Works Cited 75
Appendix A 80
Appendix B 81
Appendix C 83
Appendix D 86
Appendix E 88
Appendix F 93
Appendix G 94

List of Figures

Figure 1: ICRC SACH Foot (“Prosthetic Feet”) 6
Figure 2: SR Foot (“Lower Limb Prosthetics: The Shape&Roll”) 6
Figure 3: Clay Casting of Residual Limb and Plaster Casting of Residual Limb (CIR 2006) 9
Figure 4: Monolimb Alignment and Cast Holder (CIR 2006) 9
Figure 5: Pouring Plaster into Limb Casting, Mandrel with Positive Mold, and Cutting the Plastic (CIR 2006) 10
Figure 6: Finished Monolimb with Prosthetic Foot (CIR 2006) 10
Figure 7: CIR Monolimb (Kim) 11
Figure 8: Divisions of the Gait Cycle (Perry 1992) 12
Figure 9: Initial Contact (Perry 1992) 13
Figure 10: Loading Response (Perry 1992) 13
Figure 11: Midstance (Perry 1992) 14
Figure 12: Rockers Occurring In Gait Cycle (Perry 1992) 17
Figure 13: Flexion of Toes (Perry 1992) 17
Figure 14: Roll-Over Shape Coordinate System with Marker Locations 18
Figure 15: Diagram of Deformation ("Deformation") 19
Figure 16: Examples of SACH Feet 20
Figure 17: ICRC SACH Foot 20
Figure 18: SR Foot (Sam 2004) 21
Figure 19: Sagital Plane Cross-Section of SR Foot (Sam 2004) 22
Figure 20: SR Prosthetic Foot Pressure Mold (Sam 2004) 23
Figure 21: Aluminum Insert Piece and Attachment Point (Sam et al., 299) 24
Figure 22: Roll-Over Shape Comparisons (Sam 2004) 25
Figure 23: Niagara Foot (IDEAnet) 26
Figure 24: Jaipur Foot ("Jaipur Foot" 2005) 26
Figure 25: Jaipur Foot Mold ("Jaipur Foot" 2005) 27
Figure 27: Ground Reaction Forces During Fast Walking (Winter 1991) 28
Figure 26: Mobility for Each One (Index Award 2007) 28
Figure 28: Rosette Strain Gauge and Applicable Strain Equations (Rosette Strain Gauges 2008) 30
Figure 29: Rectangular Rosette Strain Gauge and Strain Equations (Rosette Strain Gauges 2008) 30
Figure 30: Determining Longitudinal Axis 32
Figure 31: SR Model with Longitudinal Axis 33
Figure 32: Marked Monolimb 34
Figure 33: Graph of Monolimb Center (inches) 34
Figure 34: Outline of SR Base 35
Figure 35: Datums for SR Foot 35
Figure 36: Inside Cut for SR Foot 36
Figure 37: SR Insert 36
Figure 38: Assembly of SR and Insert 36

Figure 39: CMM SACH Foot Insert 37
Figure 40: Initial Extrusion and Cut Using Spline Curves 37
Figure 41: Final Solid Model of SACH Foot Insert 38
Figure 42: SACH Model with Curves from CMM 38
Figure 43: Multiple Views of Complex SACH Model 39
Figure 44: Simplified SACH Foot 39
Figure 45: CAD Model of Monolimb Insert 40
Figure 46: CAD Model of Monolimb 41
Figure 47: Toe-off and Midstance Simple Geometry Assemblies 43
Figure 48: Y Directional Deformation in Midstance Assembly 44
Figure 49: SR Contact Surfaces 45
Figure 50: Toe Cut Contact Surfaces 46
Figure 51: Heel Cut Contact Surfaces 46
Figure 52: Meshed SR Foot Models 46
Figure 53: Refined Mesh at SR Heel 47
Figure 54: SACH Contact Surfaces 48
Figure 55: Meshed SACH Foot Models 48
Figure 56: FEA Model Constraints and Loads 49
Figure 57: Test Setup with Coordinate System 50
Figure 58: Instron to Monolimb Connection Adaptor 51
Figure 59: Toe-off Angle Block 51
Figure 60: Strain Gauge Placement on Physical Test Setup 52
Figure 61: BlueHill Program Sample Screenshot 53
Figure 62: Instron 5544 54
Figure 63: SB-10 Switch & Balance Unit and P-3500 Digital Strain Indicator 55
Figure 64: Heel-strike End Loading (SR, 910N; SACH 1300N) 57
Figure 65: Heel-strike Strain Results 58
Figure 66: Pressure Paper from SR Heel-strike Test at (top down) 130N, 650N, 910N 58
Figure 67: Midstance Strain Results 59
Figure 68: Toe-off End Loading (SR, 520 N; SACH, 910) 60
Figure 69: Toe-off Strain Results 61
Figure 70: Pressure Paper from SR Toe-off Test at 130N and 650N 61
Figure 71: Pressure Paper from SACH Test at 910N 61
Figure 72: von Mises Stress (Engineer's Edge 2008) 63
Figure 73: Toe-off Strain Results 66
Figure 74: Heel-strike Strain Results 66
Figure 75: von Mises Stresses with SR for Heel-strike, Midstance, and Toe-off (scale in MPa) 69
Figure 76: von Mises Stresses with SACH for Heel-strike and Toe-off (scale in MPa) 69
Figure 77: Deformation at SR Heel 70
Figure 78: Von Mises Stress at SR Heel During Heel-Strike 70
Figure 79: SR - Heel-strike- Normal Strain 94

Figure 80: SR - Heel-strike - Maximum Principal Stresses 95
Figure 81: SR - Heel-strike - Minimum Principal Stresses 95
Figure 82: SR – Heel-strike - von Mises Stress 96
Figure 83: SR - Midstance - Normal Elastic Strain 96
Figure 84: SR - Midstance - Maximum Principal Stress 97
Figure 85: SR - Midstance - Minimum Principal Stress 97
Figure 86: SR - Midstance - von Mises Stress 98
Figure 87: SR - Toe-off - Normal Strain 98
Figure 88: SR - Toe-off - Maximum Principal Stresses 99
Figure 89: SR - Toe-off - Minimum Principal Stress 99
Figure 90: SR – Toe-off – von Mises Stress 100
Figure 91: SACH - Heel-strike - Normal Elastic Strain 100
Figure 92: SACH - Heel-strike - Maximum Principal Stress 101
Figure 93: SACH - Heel-strike - Minimum Principal Stress 101
Figure 94: SACH - Heel-strike - von Mises Stress 102
Figure 95: SACH - Toe-off - Normal Elastic Strain 102
Figure 96: SACH - Toe-off - Maximum Principal Stress 103
Figure 97: SACH - Toe-off - Minimum Principal Stress 103
Figure 98: SACH - Toe-off - von Mises Stress 104

List of Tables

Table 1: Polypropylene Copolymer Properties 10
Table 2: Coefficient of Friction Results 42
Table 3: Contact Properties Between Surfaces 43
Table 4: SR Contact Surfaces 45
Table 5: SACH Contact Surfaces 47
Table 6: Test Procedure 54
Table 7: Strain Data from Physical for Comparison 62
Table 8: Compression from Physical Testing 62
Table 9: Strain Data from FEA 63
Table 11: Total Prosthetic Displacement 64
Table 12: Comparison of Strains from Physical Tests and FEA 67
Table 13: Total Prosthetic Compression for FEA and Physical Testing 68

Executive Summary

The Center for International Rehabilitation (CIR) is a non-profit organization working in developing countries to rehabilitate those who have lost their mobility after an amputation. These amputees are generally victims of landmines. CIR has developed a lower limb prosthetic (monolimb) for transtibial amputees, which is rigidly attached to a prosthetic foot. CIR requested a study of the effect of coupling their monolimb with two existing prosthetic foot designs: the International Committee of the Red Cross's Solid Ankle Cushioned Heel (SACH) foot and Northwestern's Shape and Roll (SR) prosthetic foot.

These prosthetics are low cost appropriate technologies for developing countries. The monolimb is custom made from a polypropylene polyethylene plastic to fit each user. The SACH foot, which is imported into the developing countries, is created using injection molding of polyurethane foam. The SR foot, which is able to be manufactured within developing countries, is made by heating copolymer sheets with an aluminum stock material inserted into the base of the foot to provide extra support.

Both physical testing and finite element analysis (FEA) were performed to compare the effect that each foot has on the monolimb. The orientations and loading for the physical testing were drawn from ISO standards. ISO 10328 [Structural testing of lower-limb prostheses] specified testing methods, loading conditions, and other parameters. The 2006 ISO 22675 [Testing of ankle-foot devices and foot units] states the loading conditions that can be used to mimic natural gate loading and specifies a static test that can be performed on prosthetic ankle-foot devices. In addition, the alignment of the foot to the prosthetic leg is stated.

The prosthetics were tested in an Instron 5544 compression/tension machine. The evaluation of the prosthetic feet was conducted at three orientations in both the physical testing and FEA. The first position was the heel-strike that occurs during the initial contact, the second position was midstance, where the foot is flat and the third position was pre-swing, where the majority of the weight is on the toe before the swing phase,. The heel-strike and toe-off orientations required the use of an angled block to simulate the angle the foot makes with the ground. This angle was 15° for heel-strike and 20° for toe-off.

For the physical testing, the appropriate angle block was attached to the base of the Instron 5544 with a rod through the center of the angle block. Tests of the monolimb/foot assembly were performed at

10% load increments to 1300N at a rate of 75N/min, or until the experimental set-up showed signs of potential damage to the equipment or sample. The tests were held after each 10% increment for 45 seconds to allow for data collection. Each test was performed twice, once using pressure paper to indicate if there were any irregularities in orientation and pressure with the angle block and once without the paper. Strain gauges were applied on the anterior and posterior of the monolimb just above the metal insert that is used to attach the foot. This was identified as a critical region by CIR based on a case study. A rosette strain gauge was attached to the anterior section of the monolimb and a uniaxial strain gauge was attached to the posterior seam. The tests were controlled and loading and displacement data were recorded using the BlueHill software program. The strain gauges were read using Vishay's SB-10 Switch & Balance Unit and Vishay's Model P-3500 Digital Strain Indicator.

For the FEA, all of the prosthetics were reverse engineered in Pro/Engineer Wildfire 2.0. Accurate computer aided design (CAD) models were made for the monolimb, SR foot, and SACH foot. A simpler, less accurate model of the SACH foot was also modeled to ease meshing in the FEA. ANSYS Workbench was chosen as the FEA software package because of its ability to accept a 3D CAD model and an assembly of high complexity. In addition to the modeling of contact surfaces and large deflection, the ANSYS program also allowed for the accurate placement of angled pressures and loads. The FEA models were evaluated at the full loading of 1300N. Each foot in each orientation had the same constraints and loads applied. The bottom surface of the angle or midstance block was selected as a fixed surface and the top block connected to the monolimb was constrained by a fixture to only allow movement in the vertical direction. In addition, the foot was frictionally connected to the angle or midstance block.

The results of the physical testing and FEA were compared to draw conclusions regarding the performance of the foot monolimb combinations. From the physical testing, it was apparent that higher strains were exhibited on the posterior uniaxial gauge positioned vertically (90^{o}) and the anterior 90° rosette gauge when the SR foot was affixed to the monolimb as compared to the SACH foot in both heel-strike and toe-off orientations. The heel-strike test for the SR foot was stopped at 910N because plastic deformation began to occur near the heel of the foot; the foot did not undergo fracture. The SACH foot was loaded to the full 1300N. Under the same loading conditions the magnitude the strains recorded by the uniaxial and 90° rosette gauge were greater in magnitude for the SR foot. For example, at 910N the SR uniaxial gauge showed an average reading of -1745με and the 90° rosette gauge showed

an average reading of 614 με. For the SACH, at 910N the uniaxial gauge showed an average reading of -1280με and the 90° rosette gauge showed an average reading of -78 με.

To aid in comparing the FEA testing to the physical testing, the physical test data were linearly extrapolated to show trendlines. These trendlines were used to predict potential strain values that may have occurred if the physical testing was run to the full loading of 1300N. Comparing these potential trendlines adds some validity to the FEA generation of the SR foot because these trendlines show strain values on the monolimb similar to the FEA results at full loading (1300 N). In addition, the FEA for the SR foot showed that both the von Mises and principal stresses in the heel exceeded the yield strength of the SR polypropylene copolymer during heel-strike at the 1300N load. The plastic deformation that occurred in the physical testing appeared at 910N. For the SACH foot the FEA results did not parallel the physical results, possibly due to inaccuracies in modeling the SACH foot.

The physical results for compression of the monolimb with the SACH foot and SR were compared from the physical testing. For the heel-strike orientations for both of the prosthetic combinations at 910N (where the SR test was stopped), the monolimb with the SR and SACH compressed in magnitude by 10.8mm and 18.0mm respectively. These results showed that the prosthetic assembly with the SACH foot compresses more therefore showing that the monolimb with the SACH foot is less stiff than the monolimb with the SR.

The assembly of the monolimb with the SR foot causes strains of a greater magnitude to occur in the monolimb than the assembly with the SACH foot. The resulting von Mises stresses and the principal stresses in both assemblies from the FEA are less than the tensile yield strength of the polypropylene copolymer of the monolimb. This therefore indicates that the monolimb will not undergo plastic deformation when affixed with the SACH foot or the SR foot. This conclusion can only be made based the on the static loading conditions that were performed in this study.

It is recommended that future physical tests be performed to take into consideration cyclic and dynamic loading. Because the SR foot underwent plastic deformation before reaching 910 N in our heel-strike test, we are led to believe that repeated cyclic loading at even lesser values would produce similar plastic deformation. Completing this test according to the ISO standards mentioned earlier could lead to a better understanding of the longevity of the SR foot.

The potential errors that affected our FEA results were primarily associated with the SACH foot. The intricate CAD model that was developed did not run in ANSYS because of its complex shape and rounds. More models of the SACH need to be made to analyze in ANSYS. The complexity of the foot made it difficult for the program to mesh the features. If a future study is performed on the SACH foot, the two types of polyurethane foam used in the foot need to be modeled. This would yield more accurate results because the model that was used for this study did not include the two material properties for the base of the foot and the body of the foot. Also, time should be spent to find the exact material properties through material testing.

This study compared the interaction of the traditionally used SACH foot and the new, low-cost Shape and Roll prosthetic foot with the Center for International Rehabilitation's monolimb. Through the static physical testing and FEA it was seen that the stiffer Shape and Roll assembly produced higher strains on the monolimb, but did not exceed the yield strength of the monolimb. This information will aid in the future development and refinement of low cost prosthetics for low income countries.

1. Introduction

Global conflict is something that has been prevalent for years. The sad fact of combat is that many of those affected are not soldiers. Victims are still being counted for wars that have taken place years ago. Landmines have killed or injured over one million people since 1975. Afghanistan, Angola and Cambodia have suffered eighty-five per cent of the world's land-mine casualties. Currently, there are over one hundred million active landmines around the world (Landmines: A Deadly Inheritance 2005). While the cost for making one landmine is on the order of three dollars, the cost to deactivate a landmine is one thousand dollars. The cost to deactivate these landmines is not feasible for the developing countries in which many of the landmines are located. It has been estimated by the World Health Organization that "ten percent of the global population, or more than five hundred million people, have a disability. Two-thirds of those people live in developing countries, and that number is rising due to poverty, poor healthcare, disasters, landmines, war, and other forms of violence" (Stanton 2006).

Landmine victims lose their place in society along with losing their limbs. Many countries see amputees as a burden since they lack mobility and the skills to work. Many organizations have gathered to combat this issue by having countries sign treaties against the use of landmines. The most well-known treaty, which bans the use of landmines, was presented at the Ottawa Convention in 1997. The treaty was supported by governments, the United Nations, and international organizations such as the International Committee of the Red Cross (ICRC), and over 1,400 non-governmental organizations (Metzger 2007).

Although great strides have been made in landmine awareness, there are still countless victims in need of assistance and rehabilitation. The Center for International Rehabilitation (CIR), started by Physicians Against Landmines, is working to provide appropriate prosthetic technology to help integrate victims back into society. As part of this effort they are in the process of developing a monolimb; a simple prosthetic leg that can be coupled with a prosthetic foot.

This Major Qualifying Project has been conducted to test the interaction of the Solid Ankle Cushioned Heel (SACH) and Shape and Roll (SR) prosthetic feet when coupled with the CIR's monolimb. The SACH foot, (Figure 1) has been traditionally used in low-income countries, while the SR foot (Figure 2) was recently developed by researchers at Northwestern University. There is concern among the researchers that the new SR foot might be too stiff to couple with the monolimb, thus potentially causing premature

failure to the monolimb. By evaluating and comparing these prosthetic foot designs through both computer modeling and experimentation, we were able to understand the interaction between the prosthetic feet and monolimb.

Figure 1: ICRC SACH Foot ("Prosthetic Feet")

Figure 2: SR Foot ("Lower Limb Prosthetics: The Shape&Roll")

2. Background

The Center for International Rehabilitation is developing appropriate prosthetics for low-income countries. To establish a basis for the need for appropriate prosthetics, factors that social scientists have deemed important when working with developing nations have been reviewed. The current work of the Center for International Rehabilitation, specifically their work with the monolimb for below knee amputees is important to gain a better understanding of the background of the center. Since the prosthetic feet undergo loading similar to that of a human performing natural gait, overviews of the multiple phases that occur in the gait cycle are explained, including the contribution of the foot and ankle through each stage of the gait cycle. The forces and moments that occur within the foot and ankle system are also included. Other current foot prosthetics available for low-income countries are investigated to gain a better understanding of similar technology. The manufacturing processes and the properties of the ICRC's SACH and the SR foot are presented. Finally, the International Organization for Standardization (ISO) Standards that apply to testing prosthetic feet are explained, in order to develop a valid methodology for the testing and analysis of these low cost prosthetics.

2.1. Prosthetics in Developing Nations

This project aims to model and analyze the mechanical functioning and interactions of the SACH foot and SR foot when coupled with the CIR's monolimb. For the overall success and sustainability of the prosthetic foot and monolimb, the product must be able to be made, distributed, and used in the country where it is needed. The distributors and users of the foot also need it to have the longest potential lifespan where funding and technology to repair the prosthetic may be limited. Industrialized nations often overlook this aspect when they are seeking to provide aid.

Vossberg writes in *Prosthetics and Orthotics International* that imported products strain the local budget and require developing countries to be dependent upon foreign aid. He suggests the following six factors that one must be aware of when providing technical assistance: economic, social, cultural, pathological, environmental, and humanitarian. A country should be assessed and each factor established when research is being done for the prosthetic design and implementation procedures. Economic factors are a concern because if the cost is too high then a country will not be able to sustain its growth. Since most of the amputees in need of prosthetics are destitute, they will not be able to provide for their medical costs, nor will they likely be able to receive assistance from their governments. Socially, people in some cultures may not be accepting of those with prosthetics, so the prosthetist

should aim to bring someone back into society. Additionally, cultures have different needs, making it unfeasible to create a universal design. Pathological factors are a concern where many of these countries are located in disease ridden areas. Environmental factors limit the resources that are available to produce the prosthetics. The humanitarian factor means that not all of the most costly donated items will be the best in non-industrialized environments (Vossberg 1999). The consideration of all these factors can increase the chances that a prosthetic will be accepted and continually used.

2.2. Center for International Rehabilitation

The Center for International Rehabilitation (CIR) was started in 1998 in the city of Chicago by William Kennedy Smith and a group of doctors. Prior to starting the CIR these doctors were involved in an organization called Physicians Against Landmines (PALM). The center focuses its efforts toward rehabilitating amputee victims affected by landmines. The CIR's mission is "to assist people with disabilities worldwide in achieving their full potential" (The Center for International Rehabilitation 2007).

The CIR's efforts span the globe, offering education, technology, and resources to the following regions: Africa, North America, Central America, Middle East, Europe, Asia, and South America (Stanton 2006). The CIR is able to reach out to these countries through E-learning initiatives to teach international prosthetic technicians. The CIR aims to produce products that are sustainable and can be produced in the host country using local materials and tools. The CIR also operates a Rehabilitation Engineering Research Center (RERC) which is nationally recognized for its accomplishments (The Center for International Rehabilitation 2007).

2.3. CIR's Monolimb

In an attempt to bring effective and inexpensive prosthetics and orthotics to low-income countries, the Center for International Rehabilitation has developed a transtibial prosthetic leg and foot unit. They have developed and are in the process of refining a monolimb, which is the prosthesis between the knee and prosthetic foot.

The first step of developing the monolimb is measuring the patient to find the center of the knee. Each monolimb is custom made for each patient. A cast of the residual limb is then made using clay. The clay is built up as seen in Figure 3.

Figure 3: Clay Casting of Residual Limb and Plaster Casting of Residual Limb (CIR 2006)

A nylon sheath is then applied over the clay and layers of plaster are put over the sheath. As the plaster is layered, splints are added to add to the structure of the casting. When the casting has dried, the alignment marks are put onto the cast. The cast is then put onto a system where a positive plaster mold will be made of the monolimb. The cast is put onto a mandrel and plaster is poured into the cast as seen in Figure 5.

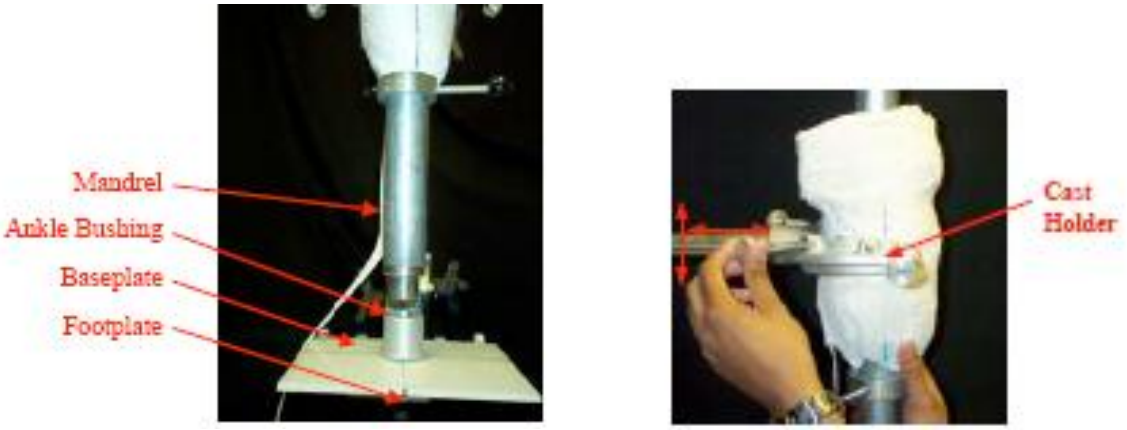

Figure 4: Monolimb Alignment and Cast Holder (CIR 2006)

The next step is to make the actual monolimb. The mandrel must be sanded and prepped. The mandrel with the positive mold is then covered by a stockinette and covered in talcum powder. The plastic is prepped by heating it in an oven for 27 minutes until it turns completely clear. The clear plastic is then drape molded over the mandrel and positive mold. From the distal end of the mandrel, the plastic is pressed together to seal it around the mold. This is done until the mold is completely encased with the plastic.

Figure 5: Pouring Plaster into Limb Casting, Mandrel with Positive Mold, and Cutting the Plastic (CIR 2006)

The excess plastic is then cut off and when it cools, edges are sanded and smoothed.

Figure 6: Finished Monolimb with Prosthetic Foot (CIR 2006)

The monolimb is made of 90% polypropylene and 10% polyethylene. The properties are found in Table 1. The shank of the monolimb is a hollow cylinder two inches in diameter and 0.2 inches thick (Kim 2006).

Property	Value
Modulus of Elasticity	1500 MPa
Poisson's Ratio	0.3
Tensile Yield Strength	30 MPa
Compressive Yield Strength	50 MPa

Table 1: Polypropylene Copolymer Properties

According to Kim Reisinger, Ph.D. former Director of Engineering Research at the CIR, the monolimb is to be attached to a separate prosthetic foot by a standard bolt. Researchers from CIR are currently performing field testing of the monolimb with the SR foot. These tests have occurred in Nicaragua and are planned for Guatemala and Honduras. The preliminary feedback from the tests has been largely

positive. There are currently about sixty users in the field that are using this circular cross sectioned monolimb with the SR prosthetic foot. The monolimb is used by the thousands with the ICRC's SACH foot (Personal Communication, Casanova, Feb. 21, 2008).

One concern has arisen from a study done on the SR foot with the monolimb in the United States. Stress marks have appeared on the anterior of the monolimb directly above the metal insert. This took place when a larger user, of about 185 pounds was using the monolimb for rigorous activities, like karate. Generally, the monolimb is prescribed for users less than 165-175 pounds. The concerns that were raised from the test where stress marks were found brought up some concern for the overall stiffness that is exhibited when the SR foot is coupled with the monolimb when used by more active and heavier patients.

Previous analysis of the monolimb has been conducted in China to study ability of the monolimb to withstand the forces applied during gait. One study had found that the depth of the posterior seam on the back of the monolimb had little effect on the stresses that occur on the monolimb (Lee 2005). A study conducted at Worcester Polytechnic Institute modeled the monolimb, seen in Figure 7, to study the peak stresses that occurred at the connection between the socket and shank portion of the monolimb (Kim 2006). There have not been any experimental studies done regarding the interaction between the monolimb and the ICRC's SACH foot or the SR prosthetic foot.

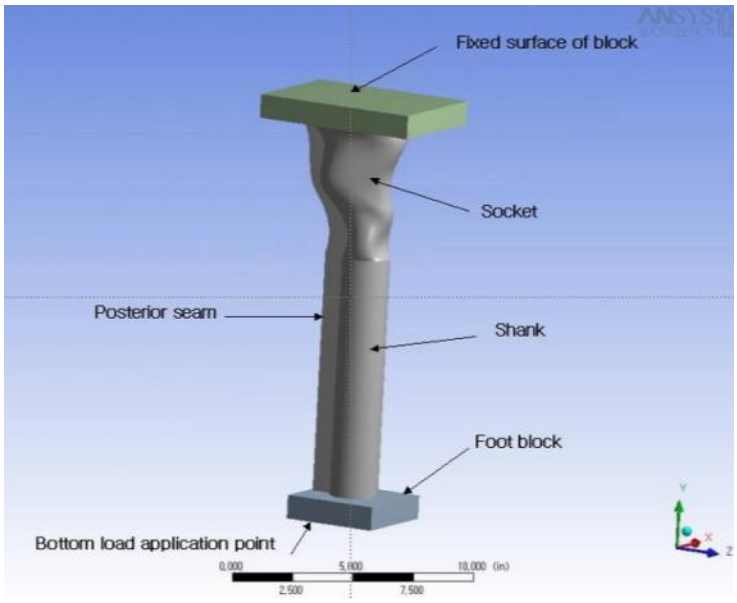

Figure 7: CIR Monolimb (Kim)

2.4. The Gait Cycle

In order to understand the behavior of lower limb prosthetics, the act of walking must be understood. The process of walking is broken down into a series of repeated events in which a person's weight is supported by one leg while the other leg moves forward, with the weight being transferred between the two. This sequence of actions, occurring on one leg, is called the gait cycle (Perry 1992)

The gait cycle is broken into two periods, the stance period and the swing period. The term stance refers to the "period of time that the foot is on the ground." The term swing refers to the "time that the foot is in air for limb advancement" (Perry 1992). The gait cycle can also be subdivided into three main tasks: weight acceptance, single limb support, and limb advancement. These main tasks are accomplished through the eight distinct phases that occur within the gait cycle, as seen in Figure 8.

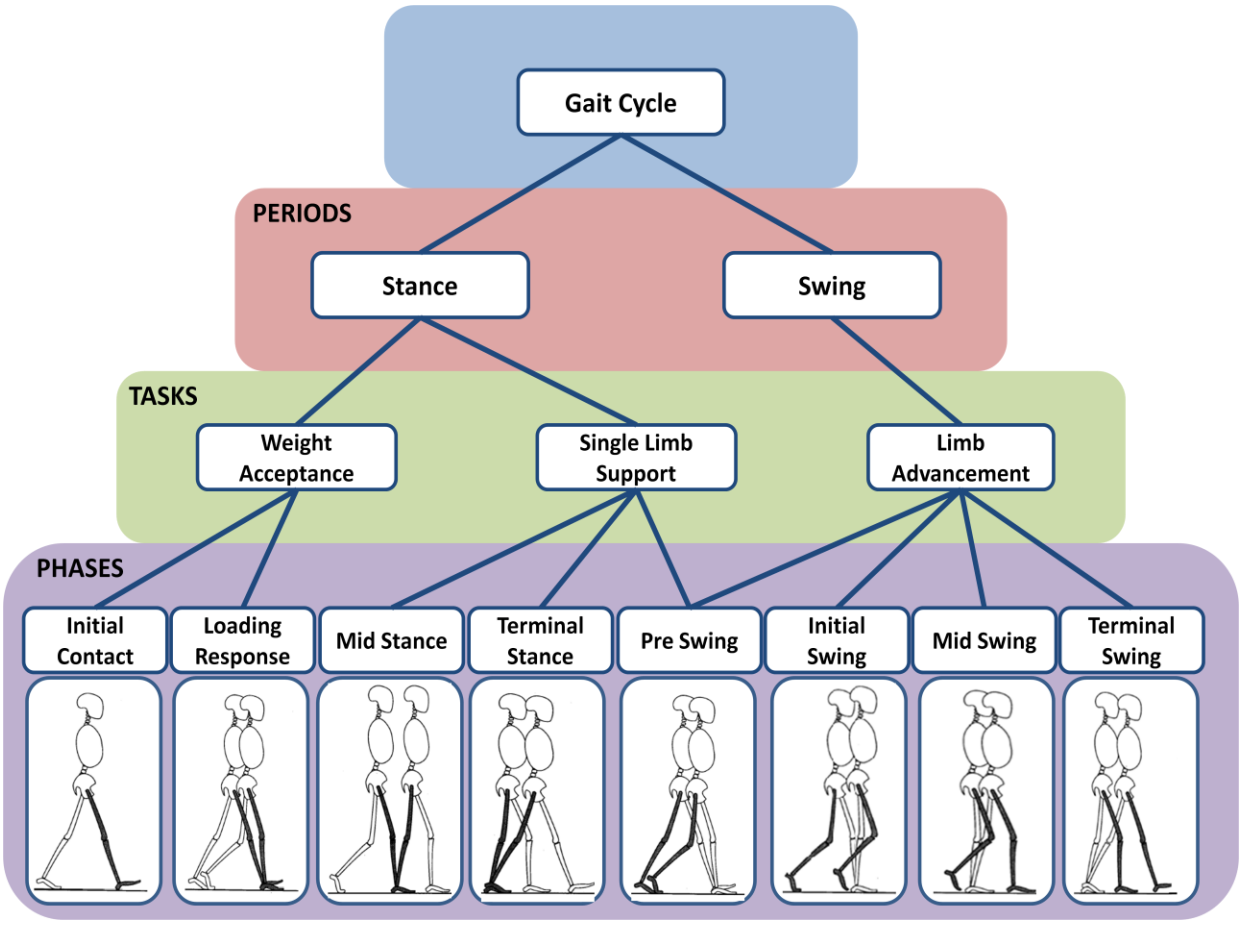

Figure 8: Divisions of the Gait Cycle (Perry 1992)

The body's weight is accepted onto the limb during the initial contact and loading response phases. There is then single limb support, where only one limb is supporting the weight of the body, during the midstance, terminal stance, and pre-swing phases. Finally, the limb advances forward during the pre-swing, initial swing, mid swing, and terminal swing phases.

2.4.1. Stance Period

Weight Acceptance: Initial Contact

The initial contact phase (Figure 9) occurs in the first 0-2% of the gait cycle, and begins the moment the foot touches the ground. At this point the other limb is at the end of the terminal stance.

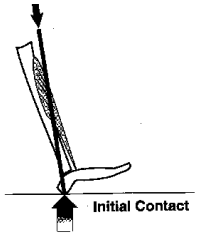

Figure 9: Initial Contact (Perry 1992)

In the initial contact phase, the foot is at a neutral position perpendicular to the lower leg. The heel is in contact with the ground, in preparation for the upcoming loading phase in which it acts as a heel rocker (Perry 1992).

Weight Acceptance: Loading Response

The loading response phase (Figure 10) occurs in the first 0-10% of the gait cycle and allows for shock absorption, weight bearing stability, and the continuation of progression. This phase starts from the foot's initial contact with the floor through until the other foot lifts from the ground to begin the swing period. The other limb is in pre-swing phase at this time.

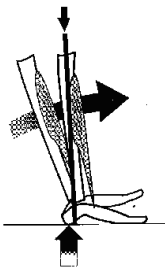

Figure 10: Loading Response (Perry 1992)

In the loading response phase, the ankle undergoes plantar flexion as the foot rapidly rotates about the heel to the ground. As the foot drops to the ground pretibial muscles act to decelerate the drop, and as result the tibia moves forward. This causes the body's weight to shift from behind the heel to in front of it. This is called the heel rocker. Since the pretibial muscles act to decelerate the falling foot, some of the force due to initial contact is reduced. If the body is unable to achieve exactly neutral position at initial contact, instead having 3 to 5° of ankle plantar flexion, the heel rocker is reduced (Perry 1992).

Single Limb Support: Midstance

The midstance phase (Figure 11) occurs during the 10-30% of the gait cycle, and in this phase the body moves forward over the stationary foot while maintaining stability. This phase starts when the other foot ends contact with the ground and ends when the weight of the body is directed over the forefoot. At this time the other limb is in the mid-swing phase.

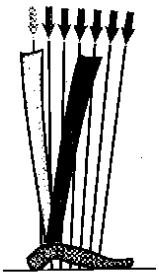

Figure 11: Midstance (Perry 1992)

In the midstance phase, the ankle undergoes dorsiflexion and acts as an ankle rocker. The foot remains fully on the ground while the tibia rotates forward to an eventual 5 ° dorsiflexion. During midstance the soleus muscle, which connects the tibia and heel, provides the majority of force to decelerate the ankle dorsiflexion (Perry 1992).

Single Limb Support: Terminal Stance

The terminal stance phase occurs during the 30-50% of the gait cycle, and in this phase the body continues to move forward past the foot on the ground. This phase begins as the heel of the foot rises and ends when the other foot first comes in contact with the ground. The other limb is in the terminal swing phase during this time.

In the terminal stance phase, the tibia is continuing its movement forward, but at this phase raises the heel as it moves forward. The foot rotates about the forefoot, which consists of the metatarsal heads

and proximal phalanges. With the rising of the heel and dorsiflexion of the ankle, the body's center of gravity moves anterior to the point of rotation on the foot. This causes the foot to rotate further, and leads to a point where the center of gravity has moved so far that the foot cannot support the body on its own. At this point the other foot touches the ground and the terminal stance phase is complete (Perry 1992).

2.4.2. Swing Period

Limb Advancement: Pre-Swing

The pre-swing phase occurs during the 50-60% of the gait cycle, and in this phase support of the body's weight is transferred to the other foot in preparation for the swing period. Because of this, the pre-swing phase is also called the weight release or weight transfer phase. This phase begins when the other foot touches the ground and ends when the foot being studied lifts off the ground. The other limb is in the loading response phase.

In the pre-swing phase, as soon as the other foot comes in contact with the floor, the ankle begins to plantar flex to 20°. The soleus and gastrocnemius muscles, which had been working in the terminal stance phase, quickly reduce their activity, which in turn accelerates the limb forward. The foot plantar flexes, which allows the toe to be stabilized on the ground (Perry 1992).

Limb Advancement: Initial Swing

The initial swing phase occurs during the 60%-73% of the gait cycle, and during this phase the foot clears the floor while the leg begins to move forward. It begins when the foot has ended contact with the floor through until the foot is in line with the other foot on standing on the ground. The other limb is in the beginning of the midstance phase.

In the initial swing phase, the foot begins in plantar flexion of 20°. The foot is not interfering with the advancement of the leg because of this position. The foot then begins to dorsiflex until it is at 5° of plantar flexion by the time it crosses the other foot in stance position. The toes of the foot also undergo dorsiflexion at this time (Perry 1992).

Limb Advancement: Mid Swing

The mid swing phase occurs during the 60-73% of the gait cycle, and during this phase the leg advances while the foot continues to remain above the floor. This period starts when the swinging limb and other stance limb are opposite each other, and ends when the swinging limb is in front of the body with the tibia in a vertical position. The other limb is in the latter part of the midstance phase (Perry 1992).

In the mid swing phase, the ankle continues its dorsiflexion. It moves to a neutral position, or just below, in the early part of this phase, but this position is not maintained completely throughout (Perry 1992).

Limb Advancement: Terminal Swing

The terminal swing phase occurs during the last 87-100% of the gait cycle, and during this phase the body completes moving the limb forward while preparing to enter the stance period. This phase begins when the tibia is vertical, continues as the lower leg moves ahead of the thigh, and ends the moment the foot comes in contact with the floor. The other limb is in early terminal stance (Perry 1992).

In the terminal swing phase, the ankle is held at the neutral position. While pretibial muscles act to hold this position, the ankle will often move to 3 to 5° of plantar flexion. This is in preparation for the initial contact phase that will be occurring (Perry 1992).

2.4.3. Biomechanics of the Foot and Ankle

As seen by the gait cycle, the ankle-foot group has complex movement and does not stay in the same configuration the entire time. The ankle and subtalar joints have a range of motion which extends past the neutral position in both directions (Perry 1992). There are three “rockers” that occur during the gait cycle, changing the angle of the foot and ankle: heel rocker, ankle rocker, and forefoot rocker (Figure 12). Each rocker contributes to the progression of the limb.

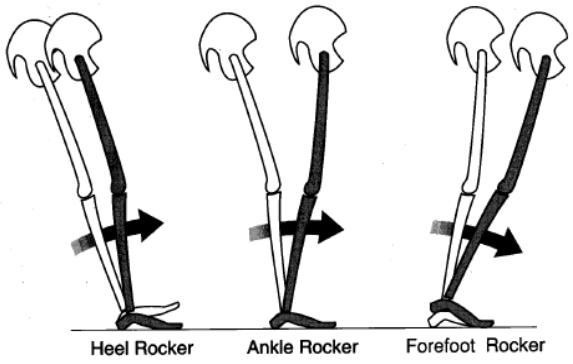

Figure 12: Rockers Occurring In Gait Cycle (Perry 1992)

In addition to the plantar flexion and dorsiflexion of the ankle during gait, the metarsaophalangeal joints, otherwise known as the toes, also move. The toes have a maximum of 55° of dorsiflexion (Figure 13), occurring during the pre-swing phase, and a minimum angle of zero (Perry 1992).

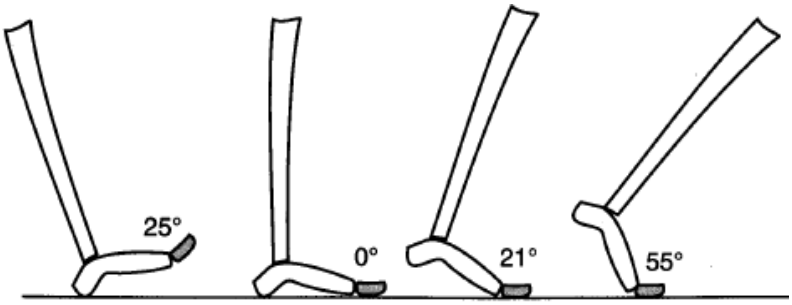

Figure 13: Flexion of Toes (Perry 1992)

2.5. Prosthetic Feet

Prosthetic feet are a highly customizable product. Each foot serves to provide for the needs of a slightly different user than the next. A prosthetic provides a stable weight-bearing surface, absorbs shock, replaces lost muscle function, replicates the anatomic joint, and restores cosmetic appearance ('Lower Limb Prosthetics').

Users of prosthetic feet can be broken down into functional levels which relate to their activity level and needs for their prostheses. A Level 0 amputee does not have the ability to go through the gait cycle due to massive injuries. A prosthetic would not help someone at a Level 0. A Level 1 has the ability to ambulate, but does not have the stability to walk on sloped ground. A Level 2 amputee can travel on some varying terrain and slopes. A Level 3 can traverse ranging slopes and conditions. They have

varying activity levels and many need a prosthesis for a vocational task. The last level, a Level 4, has high mobility and will subject their prosthetic to high impact and high stress situations (Clinical UM Guideline 2007).

2.5.1. Roll-Over Shape

The roll-over shape of a foot is better understood as the geometric representation of the shape which the studied foot takes throughout the stance period of the gait cycle, which includes the loading response, mid-stance, and terminal-stance phases. This shape is the movement of the location of the center of pressure (COP) during gait, in reference to the hip joint center position. It is believed that a better understanding of a foot's roll-over shape will explain why similar gait analysis results have been observed for feet that exhibit drastically different mechanical properties (Hansen 2005).

For a normal limb structure, the roll-over shape of a specific foot is calculated using sagital plane markers attached to the lateral malleolus (ankle), left and right anterior superior iliac spines (LASIS and RASIS), and the sacral (three lowest vertebrae). These four markers are then used to estimate a "hip joint center position," from which a coordinate system may be established (Figure 14). This coordinate system makes it possible to plot the COP throughout the gait cycle.

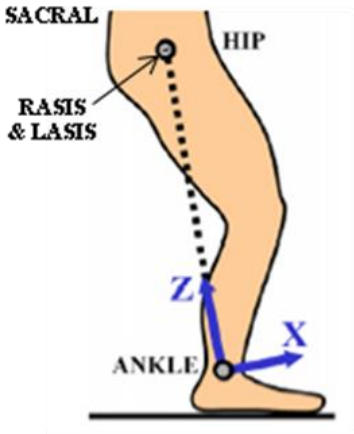

Figure 14: Roll-Over Shape Coordinate System with Marker Locations

2.5.2. Energy Storage and Return

It is important for a prosthetic foot to be able to store energy expended by the user and return it later in the gait cycle. This return of energy makes gait both less energy intensive and more realistic because human feet are naturally able to return energy throughout the gait cycle. To achieve this return of energy most feet use a deformable forefront keel to act as a leaf-spring and either a foam heel or

another leaf-spring as the heel. These leaf-springs elastically deform and then return to their original position, and thus releasing the energy originally put into them to cause deformation (Geil 2001).

2.5.3. Mechanical Properties

In the design and analysis of a prosthetic foot many different mechanical properties must be considered, including fatigue resistance, stiffness, and ductility. Fatigue resistance describes an object's resistance to changes in shape or material properties over a period of cyclic loading. The loads applied during this period may be fixed or varying to represent the loads during actual use (Fatigue Test 2007). Stiffness describes a design's resistance to deflection or deformation caused by an applied force (Figure 15). All materials and therefore prosthetic feet exhibit characteristics of both the elastic and plastic ranges of deformation over their lives. As previously mentioned to achieve energy return a foot must undergo elastic deformation, which is completely reversible. When a foot deforms past the point of elastic deformation it undergoes plastic deformation, which is only party reversible due to the fact that the foot has passed through into the plastic region.

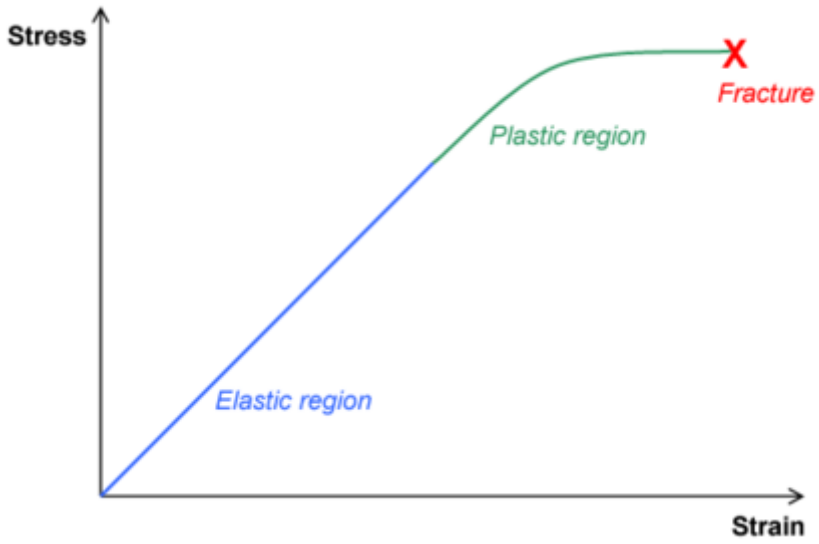

Figure 15: Diagram of Deformation ("Deformation")

2.5.4. SACH Foot

The Solid Ankle Cushioned Heel (SACH) prosthetic foot was designed in 1958 by Eberhart and Radcliffe (Gailey 2005). The SACH design has a solid ankle, made of wood, metal, or plastic, which is then surrounded by rubber or foam with a cushioned heel. The cushioned heel is for absorbing shock in the initial phases of the gait cycle to allow the user to mimic more nature gait patterns. The rigid keel also

provides a stable weight-bearing platform, which provides the user with confidence in their prosthetic. The cushioned heel lessens impact of weight transfer and the flexible material of the toe allows for a smoother rollover at the end of the gait cycle (Supan 2005). The SACH foot will be the major focus of research and comparison with the SR prosthetic.

Figure 16: Examples of SACH Feet

ICRC SACH Foot

The International Committee of the Red Cross' (ICRC) SACH foot is one of the two feet being tested in this project. The foot is currently used by 20,000-30,000 amputees in the field (personal communication, Cassanova, Feb 21, 2008). The foot is made of polyurethane foam that is injection molded in an aluminum casing. The inner keel of the foot is made of polypropylene plastic to be shown in the CAD modeling section of the report. The foot is actually manufactured by CR Equipments in cooperation with the ICRC in Geneva.

Figure 17: ICRC SACH Foot

Advantages

The SACH prosthetic design has many variations, but they are all based on a similar concept. A SACH foot is generally used when mid-stance stability is desired for the user (Supan 2005). The SACH foot has been considered the standard prosthetic prescribed to those with low function and activity levels. The SACH foot was the first prosthetic foot to exhibit roll-over shape (Hansen 2005). The minimal parts allow for easier use and maintainability. The SACH foot is available at low cost because of the minimal parts needed and is the most prescribed (Supan 2005).

Disadvantages

Several shortcomings of the SACH foot have been discovered in clinical trials and in human subject testing. A study completed at Northwestern indicated that the SACH foot often exhibits shortcomings in plantar flexion due to its rigid design (Stark 2005). This aspect of the foot also plays into its success because the rigidity in turn offers stability in the early phases of the gait cycle. The SACH foot has also had issues with low energy return when compared to the Flex Foot (Stark 2005). It has also been found that the SACH foot has a shorter roll-over shape than a human foot and other prosthetic feet, such as the SR, which means that at the toe region it is not as able to support weight (Sam 2004).

2.5.5. Shape and Roll Foot

The Shape and Roll (SR) Prosthetic foot was developed by a team of researchers at Northwestern University in 2004. It was created for use in low-income countries, as an alternative to the prosthetic feet commonly distributed. The design is based on the roll-over shape characteristics of a human foot, and can be manufactured using low cost materials (Figure 18).

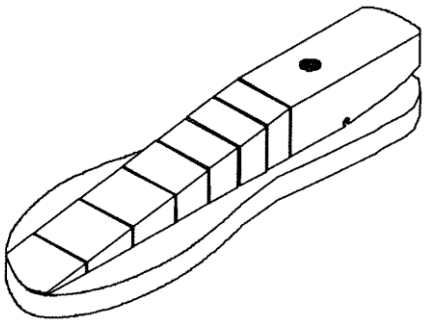

Figure 18: SR Foot (Sam 2004)

The SR Prosthetic design is based on the idea that the roll-over shape of a prosthetic foot should match the roll-over shape of a human foot. The foot consists of a wedge shape with parallel cuts through the center. The prosthetic can be used with or without a commercially available foot cover (Sam 2004).

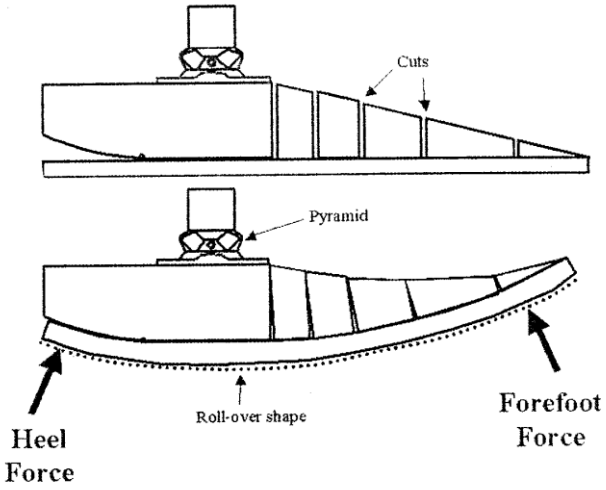

Figure 19: Sagital Plane Cross-Section of SR Foot (Sam 2004)

As seen in Figure 19 shows a sagital cross-sectional view of the foot, the height begins low at the toe region and increases in height until the ankle connection point. The spacing of the vertical cuts was determined through a computer algorithm, which attempted to give the foot the "desired bending radius based on the individual's stature" (Sam 2004). At the ankle connection point, the prosthetic has a flat surface that can be connected to a standard endoskeletal pyramid plate or other connection types. The heel of the foot has a wedge-shaped piece removed, which allows the foot to provide shock absorption during the initial contact phase when the heel-strikes the floor. This wedge also provides the foot with roll-over shape similar to a human normal foot. The foot is also hollow, in order to reduce the weight (Sam 2004).

The bottom plate of the foot can be created in various thicknesses in order to provide different levels of stiffness. This allows the foot to be used with people with different weights and different activity levels. The level of stiffness does not affect the roll-over shape, up until the point where the vertical cuts are unable to come together. Because of this, the roll-over characteristics and stiffness of this prosthetic foot can be selected independently, as required by the user (Sam 2004).

The SR Foot is made out of a polypropylene-polyethylene copolymer, because this material meets all of the desired properties: “high fatigue resistance, acceptable stiffness, easily thermoformed, available in most countries, water resistant, ductile failure characteristics, and low cost” (Sam 2004). It is compression molded using technology that is available in most countries.

Manufacturing

Copolymer sheets are placed between wooden or aluminum molds (Figure 20). The bottom part of the mold shapes the bottom part of the foot, while the middle section, otherwise known as the mandrel, shapes the hollow inside of the foot. The top part of the mold forms the top part of the foot (Sam 2004).

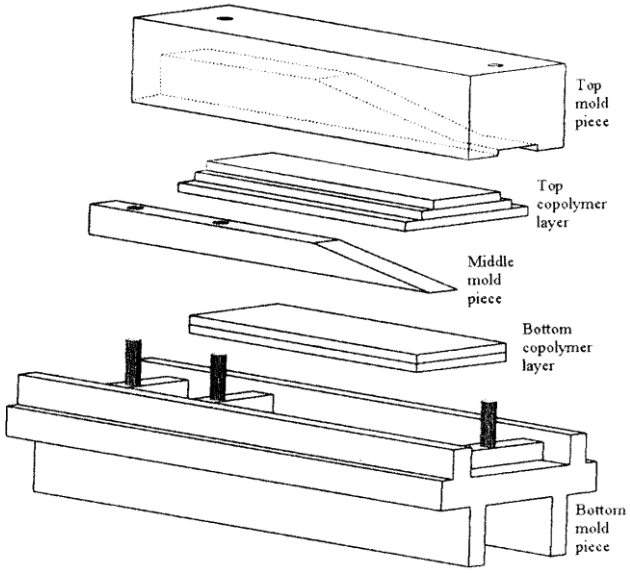

Figure 20: SR Prosthetic Foot Pressure Mold (Sam 2004)

After the heated copolymer sheets are placed between the layers of the mold the top and bottom mold pieces are bolted together to compress the copolymer and left to cool. After several hours the copolymer is removed, and the mandrel is removed using a simple tool consisting of a threaded rod and nuts on a pipe. An aluminum tube, which will be the support for the pyramid connector, is inserted into the hollow inside of the foot (Figure 21). The pre-calculated cuts are made on the top surface of the wedge and the heel wedge is removed (Sam 2004).

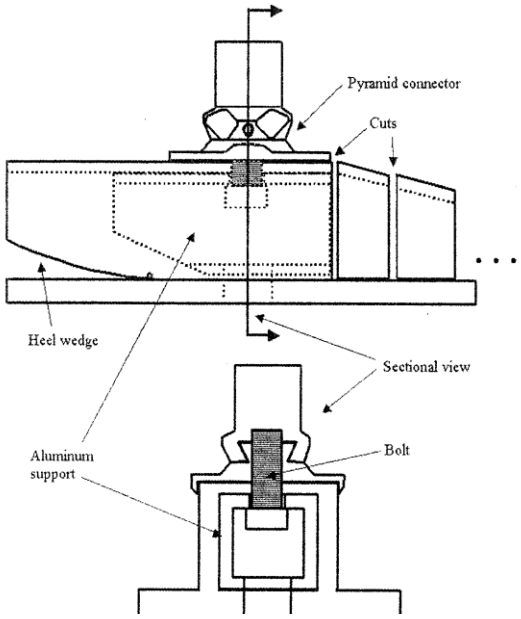

Figure 21: Aluminum Insert Piece and Attachment Point (Sam et al., 299)

There are other options for the manufacture of the SR Prosthetic Foot, including a compression molding apparatus that utilizes levers. It has been found that the lever methods reduce the number of tools and complexity of the mold, while decreasing the time required to manufacture the foot (Sam 2004).

Laboratory Testing of SR Foot

The roll-over shape of the SR Foot was created using a quasi-static roll-over method. The roll-over shape was compared to those of a Flex-Walk prosthetic, SACH prosthetic, and a typical physiological ankle-foot (AF) complex. The SR Foot has a roll-over shape similar to the normal human foot (Figure 22)(Sam 2004).

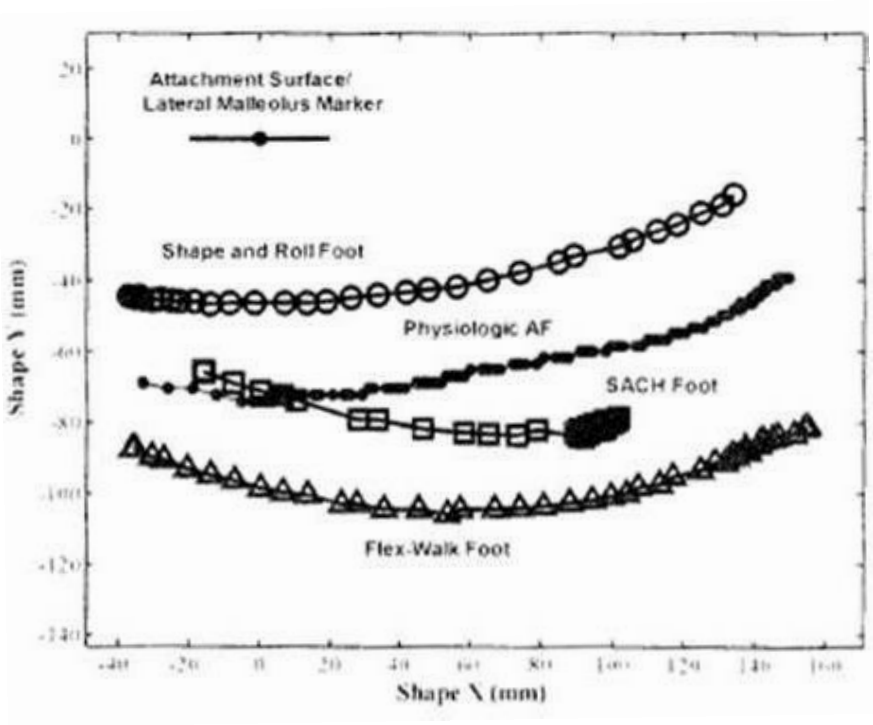

Figure 22: Roll-Over Shape Comparisons (Sam 2004)

Figure 22 shows that the distance between the prosthetic foot and place of attachment to the leg, otherwise known as the profile, is less for the SR foot than any of the other feet tested. This would allow people with longer residual limbs to use the prosthetic. (Sam 2004).

The foot was also fatigue tested on a privately made tester according to ISO standards. While ISO standards state that a sine wave loading should be applied, the researchers applied a more square-wave shape load. It was justified by the argument that a square-wave produces a more severe loading than a sine-wave. Four feet were tested to over two million cycles and another to 3.8 million cycles, all without failure, before the decision was made to stop testing (Sam 2004).

Disadvantages

Several limitations of the SR Foot have been noted by the developers. One weakness is the flat area located underneath the ankle connection attachment point. Some of the subjects that have used the foot have noticed this area, which does not bend as much as the rest of the foot during walking, but according to the designers it cannot be reduced without introducing premature failures. A second weakness is that the copolymer takes a set after being used, but it has been found that the foot still has good energy-return properties, although these results are unpublished. It is thought that using

alternative materials could provide higher energy storage and return and not undergo setting. There is also a need for testing of the foot and recording of the roll-over shape on actual subjects with and without proper alignment in order to study the roll-over shape (Sam 2004).

2.5.6. Additional Prosthetics for Developing Countries

Niagara Foot

The Niagara Foot (Figure 23) is a low-cost high energy prosthetic designed by engineers from Queen's University in Kingston, Ontario. The designers were set on the mission of designing for victims of landmines in developing countries.

Figure 23: Niagara Foot (IDEAnet)

The foot is made with impact resistant DuPont plastic in order to sustain the wear and tear of those living in rural areas. The foot's energy storing design decreases the overall muscular effort required by the user. There is considerable flexibility under loading in the heel region, which is beneficial during stride, but it can also lead to instability during standing.

Studies of the Niagara foot began in November of 2001 and several design iterations have been made, although the overall response from users has been positive. Test patients did not experience any failures in the heel of the Niagara Foot, a seemingly weak design characteristic, over a yearlong study of the device at the Aranyaprathet Clinic in Thailand. The wear was also limited in other contact areas. The study found that there were no failures of the device after one year (Niagara Foot: Pilot Study).

Jaipur Foot

The Jaipur Foot (Figure 24) is an economical prosthetic foot designed for developing countries. The foot was created in Jaipur, India by doctor Pramod Karan Sethi. The foot is made from local materials such as discarded rubber tires and waste items which are readily available in areas similar to Jaipur, India (Serlin 2001). The foot has a wooden keel with a carriage bolt to connect it to an upper prosthetic. The foot's main form is created in an aluminum mold. The body of the foot is then created using a plastic

Figure 24: Jaipur Foot ("Jaipur Foot" 2005)

which is hand cut to match the mold and then is covered in tyre cord and the foot is covered with a cushioning compound and placed back into the mold. The foot is then vulcanized in an oven.

Figure 25: Jaipur Foot Mold ("Jaipur Foot" 2005)

The Jaipur Foot is different from most prosthetics because was designed to be fitted quickly to the user, generally in less than an hour. Normal daily activities like sitting, running, squatting, and climbing can be accomplished using this prosthetic foot. The foot was designed in India after its designers discovered that most of those in need of prosthetics are below the poverty line. They designed the prosthetic to retail for less than thirty-five United States dollars. This improves the sustainability of this product.

Studies have suggested that the Jaipur Foot is preferred over the SACH foot for various reasons. The bolting of the Jaipur is just at the ankle, whereas the wooden keel of the SACH foot extends to the mid-foot restricting movement. The Jaipur Foot better mimics the appearance of a natural foot. The Jaipur Foot does not require the use of a cosmetic shoe cover, although it still remains an option. Another important aspect in many developing countries is squatting; the Jaipur Foot allows the user to squat, unlike many prosthetics. Users are able to walk barefoot. Most importantly, the Jaipur foot can be manufactured using local materials (Jaipur Foot 2005). The Jaipur foot has already helped over 900,000 amputees around the world.

Mobility For Each One

Figure 26: Mobility for Each One (Index Award 2007)

Mobility for Each One (Figure 26) is another prosthetic that has been developed for use in developing countries. This prosthetic is the winner of the 2007 Index Award for innovative design. The design can be produced for $8. The prosthetic foot can be fitted to several types of leg prostheses and it was created to meet the ICRC's standards (Index Award 2007).

The foot is made of composite material and it based on the premise of energy storage. It is made of glass fiber instead of carbon fiber, which is about ten times cheaper. The prosthetic can be molded on a wooden frame by hand. Also, less material is needed because the curved design inherently adds structure and support (Mobility for Each One 2006).

2.6.Ground Reaction Forces during Gait

There are reaction forces during the stance phase of the gait cycle as the foot interacts with the ground. These forces form a typical shape for the average person. The normalized horizontal and vertical forces during the gait cycle are seen Figure 27.

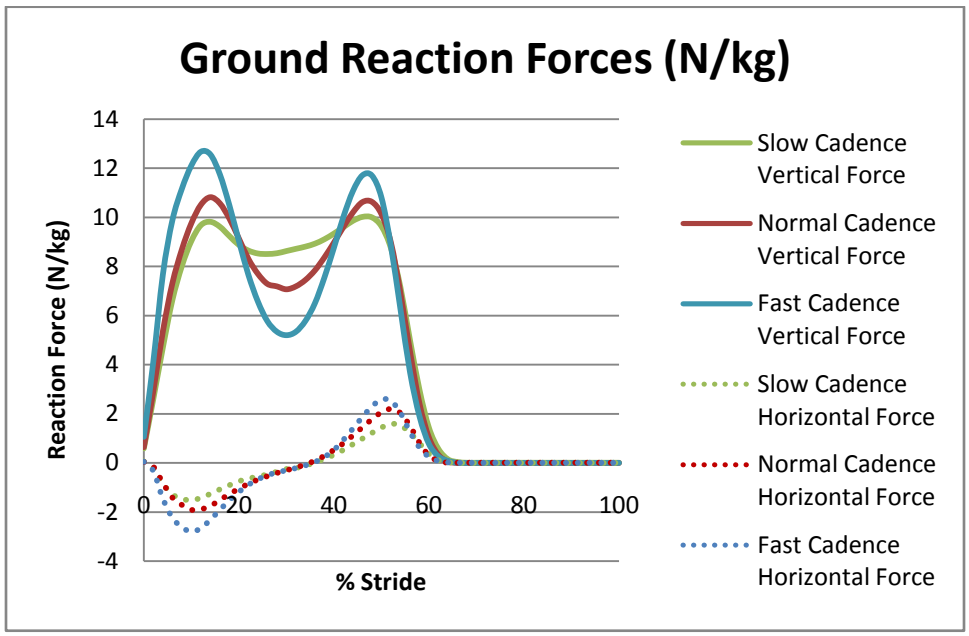

Figure 27: Ground Reaction Forces During Fast Walking (Winter 1991)

The horizontal, or lateral, forces are seen to be negative, acting in the posterior direction, during the first part of the cycle through to approximately mid-stance when they become positive, acting in the anterior direction. They peak at an average of 2 N/kg during natural walking and almost 3 N/kg for fast walking. For an 80 kg person, this would be 160N for natural walking and 240N for fast walking. The average vertical forces are much greater, at the greatest point being almost 11 N/kg during natural walking and almost 13N/kg for fast walking. For the 80 kg person, this is 880N for natural walking and 1040 N for fast walking. The vertical forces have a double hump shape, which represents the period of initial contact with the ground and the period prior to swing. During the first peak in force, the body's center of mass endures an upward acceleration as it is moving downwards. At the second peak, where the leg is pushing off before swing, the body's center of mass is again accelerated upwards (Winter 1991).

The moments of force during gait can be calculated using inverse dynamics. Inverse dynamics derives the forces and moments acting on a joint from the kinematics of walking (Kirtley 2007). Another method is to calculate the "joint moment by calculating the product of the ground reaction force vector and the perpendicular distance from the joint center to that vector" (Winter 1991). This method does not account for the moments at a joint due to the acceleration of the limbs. The errors are compounded as the moments are calculated up the ankle, knee, and hip. It also does not allow for the calculation of the moments during the swing phase. According to Winter, this method should only be used as a first approximation of the moments at a joint (Winter 1991).

2.7. Strain Gauges

The strain at the ankle is critical to the overall functioning of the coupled monolimb and prosthetic foot. If the stiffness of the foot is too high, the interaction of the foot and the monolimb could potentially result in premature deformation or fracture of the monolimb. When seeking to assist those in developing countries, the CIR would like to ensure the highest life of the monolimb that is possible. For the purposes of this project the strain gauges were used to determine the resultant strains in the monolimb due to the interaction between the monolimb and the prosthetic feet.

Uniaxial strain gauges are used to measure strain in one single axis. The strain gauge has a grid in a single direction. A rosette strain gauge provides the stresses along multiple axes. The equations to transform the strain from the gauge coordinate system to the x, y, x coordinate system are seen in

Figure 28, where ε_x is the strain in the horizontal direction, ε_y is the strain in the vertical direction, and ε_{xy} is the shear strain.

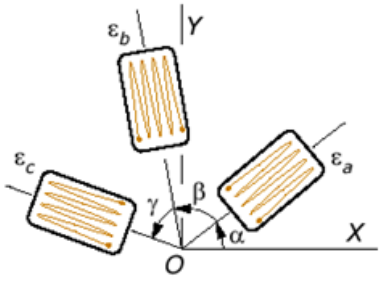

$$\varepsilon_a = \frac{\varepsilon_x + \varepsilon_y}{2} + \frac{\varepsilon_x - \varepsilon_y}{2}\cos 2\alpha + \varepsilon_{xy}\sin 2\alpha$$

$$\varepsilon_b = \frac{\varepsilon_x + \varepsilon_y}{2} + \frac{\varepsilon_x - \varepsilon_y}{2}\cos 2(\alpha+\beta) + \varepsilon_{xy}\sin 2(\alpha+\beta)$$

$$\varepsilon_c = \frac{\varepsilon_x + \varepsilon_y}{2} + \frac{\varepsilon_x - \varepsilon_y}{2}\cos 2(\alpha+\beta+\gamma) + \varepsilon_{xy}\sin 2(\alpha+\beta+\gamma)$$

Figure 28: Rosette Strain Gauge and Applicable Strain Equations (Rosette Strain Gauges 2008)

The 0, 45, 90 rosette strain gauge, also known as the rectangular rosette, is one type of rosettes used to measure strain along multiple axes. The delta rosette is another type, with gauges placed at 60 degree increments. For a 45° strain gauge (Figure 29) where α is 0°, β is 45°, and γ is 45°, the equations are simplified to the following.

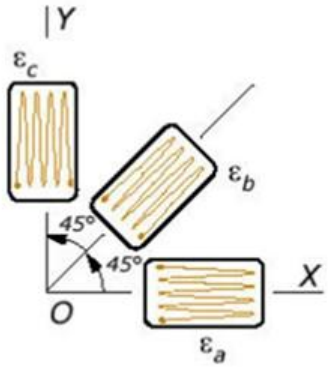

$$\varepsilon_x = \varepsilon_a$$

$$\varepsilon_y = \varepsilon_c$$

$$\varepsilon_{xy} = \varepsilon_b - \frac{\varepsilon_a + \varepsilon_c}{2}$$

Figure 29: Rectangular Rosette Strain Gauge and Strain Equations (Rosette Strain Gauges 2008)

2.8. ISO Standards

There are two standards that outline procedures for testing prosthetic leg and foot systems. These ISO standards were created for prosthetics to ensure that prostheses are adequate and safe for users.

The first is ISO 10328 [Structural testing of lower-limb prostheses]. According to ISO 10328, 'the term prosthetic means an externally applied device used to replace wholly, or in part, an absent or deficient limb segment.' The standards specify testing methods, loading conditions, and other parameters. The

standards in ISO 10328 apply to transtibial, knee-disarticulation, and transfemoral knee prostheses (ISO 10328 1996).

There are three types of testing structures indicated in ISO 10328: complete, partial, and any other structure. This research primarily dealt with the complete structure testing. In preparation for testing, all cosmetic components must be removed if they do not provide structural strength to the device (ISO 10328 1996). The products being tested were fitted normally, further description on this method can be found in the methodology.

The 2006 ISO 22675 [Testing of ankle-foot devices and foot units] standard was used more heavily in the research for this project. This ISO standard discusses the proper procedure for cyclic testing of ankle-foot devices. It reviews the loading conditions that can be used to mimic natural gait loading. In addition to the cyclic loading tests, the ISO 22675 specifies a static test that can be performed on prosthetic ankle-foot devices. It shows appropriate lines of action for the static loading tests (ISO 22675 2006).

During testing the sample must be aligned appropriately being aware of the effective ankle joint centerline, the effective ankle joint center, the effective knee joint centerline, and the effective knee joint center. All tests should be conducted using the standard's outlined worst-case alignment.

Through the use of ISO standards and following proper protocol, one can have a better chance of obtaining valuable results for a wide range of applications. The standards can also ensure safety during testing.

3. Methods

Evaluation of the foot prosthetics was conducted in two partially concurrent phases in order to determine and compare the stiffness of the prosthetic systems and the stresses that occur on the monolimb when coupled with the SACH and SR feet. The first phase was analytical modeling the foot/monolimb assemblies and conducting finite element analysis (FEA). The second phase was the validation of the FEA through the physical testing of the feet.

3.1. Determination of Axes for Prosthetic Components

In order to ensure consistent and comparable measurements and results, it was important to determine the alignment for all of the testing components. The coordinates that were used to describe the alignment were the Cartesian coordinate system with positive Y in the upwards vertical direction, positive X in the right horizontal direction, and Z outwards.

3.1.1. Prosthetic Feet

The alignment for the prosthetic feet was determined using the ISO 22675. The ISO standard indicates that the longitudinal axis of the foot should pass through two identified points. One is located at the center of the widest part of the foot, and the other is located at the center of the ankle region, specifically one quarter of the distance from the posterior of the foot. The centerline is then considered the zero/neutral axis for the alignment of the test setup. Figure 30 shows the ISO 22675 diagram for the determining the central axis for the feet (ISO 22765 2006).

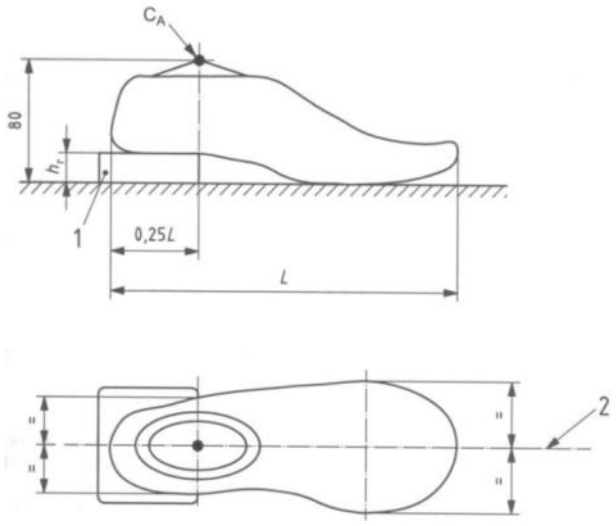

Figure 30: Determining Longitudinal Axis

The ISO 22675 indicates that the prosthetic feet should be placed at an angle of 7˚ outward from the neutral axis that was determined using the methods above (ISO 22765 2006).

Figure 31 gives an example of the calculated longitudinal datum for the SR foot, along with the rotated axis used in the model to align the foot with the monolimb.

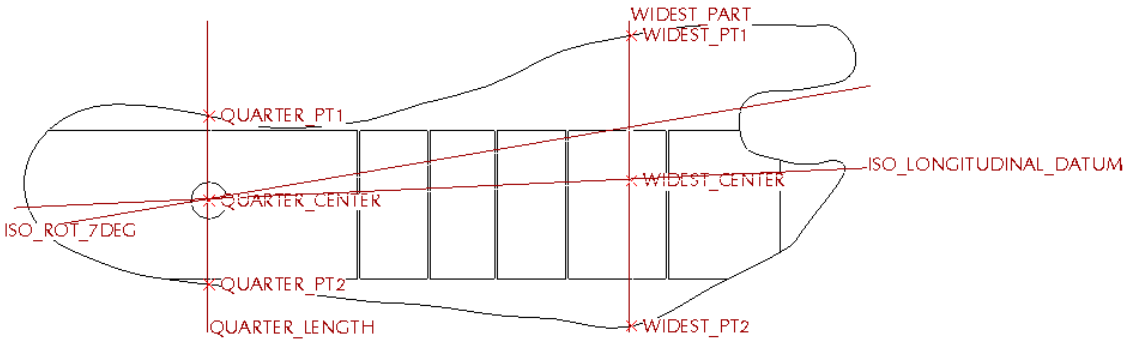

Figure 31: SR Model with Longitudinal Axis

3.1.2. Monolimb

It was important to ensure that during testing the forces applied to the prosthetic assembly occurred along a central axis. Since the monolimb was made in an environment where little precision was taken, the axis was not located in the visual center of the hole of the monolimb. The axis created by the threaded hole through the metal insert was chosen as the axis for the monolimb. The forces for testing would be applied along this axis. To ensure that the forces were applied accordingly it was necessary to determine where that axis was located in reference to the monolimb's top surface.

First, a one meter long M10 threaded rod was inserted into the metal insert and secured it using M10 washers and nuts on either side. The top surface of the monolimb was then milled perpendicular to the rod, and therefore the axis. Next, the top surface of the monolimb was marked at 22.5° intervals, with the center at the center of the threaded rod, staring from one side of the posterior seam and ending just below it (Figure 32).

Figure 32: Marked Monolimb

The distance (D_1) between the inner-wall of the monolimb and the edge of the threaded rod at each mark was measured. The total distance between the central axis of the threaded rod and the inner-wall of the monolimb (D_2) was calculated by adding the radius of the threaded rod (5 mm, 0.197 in) to each value of D_1. The points can be seen in Figure 33.

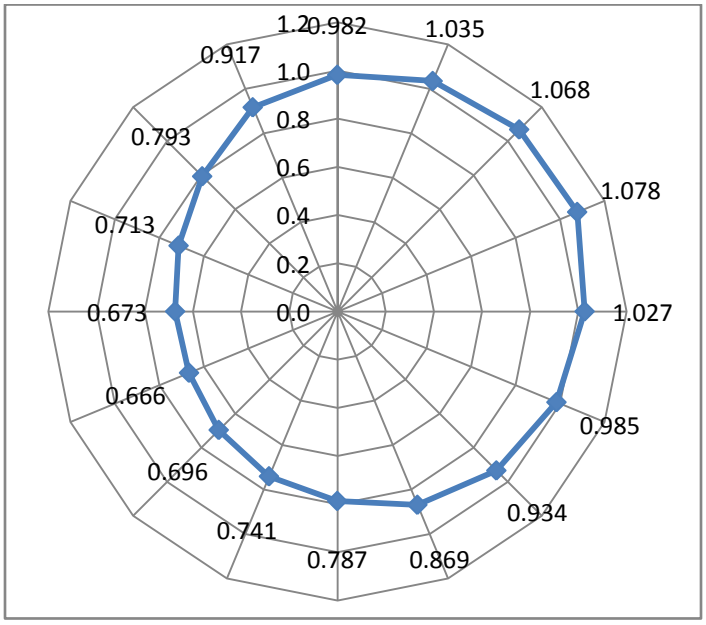

Figure 33: Graph of Monolimb Center (inches)

3.2. CAD Modeling

In order to conduct the finite element analysis, all of the components needed to be modeled. All of the components to be tested were modeled in Pro/Engineer Wildfire 2.0.

3.2.1. SR Foot

The SR foot consists of a polypropylene foot shape with a metal insert inside. Both components were measured using calipers. To obtain the shape of the bottom portion of the foot, a line was drawn

lengthwise through the foot. Points were measured at regular intervals around the outline with respect to a temporary origin (Figure 34). These points, listed in Appendix A, were then input into Pro/Engineer to form the outline of the foot. The outline was then extruded to form the base of the foot, and the bottom edge was rounded.

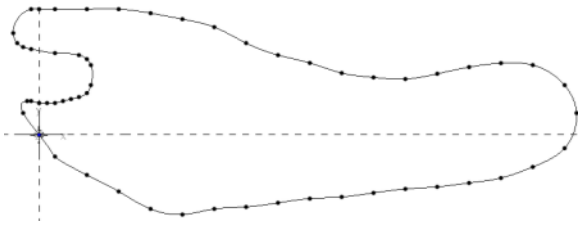

Figure 34: Outline of SR Base

The wedge-like shape was then drawn on a datum plane (DTM1). The shape used datum planes RIGHT and DTM2, which were offset from each other the exact length of the wedge, as end points The wedge was then extruded to form a solid shape, and from the outline of the base an extruded cut trimmed the overhanging sides (Figure 35).

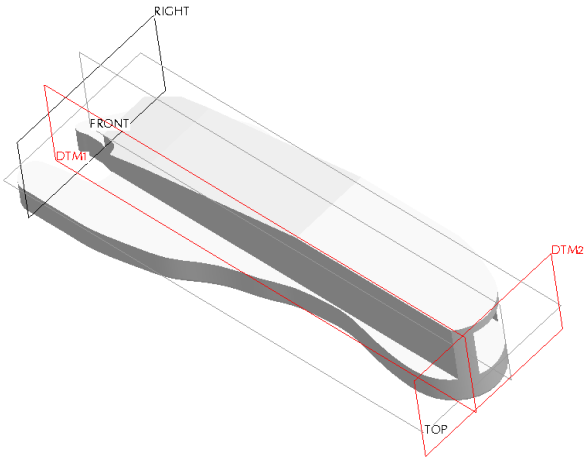

Figure 35: Datums for SR Foot

The inside of the wedge was the then cut through a sketch drawn on DTM2 (Figure 36). Next, the cuts on the top portion of the foot were then extruded at the measured intervals. Finally, the wedge shaped cut at the back of the foot was extruded through. The bolt hole at the top of the foot was placed offset from the upper cut and the side of the top of the wedge, and the larger tool access hole at the bottom of the foot was placed coaxial to it.

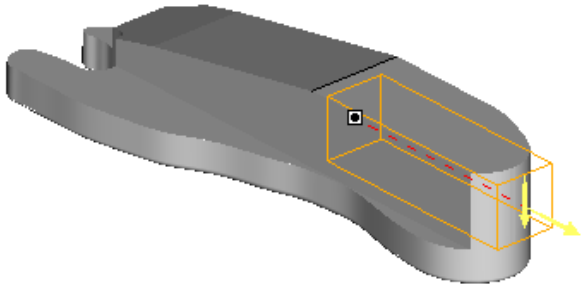

Figure 36: Inside Cut for SR Foot

The insert was first created as a single solid extrusion. The inside material was then removed in a single cut (Figure 37).

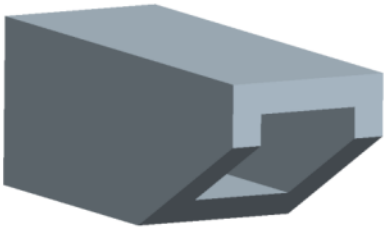

Figure 37: SR Insert

An assembly was created with the insert to ensure that there was no interference between the two parts (Figure 38).

Figure 38: Assembly of SR and Insert

3.2.2. SACH Foot

The SACH foot was more difficult to model due to the complex geometry of the foot. The SACH was modeled as an assembly of two parts, the polypropylene inner keel and polyurethane foam outer cover. The two parts were modeled separately, then assembled together and used to modify the construction of the outer cover.

The inner plastic keel of the SACH was measured using a QC-5000 Metronics Coordinate Measuring Machine (CMM). The points were then used to create spline curves on the outline of the insert (Figure 39). The coordinate system origin for the insert was selected to be the center of the bolt hole.

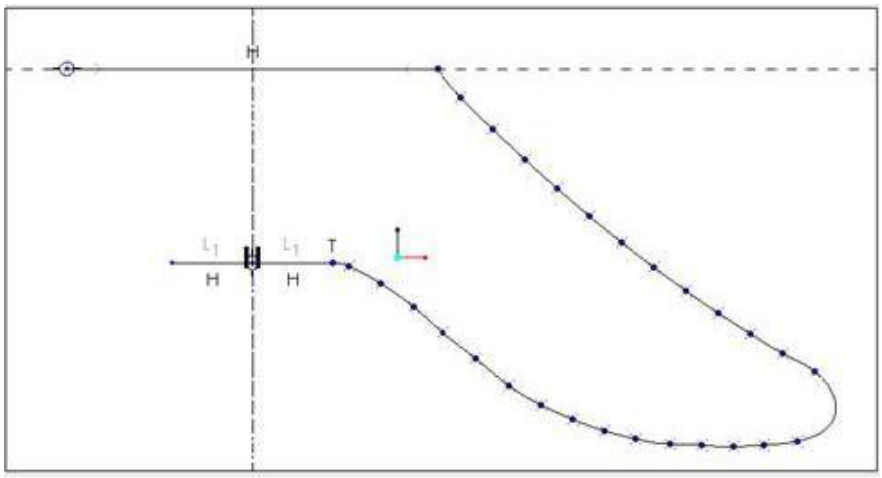

Figure 39: CMM SACH Foot Insert

The spline curves were used to accurately create the spline running down the front of the insert, the top curved surface, and the bottom curved surface. The spline curve and the bottom curved surface curves were used to make the initial extrusion, while the top curved surface curve was used to cut material away (Figure 40).

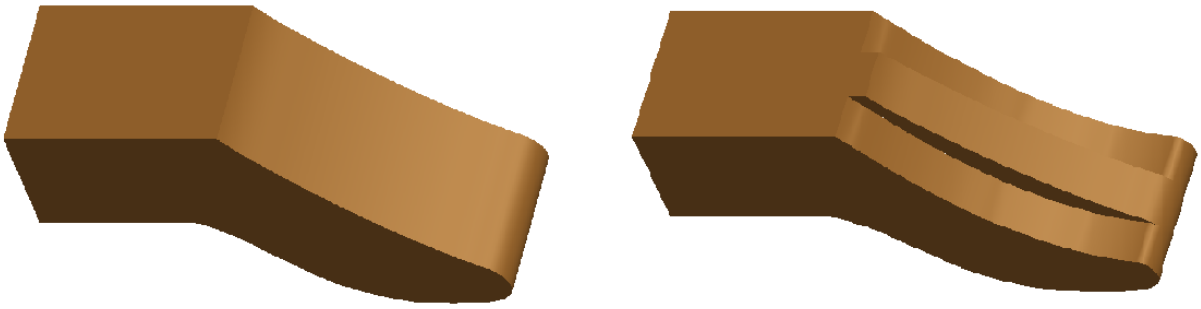

Figure 40: Initial Extrusion and Cut Using Spline Curves

The back of the foot was then cut to create the elliptical surface. From this surface the rear angled cut and support rib could be created. Finally the center hole and the pockets were modeled. The final solid model appears in Figure 41.

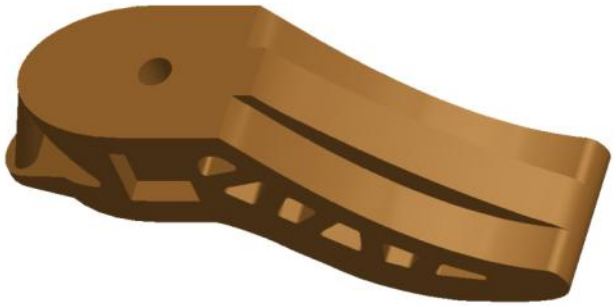

Figure 41: Final Solid Model of SACH Foot Insert

The complex outer SACH foot shell was created using the CMM. Three dimensional points were taken periodically at horizontal planes. These were taken at four parallel planes at 0.6 inch intervals. In addition, points were taken along the seam at the bottom of the SACH and along the top surface of the foot. Fourteen points were taken around each plane. These were saved as separate Excel files. These files were then converted to *.ibl files (IBasic Component Language) and imported into Pro/Engineer as datum points. Closed spline curves were then created through these points. A solid blended surface was then created using a smooth general blend from spline to spline (Figure 42).

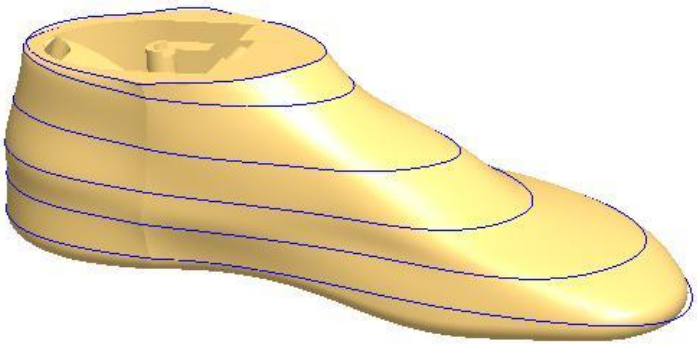

Figure 42: SACH Model with Curves from CMM

The bottom profile of the foot was also measured using the CMM and imported into Pro/Engineer using the same method as the previous spline curves. This sketch was then created from this curve and it was extruded as a cut from the bottom of the foot. The new edge was then rounded.

The SACH insert was then assembled to the SACH foot outer shell, and cut out of the shell (Figure 43). Finally, assembly datum planes were created by making a central axis based on the specifications of ISO 22675 and offsetting a datum plane from it by 7°.

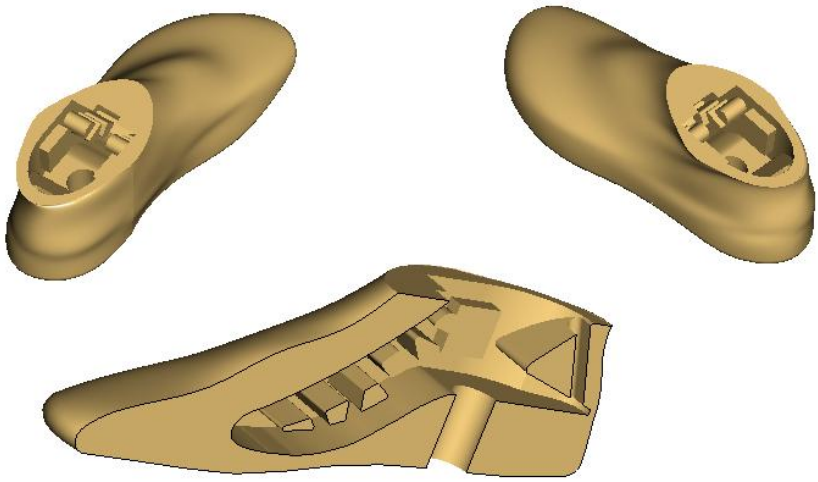

Figure 43: Multiple Views of Complex SACH Model

This model was found to be too complex when loaded into ANSYS and it was not able to mesh the foot. Because of this, a simpler, less refined model was created.

The simplified SACH foot was created using only one set of points taken from the CMM. This set was taken near the base of the foot around the outermost edge. Again the points were imported as an .ibl file and converted into a closed spline curve. This curve was then converted into a sketch and extruded to the height of the foot. A round was then placed on the bottom edge.

The profile of the fore foot was then estimated and cut from the solid model. The sharp edges of the fore foot were then rounded. Finally assembly datum planes were created by making a central axis and offsetting a datum plane from it by 7°. The SACH insert was then assembled and the insert shape was cut out.

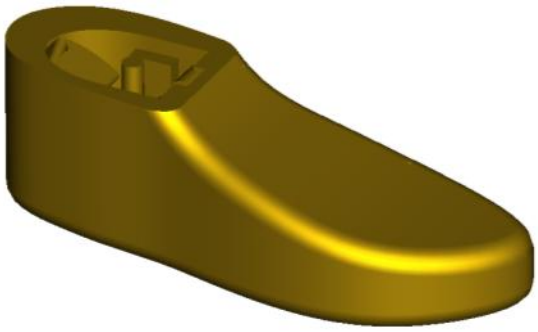

Figure 44: Simplified SACH Foot

3.2.3. Monolimb

The monolimb was measured using calipers. There is variation in the dimensions of the monolimbs created by the CIR, because of the imprecise method of construction. Because of this, the CAD model was created based on the design intent for the monolimb. The dimensions of five monolimbs were measured, identified as monolimbs A through E, and monolimb B was selected to be used for the modeling dimensions, as it had a limited number of imperfections, including variable edge thickness at the bottom and above the metal insert. The model was created to capture design intent. The actual physical monolimb does not have a perfect circular shape, as seen from Figure 33 in the determinaton of the axes. In addition, the posterior seam is not always perpendicular to the monolimb shank, and therefore its plane does not always pass through the center axis of the monlimb.. This variation was eliminated in the model, and the monolimb was modeled as a perfect cylinder with a constant wall thickness. In addition, the posterior seam was modeled to be perpendicular to the shank and aligned with the monolimb center axis.

The monolimb shank consists of a metal insert with plastic molded around it. These two components were modeled separately then joined in an assembly. The metal insert was modeled as a revolved protrusion, creating a short cylinder. The coordinate system origin was placed on the bottom surface, on the center axis, to correspond with the chosen coordinate system. Cuts were then made on either side of the front plane. The top and bottom holes were added last (Figure 45).

Figure 45: CAD Model of Monolimb Insert

The base was created as a revolved protrusion cylinder with two sections. The coordinate system origin was placed on the bottom surface, on the center axis, to correspond with the chosen coordinate system. The upper portion has a smaller diameter than the lower portion, where the metal insert is located. Side cuts were then placed on opposite sides of the monolimb. The monolimb was then shelled to a thickness of 5mm.

The posterior seam was centered on the front plane, since the design intent of the monolimb is to have the posterior seam equidistant from the flat edges of the monolimb and perpendicular to the ground.

It was determined that the most critical round on the monolimb was the bottom round, as it is in contact with the foot. Other rounds, including the ones between the posterior seam and cylinder, and around the side cuts, are formed only as a result of the manufacturing process and are not critical to the model (Figure 46).

Figure 46: CAD Model of Monolimb

An assembly of the monolimb and insert was built in order to ensure that there was no interference between the monolimb and insert. The insert was mated to the bottom inside surface of the monolimb and aligned with the assembly front plane. This meant that the flat edges of the monolimb and insert were aligned. Since interference did occur, the interfering material was cut from the monolimb.

3.3. Coefficient of Friction

In the physical testing, all of the feet were pressed against a 1/8" thick aluminum surface to limit surface deformation during testing. To have the CAD model accurately reflect the behavior of the physical testing, the coefficient of friction (μ) between each prosthetic foot and the aluminum board was determined experimentally through a slip test. Each prosthetic foot was placed on an aluminum that was later affixed to the angle blocks during the experimental testing. The plate was then tilted upward in five degree increments until the foot began to slip. The plate was moved at approximately 5° per second between increments and held for three seconds at each increment for this rough estimate. The

test was accurate within one degree. The test was rerun, starting 10° below the estimated slip angle and held at increasing one degree increments, in order to establish the angle of the plate when slipping occurs to the nearest angle. The plate was moved at one degree per second between increments for this more precise estimate. Five trials for each foot were run, in order to find the average angle of slippage. From this angle the coefficient of friction was then be estimated using the relationship $\mu = \tan(\theta)$.

The feet were each tested and the gathered results can be found in Table 2. The raw data for these tests can be found in Appendix D.

	ICRC SACH	SR
Toe Down μ	0.49	0.32
Heel Down μ	0.39	0.28

Table 2: Coefficient of Friction Results

3.4.Finite Element Analysis

ANSYS Workbench was chosen as the FEA software package because of its ability to accept a 3D computer aided design (CAD) model and assembly of high complexity. The program also allows for the accurate placement of angled pressures and loads, in addition to the modeling of contact surfaces and large deflection.

In the finite element analysis, the element type was chosen based on the geometry of the prosthetic foot, the information available to input, and the results that are to be extracted. Each element type has different available degrees of freedom, real constants, material properties, allowance of surface and body loads, and other special features (ANSYS). This analysis required element types that have three degrees of freedom, can undergo potentially large deflections, and model contact forces. Previous FEA studies of prosthetics have used tetrahedral elements, including a previous study on the monolimb (Kim, 6) and one on a SACH foot (Saunders, et al. 80). For this study 10 node 3D tetrahedral elements, SOLID187, were used as the solid elements.

3.4.1. Simple Test Case

Before the complex model of the assembly was analyzed, simple test cases were used to select the proper analysis methods and choices including element type, contact element type, and supports. For these tests a SR foot was used. The assembly was created with each part modeled with simple

geometries (Figure 47). For example, the monolimb was modeled as a cylinder. The configurations of toe-off and midstance were used for these initial test setups.

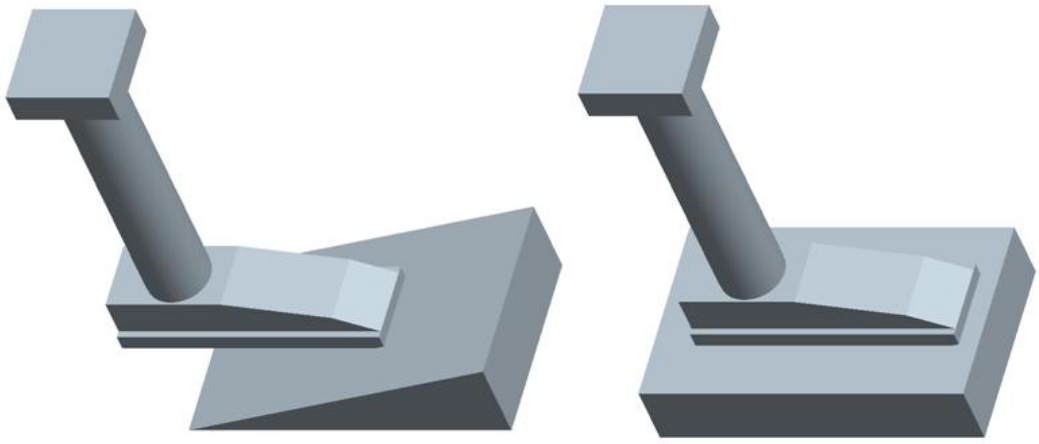

Figure 47: Toe-off and Midstance Simple Geometry Assemblies

Each assembly configuration was modeled using the contact properties seen in Table 3. The first part is the contact surface while the second part is the target surface.

No Separation	Bonded	Frictional
SR to Monolimb	SR to Bolt	SR to Lower Block
SR to Insert	SR Insert to Bolt	
Monolimb to Monolimb Insert	Monolimb Insert to Bolt	
	Monolimb to Top Block	

Table 3: Contact Properties Between Surfaces

The No Separation contact was selected for the parts that were able to move relative to each other, but would remain touching the entire time. The Bonded contact was selected for all contacts with the bolt, since in actuality the bolt would be secured with Loctite® and therefore unable to move relative to the other parts. It was also selected for the upper block, as it is only used to apply the force to the monolimb. The frictional contact, with a coefficient of friction of 0.4, was selected for the connection between the foot and lower block, since in reality there would be frictional forces between the foot and lower block. This coefficient of friction was chosen from the initial testing to determine the coefficient of friction between the SR foot and the metal plate.

It was important to ensure that the model created in ANSYS would behave similarly to the actual prosthetic setup. To confirm this, theoretical calculations using the basic equations for stress and strain

were completed to determine the approximate total axial deformation that would occur in the midstance setup under a compressive 1300N load (Appendix C).

The resulting calculated change in length was 0.311 mm. An analysis was run on the midstance setup with a compressive pressure on the top block of 1300N divided by the area of the attached block. The resulting deformation in the vertical direction can be seen in Figure 48. The total deformation was 0.288 mm, giving a percent difference of 8%. This error could be a result of the approximations made in the hand calculations. It could also be a result of the insertion of the metal inserts and bolt in the FEA model, and the interaction between the contact surfaces of the parts, which were not included in the hand calculations.

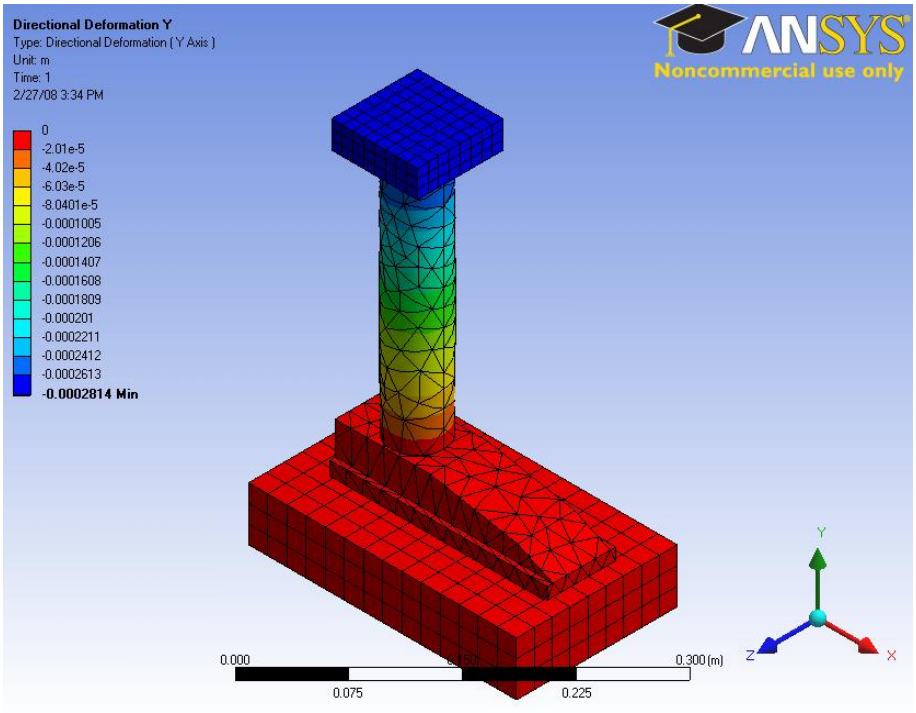

Figure 48: Y Directional Deformation in Midstance Assembly

3.4.2. Meshing of SR Foot

In the modeling of SR foot, the standard tetrahedral elements were used. The contact surfaces in Table 4 were defined. The connections between the majority of parts were bonded, in order to allow the model to solve. The connection between the contact portion of the foot and the block was frictional, with a value of 0.3, determined as an average from friction testing, as seen in Table 2 of the determination of the coefficent of friction. A rough connection was created between the bottom

surface of the foot and the base to allow pontential contact as the load was applied (Figure 49). A rough contact allows for gaps to occur between contact surfaces. This was important for the contact surfaces between the bottom of the foot and ground block, between the cut surfaces of the heel, and between the cuts on the forefoot, as these surfaces are either in partial contact or have no contact initially and after the applied load.

Bonded	Frictional	Rough
SR to Monolimb	Heel/Toe Contact Area to Lower Block	Bottom Foot Potential Contact Area
SR to Insert		Toe Cuts
Monolimb to Monolimb Insert		Heel Cut
SR to Bolt		
SR Insert to Bolt		
Monolimb Insert to Bolt		
Monolimb to Top Block		

Table 4: SR Contact Surfaces

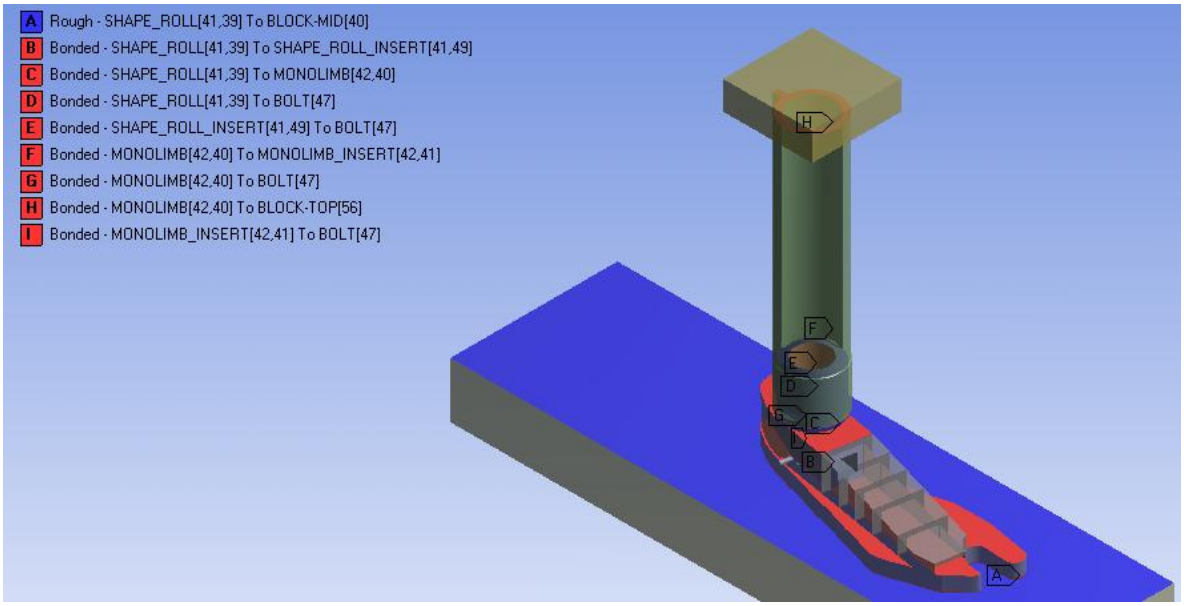

Figure 49: SR Contact Surfaces

For the toe-off and heel-strike positions, special contact surfaces were placed on the foot. In toe-off (Figure 50), contact surfaces were placed between the cuts on the top of the foot, to allow these surfaces to bend towards each other and touch. For the heel-strike position (Figure 51), contact surfaces were defined between the top and bottom portions of the heel cut, to allow the cut to touch during loading.

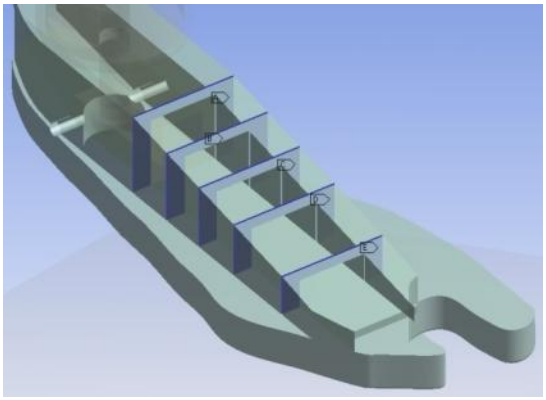

Figure 50: Toe Cut Contact Surfaces

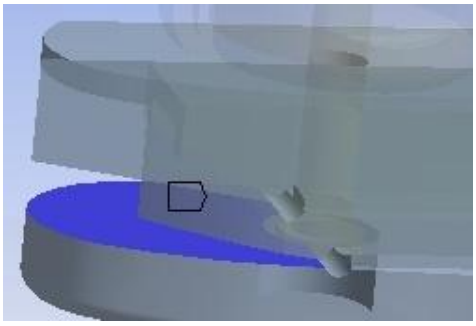

Figure 51: Heel Cut Contact Surfaces

The automatic size control was used to mesh the three models (Figure 52), with refined meshing occurring at key areas such as the bottom of the SR foot and around the heel cut (Figure 53).

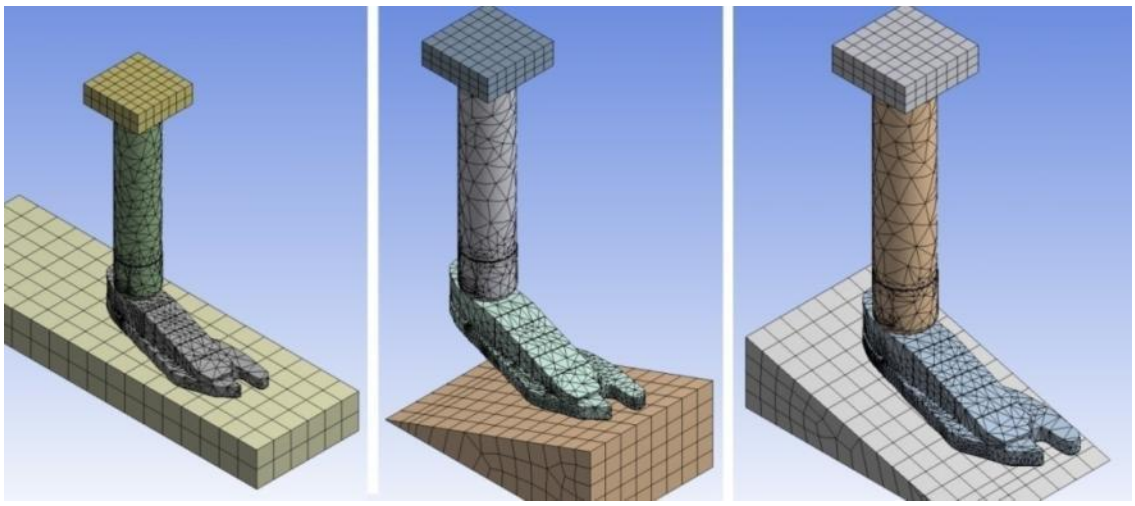

Figure 52: Meshed SR Foot Models

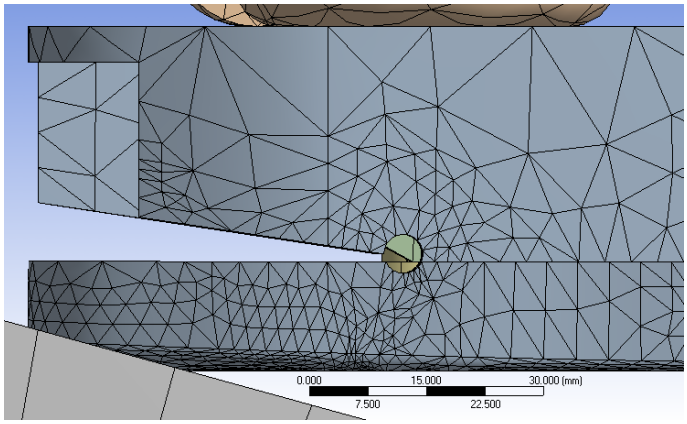

Figure 53: Refined Mesh at SR Heel

3.4.3. Meshing of SACH Foot

For the SACH foot, the initial accurate CAD model of the foot was not able to be meshed because of the complex spline surfaces. The simplifed SACH model was used for the FEA instead. In the modeling of SACH foot, the standard tetrahedral elements were used. The contact surfaces in Table 5 were defined. The connections between the majority of parts was bonded, in order to allow the model to solve. The connection between the contact portion of the foot and the block was frictional, with a value of 0.3, determined as an average from friction testing, as seen in Table 2 in the determination of the coefficent of friction. A rough connection was created between the bottom surface of the foot to allow pontential contact as the load was applied (Figure 54).

Bonded	Frictional	Rough
SACH Insert to Monolimb	Heel/Toe Contact Area to Lower Block	Bottom Foot Potential Contact Area
SACH Outside to SACH Insert		
Monolimb to Monolimb Insert		
SACH Insert to Bolt		
Monolimb Insert to Bolt		
Monolimb to Top Block		

Table 5: SACH Contact Surfaces

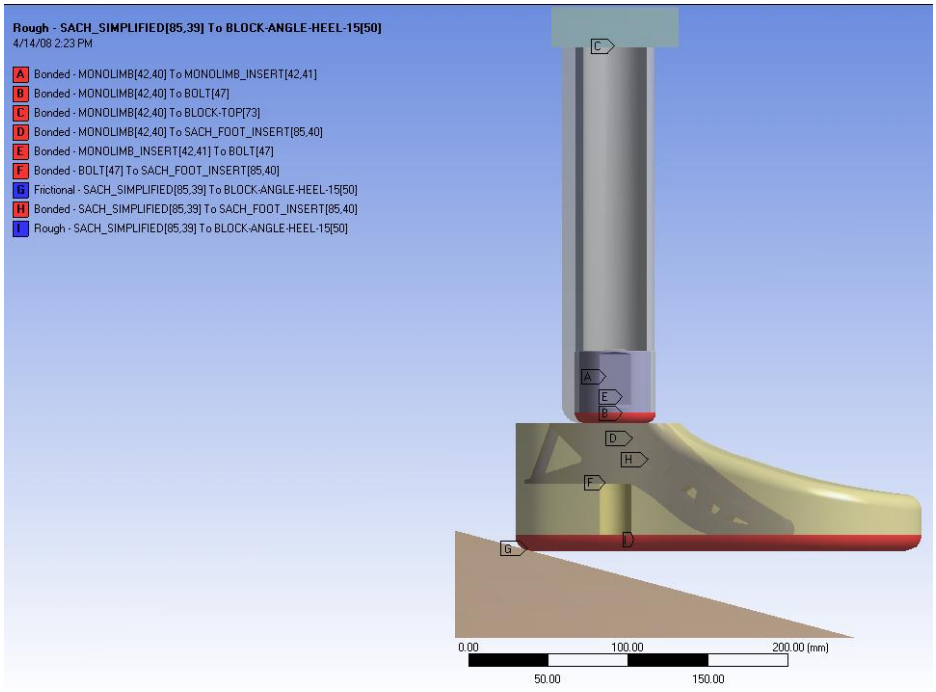

Figure 54: SACH Contact Surfaces

The automatic size control was used to mesh the heel-strike and toe-off orientations (Figure 55), with refined meshing at the bottom of the foot.

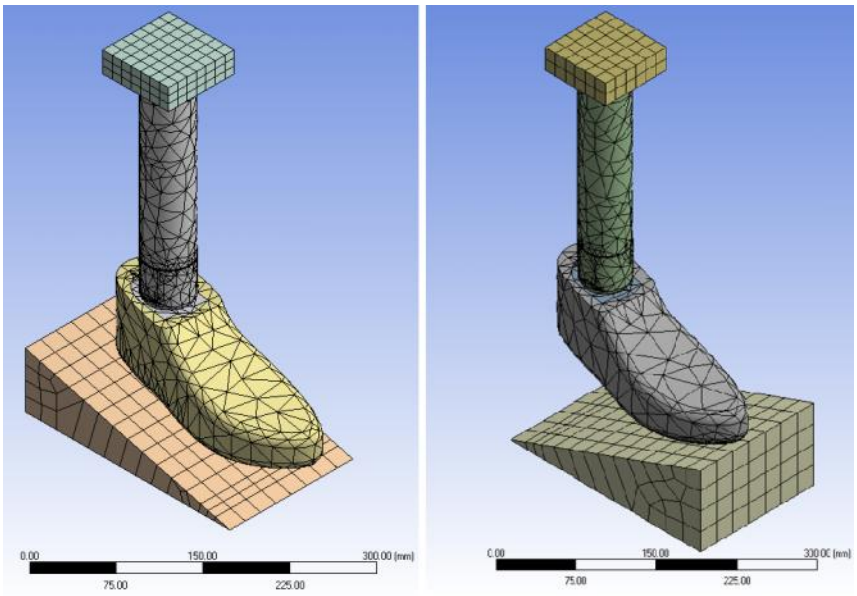

Figure 55: Meshed SACH Foot Models

3.4.4. Model Constraints

Each foot in each orientation had the same constraints and loads applied (Figure 56). The bottom surface of the block was selected as a fixed surface. The top block connected to the monolimb was constrained to no movement in the X and Z directions. Lastly, a vertical force of 1300N was applied to the monolimb. To accomplish this, a pressure of 2.03MPa was evenly applied to the top of the 0.08m x 0.08m block.

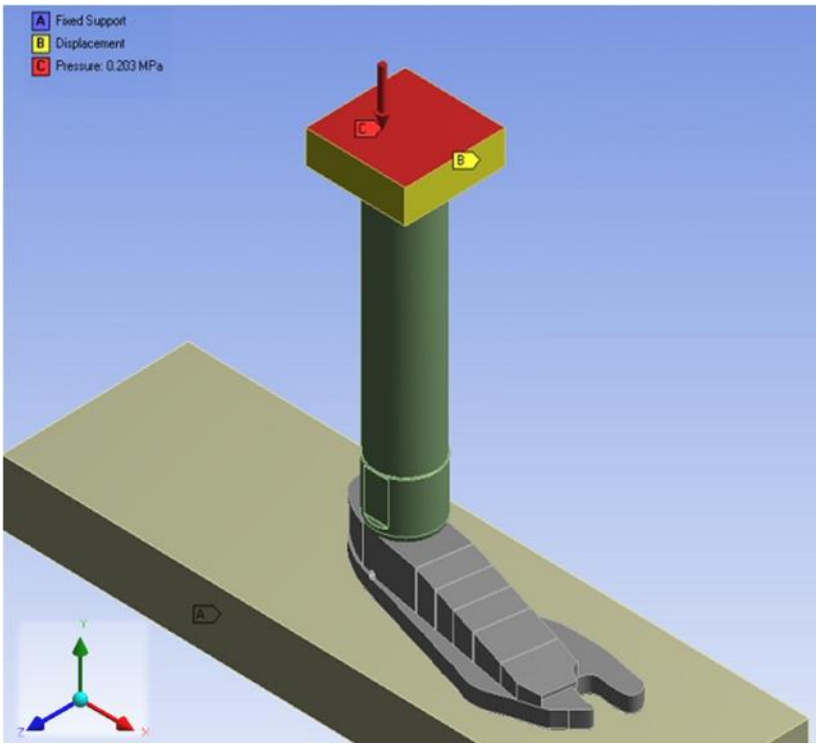

Figure 56: FEA Model Constraints and Loads

3.5.Physical Testing

Physical testing was performed to use as a method of comparison for finite element analysis. There are many components to the physical testing that was performed. The alignment of the test setup, the foot orientations, strain gages are all explained along with the BlueHill programming software for the testing, force application, data collection and analysis.

3.5.1. Alignment

The testing of the prosthetic feet took place on an Instron 5544. A coordinate system was set up at the initial ankle position of the monolimb-prosthetic foot system. The origin was located in the center of the ankle joint (Figure 57).

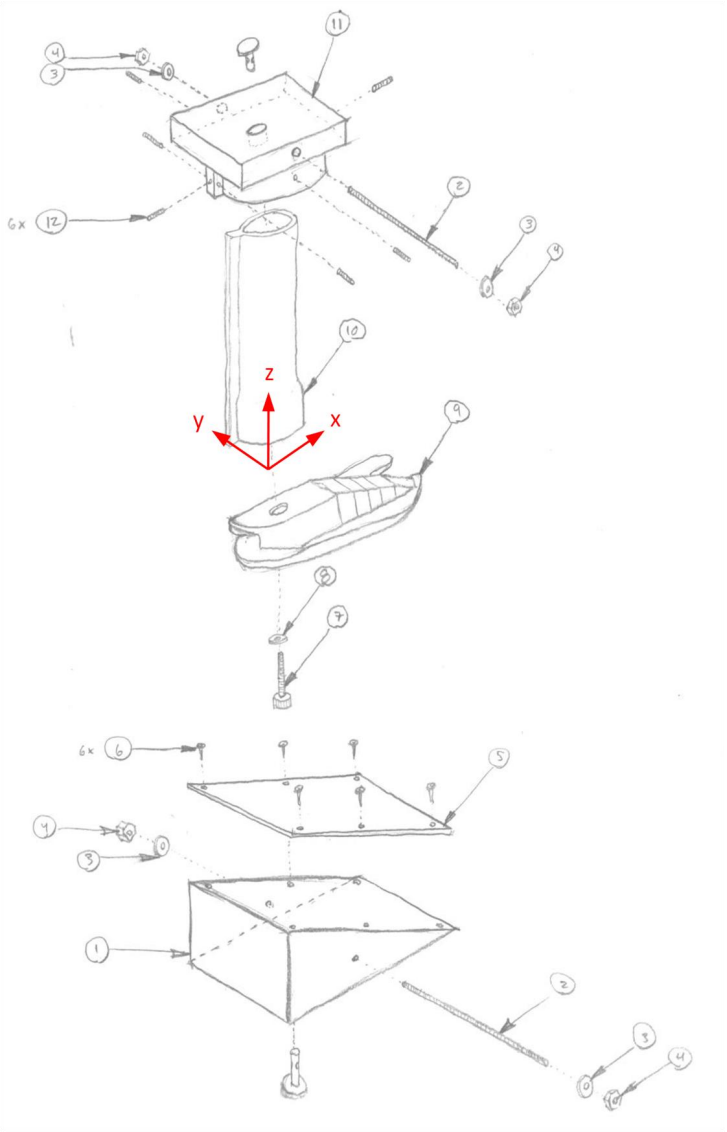

Figure 57: Test Setup with Coordinate System

In order to connect the monolimb to the Instron compression testing machine, a custom adaptor was required. This aluminum adaptor was designed so that the force was transmitted through the center axis of the monolimb as determined previously. The top of the adaptor was designed to fit around the circular protrusion at the top connection point of the Instron machine, and it was secured with a dowel pin that was inserted though the adaptor and machine protrusion. The bottom of the adaptor was designed to fit snugly inside the top of the monolimb, with set screws used to secure the monolimb in place. The monolimb profile was determined previously, and the points were used to design the bottom face of the adaptor. The final design can be seen in Figure 58, with the red dashed line showing the axis of alignment.

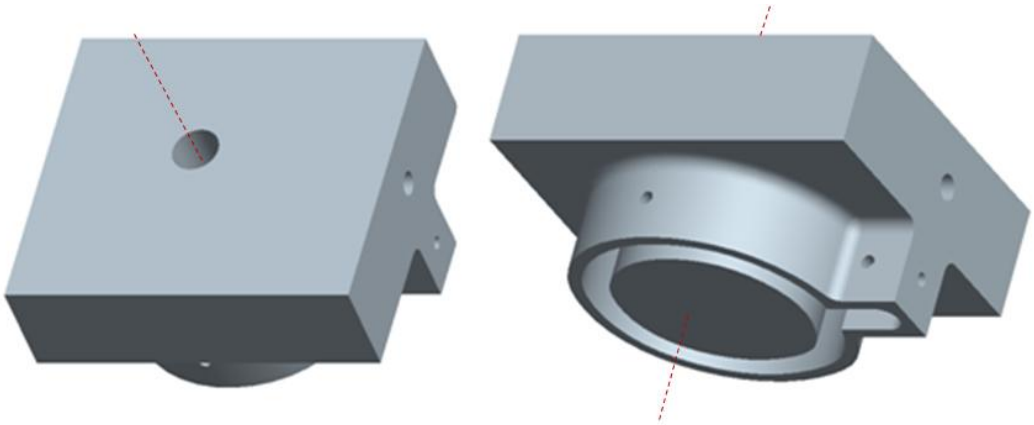

Figure 58: Instron to Monolimb Connection Adaptor

3.5.2. Foot Orientations

Testing of the prosthetic feet was conducted at three orientations. The first position was the heel-strike that occurs during initial contact, henceforth referred to as heel-strike. This was accomplished in the physical testing through the use of a 15° angle block made out of wood with a 1/8" thick aluminum surface to limit surface deformation during testing. The aluminum surfaces were affixed by six nails attached to the sides of the angle block as to not interfere with the contact surface where the feet were tested. The second position was midstance, where the foot is flat on a level 1/8" piece of aluminum. The last position was pre-swing, where the majority of the weight is on the toe before the swing phase, henceforth referred to as toe-off. This required the use of a 20° angle block also with an aluminum surface mounted to the surface (Figure 59). These blocks were attached to the base of the Instron 5544 with a rod that was inserted through the center of the angle block and connection cylinder on the Instron machine.

Figure 59: Toe-off Angle Block

During the physical testing, pressure paper was placed between the foot and the angle block, as described in the next section. It was attached using tape lined up against a mark on the block. This position was determined when the final test set-up was established in the lab. This ensured that each piece of pressure paper is attached at the same spot in relation to the coordinate system.

3.5.3. Strain Gauges

In order to measure the strain that occurs on monolimb, strain gauges were attached to the monolimb shank. The strain gauges (Figure 60) were a uniaxial gauge mounted to the posterior seam and a rectangular rosette strain gauge mounted to the anterior of the monolimb. Both of the gauges were located on the outside of the monolimb, directly above the metal insert. These locations were chosen because the CIR indicated them as a critical region for failure. Failure was seen above the metal insert in a case study performed on an active 185lb male (personal communication, Cassanova, Feb 21, 2008).

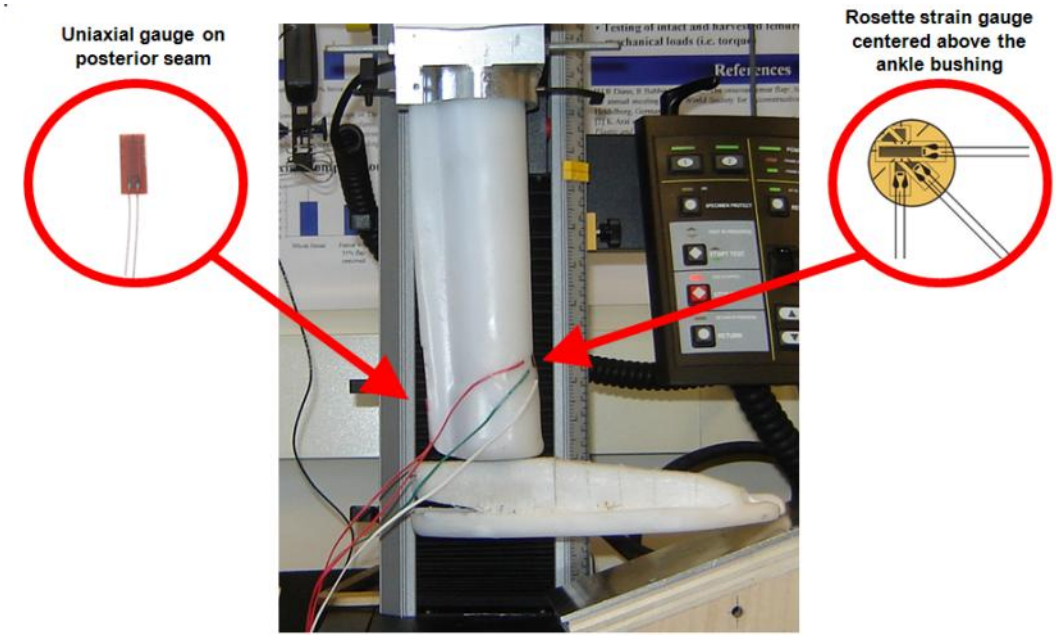

Figure 60: Strain Gauge Placement on Physical Test Setup

The rectangular rosette gauge was selected since the principal axes of the strains are not known for the monolimb. The rectangular rosette strain gauge was selected because it is easier to determine the directions of the principal strains when compared to a delta rosette. The rosette gauge so that a gauge was located horizontal (0°), 45°, and vertical (90°).

The strain gauges and the mounting surface on the ankle portion of the monolimb were prepped for testing using a fine grade polishing paper and then applying alcohol to the surface to remove any oils or fingerprints that may be on the surface. The strain gauges were then applied with super glue.

3.5.4. BlueHill Software

The testing for this project was run through the use of the BlueHill software. The BlueHill program allows for load and timing input to be read from the screw driven compression apparatus of the Instron machine (Figure 62).

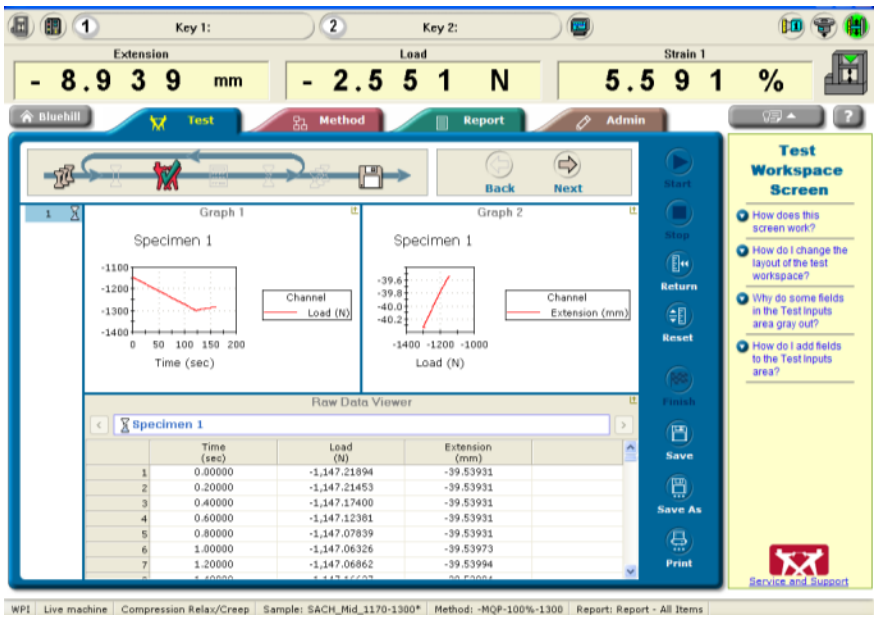

Figure 61: BlueHill Program Sample Screenshot

BlueHill is ideal for this test because it allows for the user to generate a custom test based upon the loading, materials, and timing required for each experiment (BlueHill 2007). For the purposes of this study, only compression tests were used. Ten separate BlueHill files were created to apply the forces for the physical testing. Specifically, the individual tests were 0-130N, 130-260N, 260-390N, 390-520N, 520-650N, 650-780N, 780-910N, 910-1040N, 1040-1170N, and 1170-1300N. After running one file, the test held the force so that the data from the strain gauges could be recorded. Time, force, and extension were automatically read from the BlueHill program and recorded to Excel.

3.5.5. Compression Testing Machine

For the testing of the prosthetic feet coupled with the monolimb, the Instron 5544 compression/tension machine was used (Figure 62). The Instron 5544 is capable of applying 2000N of force, where the

testing for this project only required a maximum of 1300N. Since the test required only about one foot of vertical test space, the forty-two inches of available space with the Instron machine easily met the needs of the experiment. The machine is capable of ± 0.5% load accuracy and has a precision accuracy of ±0.02mm.

Figure 62: Instron 5544

3.5.6. Force Application

The prosthetic foot and monolimb were attached to the top grip location of the Instron machine. To begin, a baseline measurement was taken at 10N of force which allowed for the initial compression of the gaps in the assembly. The force was applied to the monolimb/foot setup at 75N/min. The force was applied to the levels indicted in Table 6. The position was then held for 45 seconds while the strain gauge data was manually recorded from the P-3500.

Test #	Percent Total Loading	Force Applied (N)	Pressure Paper?
1	10%	130	*
2	20%	260	
3	30%	390	
4	40%	520	
5	50%	650	*
6	60%	780	
7	70%	910	
8	80%	1040	
9	90%	1170	
10	100%	1300	*

Table 6: Test Procedure

Each test shown in Table 6 was performed twice for each foot in each orientation. The first test run included the use of pressure paper while the second test was just the force application. The same alignment was used, so that the data gathered from the pressure paper and any realignment was carried

through each test. The purpose of the pressure paper was to determine if there were any loading irregularities or pressure distributions that were not expected. The pressure paper that was needed was predetermined by predicting the expected contact area and force relationship. The table of these predictions can be found in Appendix E.

The asterisks on the table indicate the tests where the pressure paper was used. The 130N force was applied, the load arm was lifted and the pressure paper was removed and read. In the event of any discrepancies, like spotting or other unexpected loading, the alignment of the assembly was modified and the test was rerun. Once there were no issues with the pressure paper, a new paper was mounted and the foot was reloaded and the force was applied to 50% as indicated in the table, the tests were run to each 10% increment and strain gauge data were recorded. The paper was checked again at 50% and if there were no errors, a new paper was inserted and the test was run at 10% increments of force up to 1300N.

3.5.7. Data Collection

Figure 63: SB-10 Switch & Balance Unit and P-3500 Digital Strain Indicator

Data were collected using the uniaxial and rosette strain gauges as seen in Figure 60. The strain gauge data were read using Vishay's SB-10 Switch & Balance Unit and Vishay's Model P-3500 Digital Strain Indicator. The SB-10 Switch & Balance Unit is designed to provide a method of reading the output of ten strain gauges on a single strain indicator. For the purposes of this test, only four strain gauges were used, each in a quarter bridge configuration. The strains were read on the P-3500 which is a portable battery powered strain gauge reader.

3.5.8. Data Analysis

The loading and displacement were recorded from the physical testing and were compared with the FEA along with the posterior uniaxial, anterior 90˚, and anterior 0˚ strain values. The principal strains were calculated using the rosette strain 0, 45, and 90˚ gauges. The stiffness of the foot-monolimb system, *k*, was calculated from the displacement of the Instron arm. This displacement is measured from the center of the Instron arm and was set to zero when the load equaled 10N in compression. This was done to compensate for any movement in the test setup. The vertical displacement of the top surface of the top block from the neutral zero force position to final deformed position in the FEA model was also recorded. The equation $k = F/d$ was used to calculate this stiffness, where *k* is stiffness, *F* is the force applied, and *d* is the displacement.

4. Results

From the physical testing and FEA models, data were collected regarding the strain on the monolimb and the compression of the prosthetic assembly. In addition, information collected from the FEA included the principal stresses on the monolimb and the von Mises stresses.

4.1.Physical Results

The physical testing that was performed was directed at establishing the reactions that the monolimb displayed when under the specified loading conditions. Each foot and monolimb combination was loaded as indicated in the methodology. The uniaxial gauge located on the posterior seam of the monolimb, and three strain gauges of the rosette were read and recorded. The data from these tests are compared in the analysis section of this report. Values may be seen in Appendix E.

4.1.1. Heel-strike

During the heel-strike test for the assembly with the SR foot was stopped at a load of 910N because plastic deformation began to occur near the heel of the foot. This deformation is shown as a bright white spot on the foot indicated with the arrow in Figure 64a. The foot did not undergo fracture. The SACH foot assembly was run to the full 1300N loading (Figure 64b).

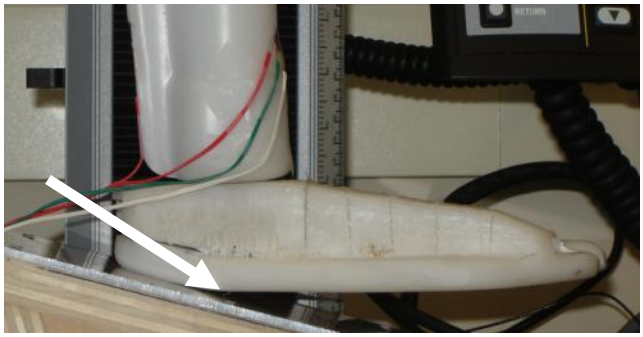

(a)

(b)

Figure 64: Heel-strike End Loading (SR, 910N; SACH 1300N)

The results from the heel-strike testing of both the SR and SACH foot assemblies are shown in Figure 65. Data collected from uniaxial strain gauges are labeled as “Uniaxial” while data collected from the rosette strain gauges is labeled by the angle of the corresponding strain gauge. The 0° gauge was horizontal while the 90° gauge was vertical. Each point represents the averaged value of two tests.

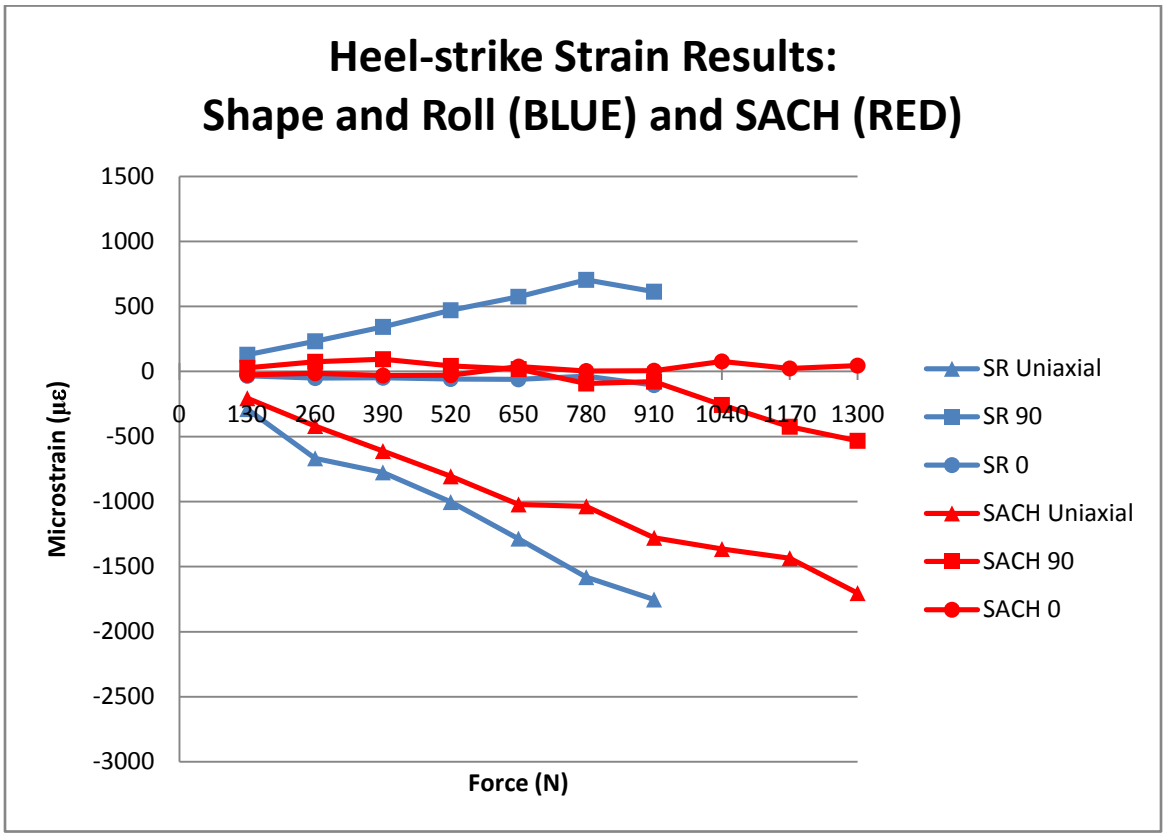

Figure 65: Heel-strike Strain Results

The foot loading was distributed as seen in Figure 66 on the pressure paper. There were not any concerns with the loading distribution.

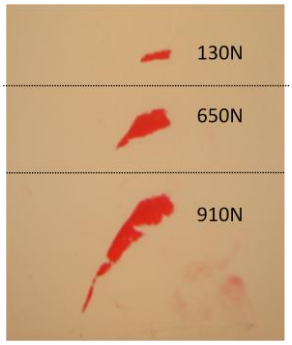

Figure 66: Top View of Pressure Paper Results from SR Heel-strike Test

4.1.2. Midstance

The results from the midstance testing of both the SR and SACH feet are shown in Figure 67. Data collected from uniaxial strain gauges are labeled as "Uniaxial" while data collected from the rosette strain gauges are labeled by the angle of the corresponding strain gauge. Each point represents the averaged value of two tests.

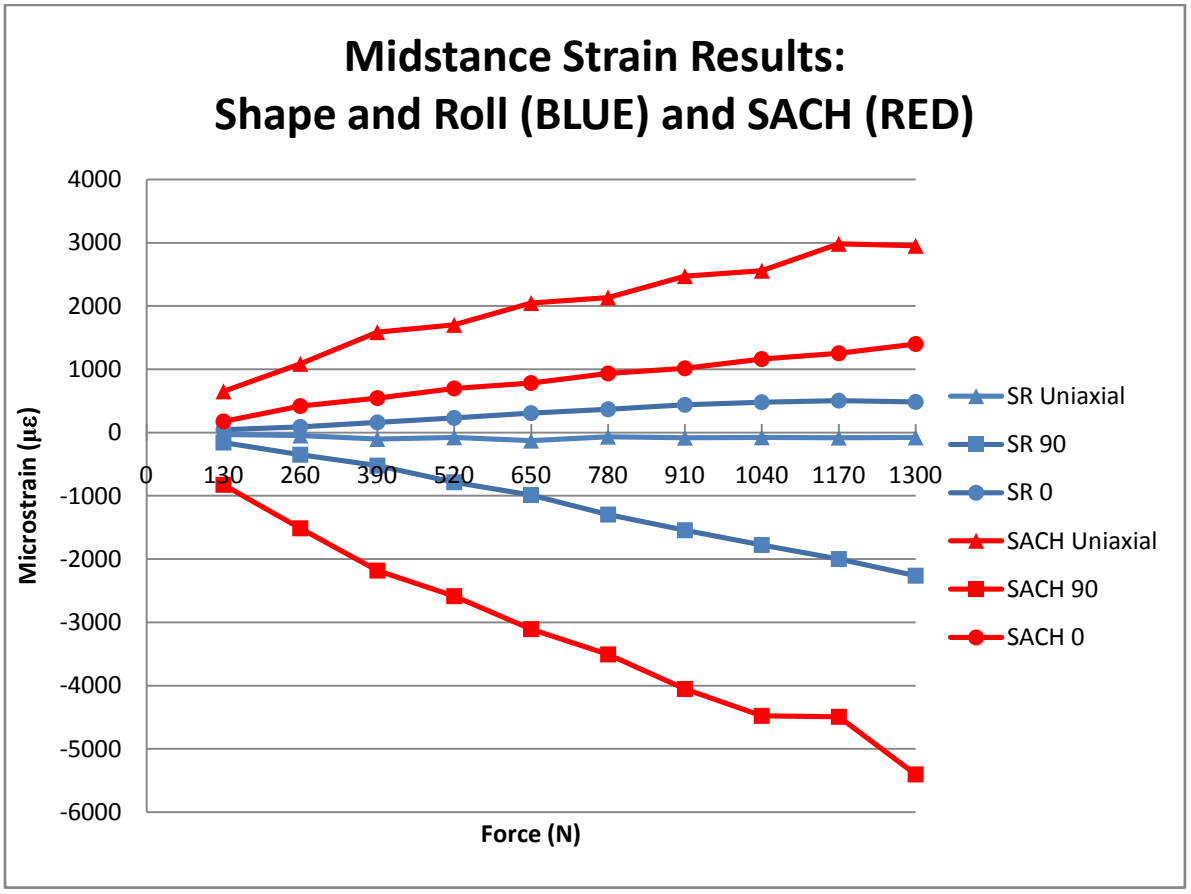

Figure 67: Midstance Strain Results

4.1.3. Toe-off

The toe-off test for the SR foot assembly was stopped at 520N because the test setup was creating a torsional force on the Instron machine that could have been detrimental to the test setup (Figure 68b). The SACH foot assembly test was stopped at 910N for the same reason (Figure 68a).

(a)

(b)

Figure 68: Toe-off End Loading (SR, 520 N; SACH, 910)

The results from the Toe-off testing of both the SR and SACH feet are shown in Figure 69. Data collected from uniaxial strain gauges are labeled as "Uniaxial" while data collected from the rosette strain gauges are labeled by the angle of the corresponding strain gauge. Each point represents the averaged value of two tests.

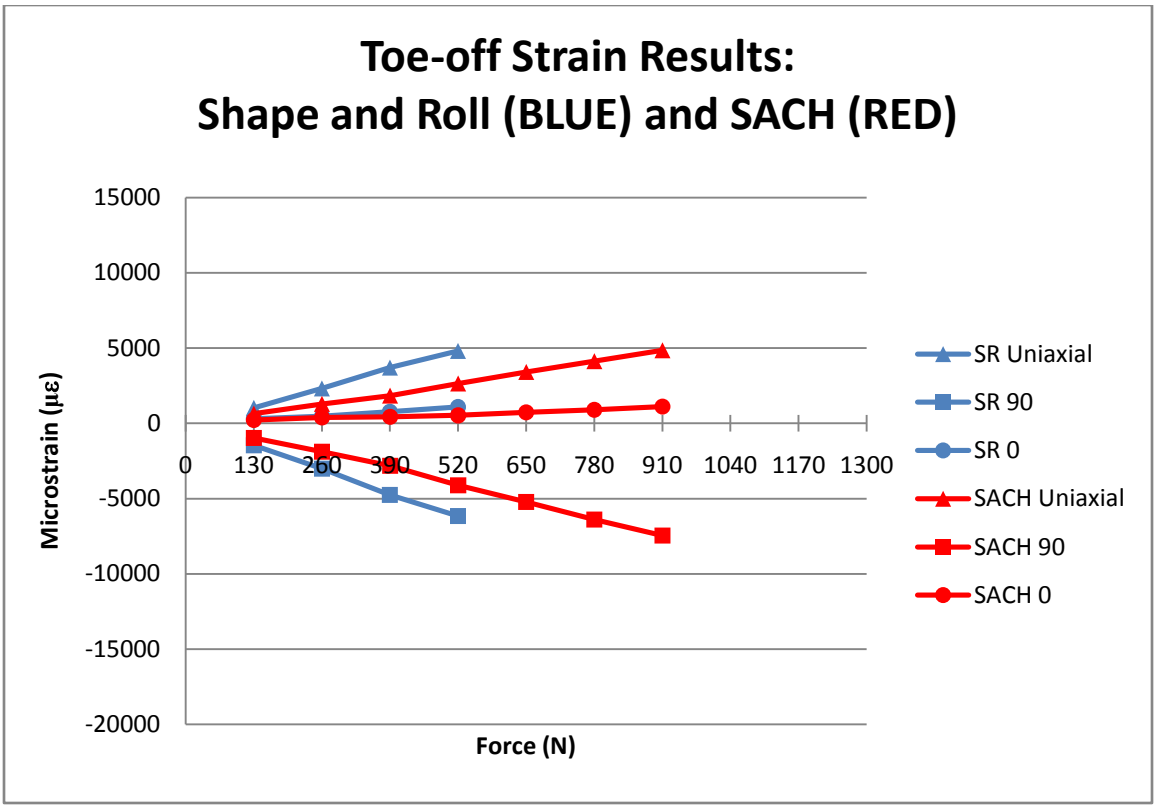

Figure 69: Toe-off Strain Results

The foot loading was distributed as seen in Figure 70 and Figure 71 on the pressure paper. There were not any concerns with the loading distribution.

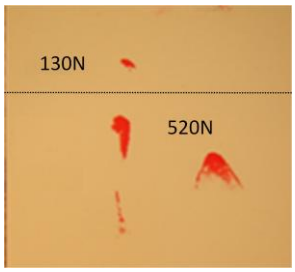

Figure 70: Top View of Pressure Paper Results from SR Toe-off Test

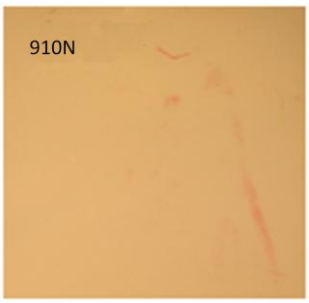

Figure 71: Top View of Pressure Paper Results from SACH Test Toe-off Test

A summary of the strain data at the maximum loading applied for each test from the physical testing is shown in Table 7.

Table 7: Strain Data from Physical for Comparison

		Load (N)	Posterior Uniaxial Strain (με)	Anterior Uniaxial Strain (με)	Anterior Horizontal Strain (με)
SR	***Heel-strike***	910	-2542	942	-95
	Midstance	1300	-80	-2262	463
	Toe-off	520	14780	-15567	5052
SACH	***Heel-strike***	1300	-1538	-362	178
	Midstance	1300	2942	-5403	1397
	Toe-off	910	5896	-10690	317

4.1.4. Compression Results

The displacement of the Instron arm, from the starting position at a loading of 10N to the final loading condition was recorded. The total compression for each test found in Appendix F. Table 8 shows the average of two trials of vertical displacement of the top arm of the Instron from 10N to position to final position at the given loading.

Table 8: Compression from Physical Testing

		Loading (N)	Compression (mm)
SACH	***Heel-strike***	1300	22.60
	Toe-off	910	41.62
SR	***Heel-strike***	910	10.79
	Toe-off	520	33.86

The tests were stopped at different final loading conditions. it was shown that under heel strike, the SACH foot assembly deformed more than the SACH foot assembly. At 910N (where the SR assembly test was stopped) the assembly with the SR and SACH compressed in magnitude by 10.79mm and 18.08mm respectively, thus showing that the SACH foot assembly deformed almost 7mm more than the SR.

4.2.FEA Results

FEA was performed at the maximum loading of 1300N to compare to the physical testing. The FEA testing showed the following results for the SR foot assembly and the SACH foot assembly. The data points were called out on the FEA at the specific sites of the strain gauge application on the FEA for each experimental test that was run, specifically the SR assembly at heel-strike, midstance, and toe-off, and the SACH assembly at heel-strike and toe-off (Table 9). For each model, ten points were sampled within a circular 10 mm in diameter located 10 mm above the metal insert. The data are further explained and compared in the analysis section of the report. The FEA screenshots of the models can be found in Appendix G.

Table 9: Strain Data from FEA

		Posterior Vertical Strain (με)	Anterior Vertical Strain (με)	Anterior Horizontal Strain (με)
SR	***Heel-strike***	-2550 to -2650	650 to 990	-240 to -420
	Midstance	-280 to -350	-1550 to -1580	80 to 85
	Toe-off	7300 to 7600	-9300 to -11000	2700 to 3600
SACH	***Heel-strike***	-0.0009	-0.0012 to -0.0013	0.0006
	Toe-off	6400 to 6800	-7800 to -8850	2900 to 3400

The von Mises stresses were also extracted from the FEA models, and the resulting images can be found in Appendix G. The von Mises stress (Figure 72) will be important for the analysis of the monolimb and the feet. The von Mises stress is an indicator of failure. It is an index that combines the three principal stresses of the material. Although the material may not indicate failure based on the principal stresses alone, the von Mises stress can show how these principal stresses combined can potentially cause a failure in the material. For analysis the von Mises stress is compared to the tensile yield strength of the material (Engineer's Edge 2008).

$$\sigma_v = \sqrt{\frac{(\sigma_1 - \sigma_2)^2 + (\sigma_2 - \sigma_3)^2 + (\sigma_1 - \sigma_3)^2}{2}}$$

where $\sigma_1, \sigma_2, \sigma_3$ are principal stresses.

Figure 72: von Mises Stress (Engineer's Edge 2008)

The compression of the entire prosthetic assembly was also extracted. Table 10 shows a summary of the vertical displacement of the top surface of the top block from the neutral zero force position to final deformed position in the FEA model.

Table 10: Total Prosthetic Compression

		Compression (mm)
Shape & Roll	***Heel-strike***	7.40
	Midstance	0.253
	Toe-off	21.33
SACH	***Heel-strike***	14.90
	Toe-off	19.43

5. Analysis

After gathering the data from the physical tests and FEA, the data were analyzed and compared in order to draw conclusions about the interaction of the SR foot and the SACH foot with CIR's monolimb. The strain data collected from the physical testing were compared to the data computed using FEA. The FEA results were then used to determine the stresses on the monolimb and their effects. The observed behavior of the SR heel during the physical testing was very similar to the observed behavior of the FEA model, while the SACH model did not exhibit the same behavior during physical testing as the FEA model.

5.1.Strains on the Monolimb

The physical testing indicated that the strain produced on the monolimb by the SR foot was higher under the same loading conditions as compared to the SACH foot (Figure 73 and Figure 74). This comparison can be seen in the blue lines of the SR uniaxial and 90˚ rosette strain gauge readings as compared to the red lines of the SACH uniaxial and 90˚ rosette strain gauge readings.

The extended trend lines of the physical data, shown as dotted lines, represent the predicted values for the strains at higher loading conditions. These trend lines were calculated using a regression analysis to fit a first order polynomial to the measured data points, averaged from the two trials. These equations were used to calculate the expected values at higher loading conditions. These trend lines may be inaccurate due to the fact that the relationship between strain and loading will not be linear if the monolimb undergoes any plastic deformation.

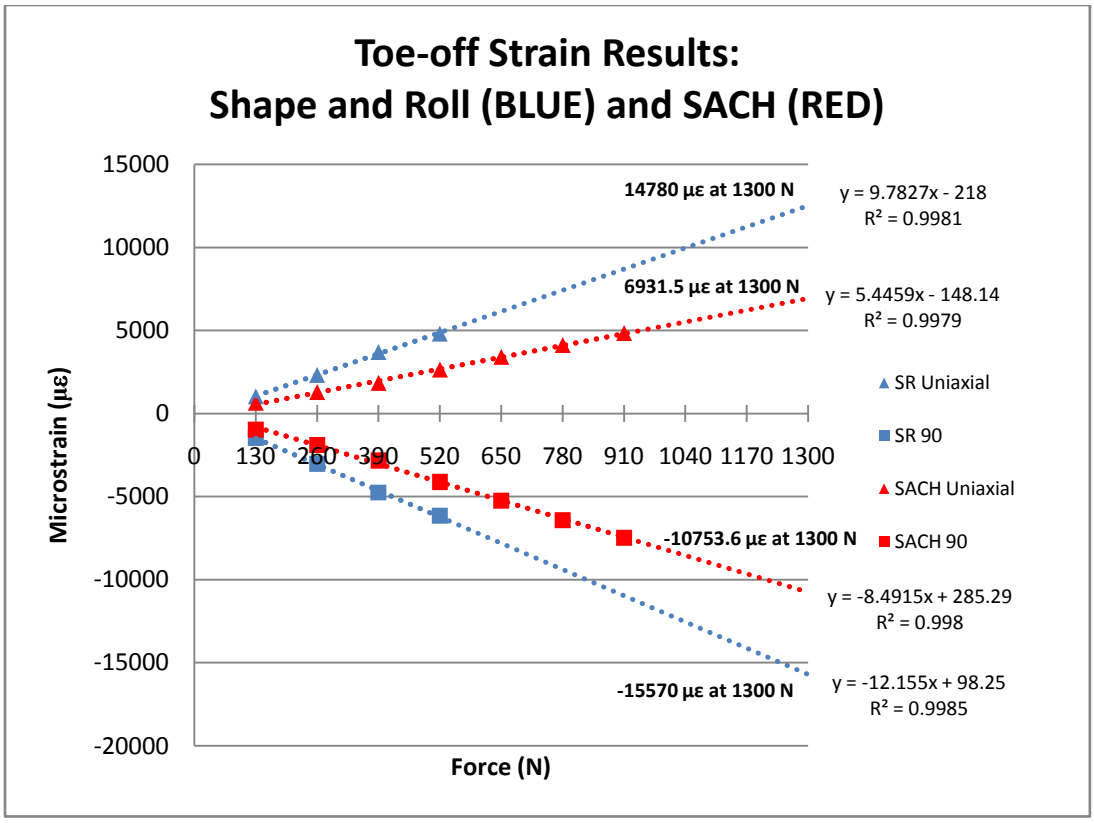

Figure 73: Toe-off Strain Results

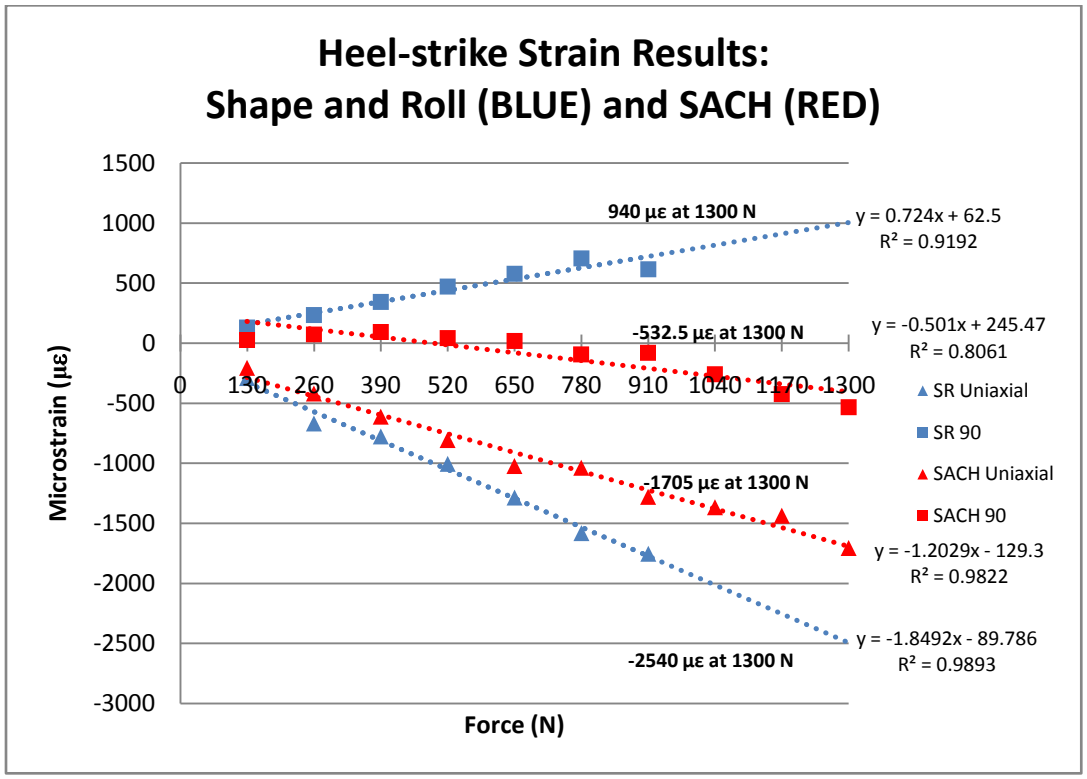

Figure 74: Heel-strike Strain Results

The extrapolated points were compared to the values from the FEA at 1300N. The strain data from the FEA appears in Table 11. The table shows that the data from the FEA was approximately equal to the physical data and actually very comparable for the heel-strike. The values calculated from the extrapolated physical test data for the heel-strike uniaxial gauge was 940 με as compared to the FEA value range of 650 με to 990 με. The values calculated from the extrapolated physical test data of the 90˚ rosette strain gauge mounted to the anterior of the monolimb showed a predicted value of -2540 με as compared to the value of -2550 to -2650 με.

Table 11: Comparison of Strains from Physical Tests and FEA

		Posterior Vertical Strain (με)		Anterior Vertical Strain (με)		Anterior Horizontal Strain (με)	
		FEA	**Physical**	**FEA**	**Physical**	**FEA**	**Physical**
SR	***Heel-strike***	-2550 to -2650	-2542*	650 to 990	942*	-240 to -420	-95*
	Midstance	-280 to -350	-80	-1550 to -1580	-2262	80 to 85	463
	Toe-off	7300 to 7600	14780*	-9300 to -11000	-15567*	2700 to 3600	5052*
SACH	***Heel-strike***	-0.0009	-1538	-0.0012 to -0.0013	-362	0.0006	178
	Toe-off	6400 to 6900	5896*	-7800 to -8850	-10690*	2900 to 3400	317*

** Values linearly interpolated from test data*

Due to the correlation of the data between the physical strain data and the calculated FEA strains, the FEA models for the SR were accepted to be an accurate model of the behavior of the prosthetic assembly. There were some varying values, but this could be due to experimental error. The strain values from the FEA on the monolimb coupled with the SACH foot for heel-strike were much less than the strains actually exhibited in the physical testing. This difference could be attributed to the simplified SACH model that was used for the FEA.

5.2.Stiffness of Prosthetics

The CIR was concerned that the SR foot would cause more strain on the monolimb than the SACH foot because it is stiffer than the SACH foot. Stiffness (k) is defined as the force applied over the displacement, or $k = F/d$. Rearranging this equation gives $F = kd$. This means that for two objects, at the same applied force, the stiffer object will deform less than the other. A comparison of the compression

of the foot and monolimb combinations can allow for comparison of the stiffness of the feet. This is because all of the components in the assembly were the same in each case, except the foot that was coupled with the monolimb. Table 12 contains a summary of the final compression values for the FEA and physical testing.

Table 12: Total Prosthetic Compression for FEA and Physical Testing

		Compression (mm)	
		FEA	**Physical**
Shape & Roll	***Heel-strike***	7.40 at 1300N	10.8 at 910N
	Toe-off	21.33 at 1300N	33.9 at 520N
SACH	***Heel-strike***	14.90 at 1300N	22.6 at 1300N
	Toe-off	19.43 at 1300N	41.6 at 910N

The displacements for the physical testing were greater than the FEA results, even though the physical tests with the SR at heel-strike and toe-off and with the SACH at toe-off stopped at a lower loading level. In addition, the compression of the assembly with the SR foot was always less than the compression of the assembly with the SACH foot. Since a smaller deflection means a stiffer assembly, the SR foot assembly can be considered stiffer than the SACH foot assembly.

5.3.Stresses On Monolimb

From the FEA, the maximum and minimum principal stresses that occurred throughout monolimb with the full 1300N load were extracted (Appendix G). The principal stresses on the monolimb were found to be lower than the tensile yield strength, 30 MPa, and compressive yield strength, 50 MPa, of the polypropylene copolymer. The stresses apparent at the top of the monolimb were neglected because the bonding of the steel top block to the monolimb is not how the monolimb is attached to a body. The actual monolimb's shank is attached to the socket of the prosthetic that attaches to a person's leg.

Because the forces applied to the prosthetic assembly are not just uniaxial, the von Mises stresses on the monolimb are important to consider, in addition to the principal stresses. The failure criterion for von Mises stress is the tensile yield strength, which is 30 MPa. The von Mises stresses on the monolimb shank for both the SACH (Figure 75) and SR foot (Figure 76) are under this limit. The von Mises stresses (Figure 72) on the monolimb are higher during toe-off than during heel-strike, but the highest value, approximately 20 MPa, is still less than the tensile yield strength.

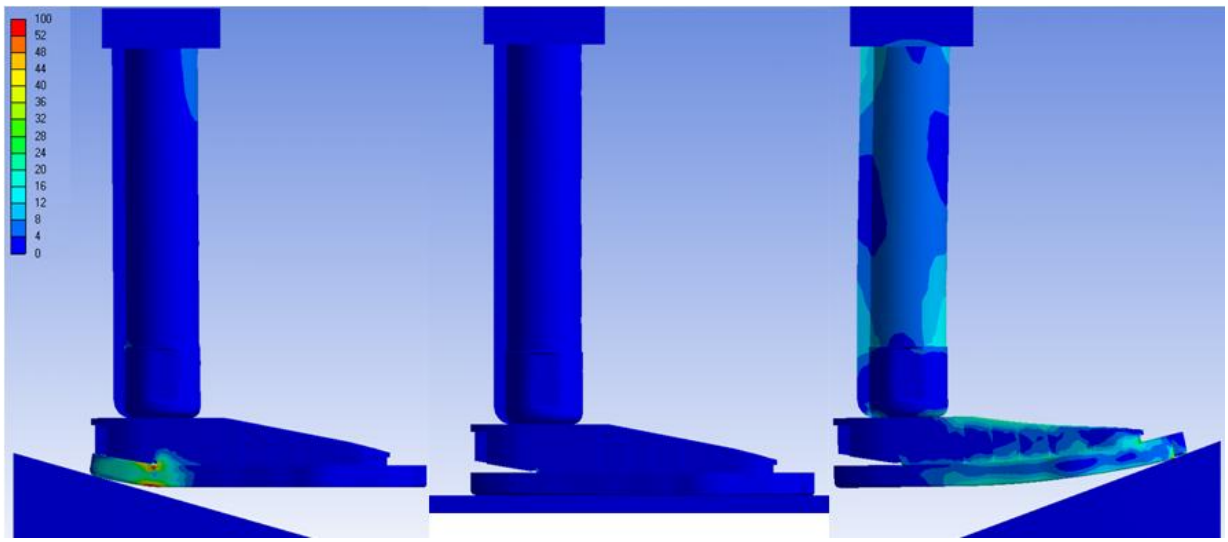

Figure 75: von Mises Stresses with SR for Heel-strike, Midstance, and Toe-off (scale in MPa)

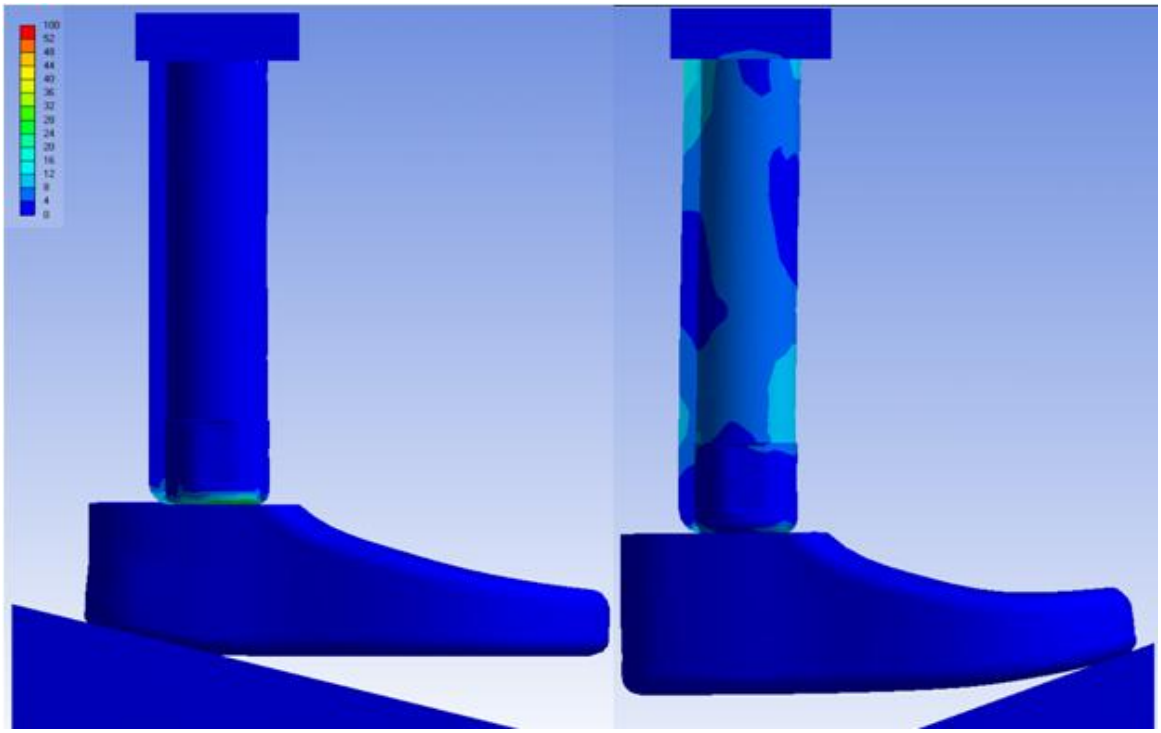

Figure 76: von Mises Stresses with SACH for Heel-strike and Toe-off (scale in MPa)

5.4.Deformation of SR Heel

During physical testing, the SR foot deformed at the heel in the heel-strike orientation (Figure 77). This picture shows the SR heel at 910N, with the circled region containing the area where white markings appeared.

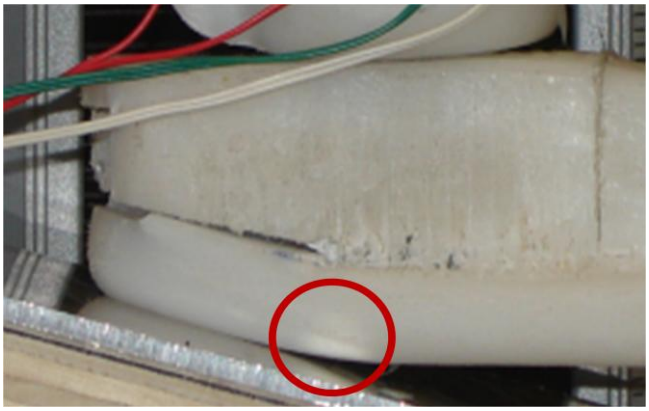

Figure 77: Deformation at SR Heel

This area is similar to the areas that exhibited high stresses in the FEA study on the SR foot at 1300N. The von Mises stresses around the cut and bottom surface of the foot (Figure 78) are above the tensile yield strength of polypropylene, 30MPa. The von Mises stress at the bottom surface is double the yield strength, while the cut area has a maximum three times the yield strength. Since these values are above the tensile yield strength, the material will fail and deform plastically at the 1300N loading.

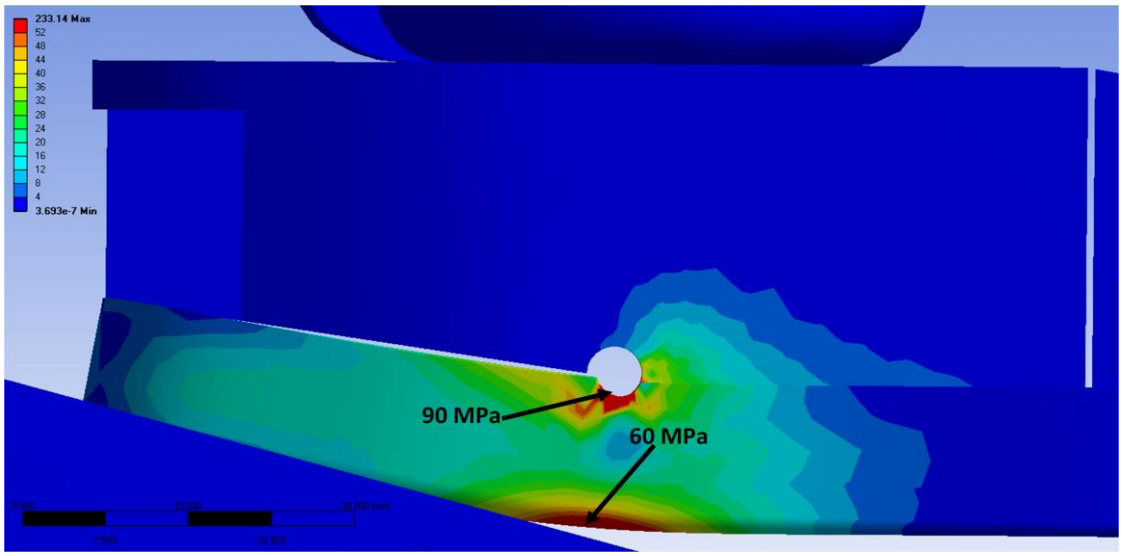

Figure 78: Von Mises Stress at SR Heel During Heel-Strike

The foot began to show deformation marks at 910N, which is 70% of the 1300N applied to the FEA. This suggests that at 910N, the von Mises stresses were near 70% of the stresses seen at 1300N. At 1300N the von Mises stresses at the bottom surface of the heel were 60 MPa, so at 910N the stresses were approximately 40 MPa. That is well over the tensile yield strength of polypropylene, and it can be assumed that the foot was deforming plastically at that point.

6. Discussion

The goal of this study was to investigate the interaction of the monolimb coupled with the SACH and SR under static loading conditions. The study compared the physical testing of the monolimb-foot assemblies to FEA models under the same conditions. Using the results and analysis, conclusions were made regarding the acceptability of the SR foot coupled with the monolimb. Suggestions were also given for future testing and design changes to the SR foot.

6.1. Comparison of FEA and Physical Testing

The physical testing results of the prosthetic assemblies were compared to the FEA models. This was done in order to provide evidence that the FEA model was an accurate representation of the behavior of the prosthetics. The strains on the monolimb and total compression of the prosthetics were used to compare the accuracy of the FEA for each assembly.

The SR assembly heel-strike FEA model when loaded to 1300N showed strains which closely correlated with the strains seen during physical testing when the data were extrapolated. The physical tests were stopped at 910N when the test setup showed influence of large moments and plastic deformation of the SR foot. FEA results for midstance and toe-off generally had similar magnitudes of strain when compared to the extrapolated physical test data.

For the SACH foot assembly, a midstance FEA model was not created due to time constraints. The strain values for the FEA heel-strike were nearly zero compared to the values seen in the physical testing, while the FEA strain for toe-off was of a similar magnitude to the physical testing. Since there was a large difference between the FEA and physical testing strains for the assembly connected to the simplified model of the SACH at heel-strike, the corresponding FEA model was considered to not accurately reflect the behavior of the assembly.

A comparison of the total compression of the prosthetic assemblies during physical testing and FEA was to be used as a criterion for determining if the FEA model was accurate. The amount that the prosthetic assembly compressed during the physical testing was consistently much greater than what was seen in the FEA, potentially due to identified errors discussed in the following section, so the amount of assembly compression was not used to determine if the FEA model was accurate. The compression of the prosthetic assembly from the physical testing shows that the SR foot compresses approximately 7mm less than the SACH assembly in the heel-strike orientation, thus making it stiffer than the SACH assembly.

5.2. Potential Errors in Study

The results from the physical testing and FEA have highlighted areas that could be improved for future studies, in order to reduce the error. The physical testing setup was seen have multiple areas in which displacement could occur separate from the prosthetic assembly. The tolerances of the holes in the adaptor and the angle blocks may have led to some overall inaccuracies in the compression measurements that were seen in the physical testing. The hole of the aluminum adaptor that fit over the Instron shaft was one or two millimeters too large, allowing for some slight rotation. To compensate for this, extension was measured from a load of 10N, to allow for the rotation to occur prior to recording. This load may not have been large enough, as shifting could have occurred during the test. Therefore we would recommend that tighter tolerances be held in the manufacturing of test fixtures. In addition, the wooden angle blocks were surfaced with a thin aluminum plate, which may have deflected at the higher loading levels. Future testing should use a plate of at least a ¼ inch thick, to prevent this deflection.

Potential errors in the strain measurements could have come from the recording method. Since the strain data were recorded by hand, there may be some human error in the recordings; therefore it would be valuable to use LabView with National Instruments data acquisition hardware. Using such data recording methods would allow future researchers to export data in real time to Excel spreadsheets, rather than holding the prosthetics at each load and switching between each strain gauge to record them. This could provide more information regarding the behavior of the monolimb as a load is applied.

The errors that affected the FEA results were mainly associated with the SACH foot. The intricate CAD model of the SACH outer cover that was constructed was unable to mesh in ANSYS because of the complex spline curves created from the CMM. The simple SACH CAD model was not as accurately dimensioned, due to time constraints, and the differences might have affected the behavior of the model. In addition, the SACH outer cover was modeled as only one material. Future SACH models should include the two materials that make up the outer SACH cover. The modulus of elasticity used for the current study was found using simple weights and measurements of deformation. More accurate material properties could provide a more accurate model of the SACH foot behavior.

6.3. Feet Acceptability

The strains above the metal insert in the monolimb were recorded on the posterior and anterior sides, as this was a location that marks had appeared during field testing with the SR foot. In the physical testing it was seen that the magnitudes of the strains were consistently higher on the monolimb with the SR than with the SACH foot. Higher strains are an indication of higher stresses occurring on the monolimb. Therefore it was important to confirm that the monolimb was able to withstand the stresses that would occur with the SR. It was seen from the FEA models that the principal stresses were less than the yield strength of polypropylene.

Because the monolimb is potentially loaded in a complex manner, the von Mises failure criteria were used to ensure that the monolimb could withstand the stresses. The von Mises stresses were found to be less than the tensile yield strength, leading to the conclusion that the monolimb, coupled with the SR foot, can withstand the 1300N loading at the three orientations evaluated. However as noted, it appears that the SR foot itself would exhibit plastic deformation at heel-strike.

6.4. Recommendations

Based on our test results we would recommend that future testing be done to take into consideration cyclic and dynamic loading. Because the SR foot underwent plastic deformation before reaching 910N in our heel-strike test, we believe that repeated cyclic loading at even lower loads could produce similar plastic deformation. Cyclic testing should be performed as outlined in ISO standards 22675. In addition, the dynamic loading, either by machine or with human subjects, will provide information regarding the strain on the monolimb during a complete gait cycle. The results of these future tests could lead to a better understanding of the longevity of the SR foot.

Regarding the SR foot, we would recommend considering altering the foot geometry to minimize the effect of the metal insert. The plastic deformation occurred directly at the back edge of the metal insert. This back edge of the insert is also coincident with the vertex of the angled cut-out on the heel of the SR foot. It is possible that selecting a different geometry for the cut-out could help to better distribute the load and prevent plastic deformation.

7. Conclusion

The Center for International Rehabilitation has created a low-cost monolimb that is to be attached to a low cost prosthetic foot. In this study, the traditionally used SACH foot was compared to the newer SR prosthetic foot. The feet were tested under static loading conditions in order to compare the behavior of the monolimb when coupled with each of the feet.

The physical testing results of the prosthetic assemblies were compared to the FEA models. The strains on the monolimb and total compression of the prosthetic assemblies were used as methods to compare the accuracy of the FEA for each assembly. The SR heel-strike FEA model showed strains which closely correlated with the strains seen during physical testing when data were extrapolated to the same loading levels. Midstance and toe-off generally had similar magnitudes of strain. For the SACH foot, the strain values for the FEA heel-strike were nearly zero compared to the values seen in the physical testing. The FEA strains for toe-off were of similar magnitudes to the strains exhibited in the extrapolated data from the physical testing. Since there were large differences between the FEA and physical testing data, the FEA model was considered to not accurately reflect the behavior of the assembly.

The compression of the prosthetic assembly from the physical testing shows that the SACH foot assembly compresses more in all orientations presented, thus making it less stiff than the SR assembly.

The physical testing also showed that the SR foot shows strains of greater magnitude than the SACH on the critical region above the metal insert. However, the resulting principal and von Mises stresses do not exceed the tensile yield strength of the polypropylene copolymer of the monolimb with either assembly. This leads to the conclusion that based on the testing conducted, both feet are acceptable during static loading conditions even though the higher strains are seen on the SR monolimb combination. More testing should be performed to verify these results, specifically through cyclic and dynamic testing.

This study compared the interaction of the traditionally used SACH foot and the new, low-cost Shape and Roll prosthetic foot with the Center for International Rehabilitation's monolimb. Through the static physical testing and FEA it was seen that the stiffer Shape and Roll assembly produced higher strains on the monolimb, but did not exceed the yield strength of the monolimb. This information will aid in the future development and refinement of low cost prosthetics for low income countries.

Works Cited

ANSYS. "Chapter 2. General Element Features" ANSYS Release 9.0 Documentation ANSYS, Inc. 2004.

Arbogast, Robert and Joseph Arbogast. "The Carbon Copy II – From Concept to Application." Journal of Prosthetics & Orthotics 1.1 (1989): 32-36

"BlueHill Power Features." Instron. 2006. http://www.instron.us/wa/products/software/bluehill/features/power.aspx#testing Accessed: 2/14/08.

The Center for International Rehabilitation. 'IDEAnet.' http://www.cirnetwork.org/content.cfm?id=5B&newCommunity&CFID=1714313&CFTOKEN=34116128. Accessed: 9/6/07.

'Clinical UM Guideline.' http://medpolicy.bluecrossca.com/policies/guidelines/DME/lower_limb_prosthesis.html. Accessed: 9/10/07.

"Deformation." Wikipedia, The Free Encyclopedia. 29 Sep 2007, 23:32 UTC. Wikimedia Foundation, Inc. 4 Oct 2007 <http://en.wikipedia.org/w/index.php?title=Deformation&oldid=161209779>. Accessed: 1/23/08

Engineer's Edge. http://www.engineersedge.com/strength_of_materials.htm. 2008. Accessed: 4/22/08

"Fatigue Test" Instron. http://www.instron.us/wa/applications/test_types/fatigue/default.aspx Accessed: 9/6/07.

"Strain gauge." Wikipedia, The Free Encyclopedia. 3 Oct 2007, 05:13 UTC. Wikimedia Foundation, Inc. 4 Oct 2007 <http://en.wikipedia.org/w/index.php?title=Strain_gauge&oldid=161955202>. Accessed: 2/13/08

Gailey, Robert. "Functional Value of Prosthetic Foot/Ankle Systems to the Amputee." Journal of Prosthetics and Orthotics 17.4s (2005): 39-41

Geil, Mark. "Energy Loss and Stiffness Properties of Dynamic Elastic Response Prosthetic Feet." Journal of Prosthetics and Orthotics 13.3 (2001): 70-73

Hansen, AH, DS Childress, and EH Knox. "Prosthetic Foot Roll-Over Shapes and Implications for Alignment of Trans-tibial Prosthesis." Prosthetics and Orthotics International 24 (2000): 205-215

Hansen, Andrew. "Scientific Methods to Determine Functional Performance of Prosthetic Ankle Foot Systems". American Academy of Orthotists and Prosthetists. http://www.oandp.org/jpo/library/2005_04S_023.asp. Accessed: 9/20/07.

Jenkyn et. al. Noninvasive muscle tension measurement using the novel technique of magnetic resonance elastography (MRE). Journal of Biomechanics. 36.12 (2003):1917-1921

"Index Award" Index. http://www.indexaward.dk/2007/default.asp?id=706&show=nomination&nominationid=163. Accessed: 9/29/07.

Kim, Donghak. "Finite Element Analysis of Monolimb." Worcester Polytechnic Institute. 2006

Kirtley, Chris. "Inverse Dynamics." Clinical Gait Analysis. 29 Nov 2007 <http://guardian.curtin.edu.au/cga/teach-in/inverse-dynamics.html>. Accessed: 12/1/07.

Krajowy Punkt Kontaktowy. http://www.kpk.gov.pl/centra_doskonalosci/coe/midi/data/603.html

"Landmines: A Deadly Inheritance." http://www.unicef.org/graca/mines.htm. 2005. Accessed: 9/21/07.

'Lower Limb Prosthetics.' http://www.emedicine.com/pmr/topic175.htm. Accessed: 9/10/07.

"Lower Limb Prosthetics: The Shape&Roll Prosthetic Foot for Use in Low-Income Countries" Prosthetics Research Laboratory and Rehabilitation Engineering Research Program. http://www.medschool.northwestern.edu/depts/repoc/sections/research/projects/ambulate/srfoot_lowincome.html. Accessed: 10/1/07.

Lee, Winson CC and Ming Zhang." Design of monolimb using finite element modeling and statistics-based Taguchi method." Clinical Biomechanics 20. (2005):759-766

Mara, GE, AR Harland, and SR Mitchell. "Virtual Modeling of a Prosthetic Foot to Improve Footwear Testing." Proceedings of the Institution of Mechanical Engineers, Part J: Journal of Materials: Design and Applications. 220 (2006): 207-213

"Mechanics Laboratory." Northwestern University. http://www.medschool.northwestern.edu/depts/repoc/sections/facilities/fac_mechanics.html. Accessed: 10/3/07.

"Mechanics Property Analysis." Shanghai Institute of Ceramics Chinese Academy of Sciences. http://www.sic.ac.cn/List/science/analysis/ceshi_xm/ceshi_11/49_1.htm. Accessed: 11/14/07

Metzger, Sherry. 'Rotary: Changing Lives in Developing Countries.' April 2007. http://www.oandp.com/edge/issues/articles/2007-08_01.asp. Accessed: 9/22/07.

Miff SC, et al."Roll-Over Shapes of the Able-Bodied Knee–Ankle–Foot System During Gait Initiation, Steady-State Walking, and Gait Termination." Gait Posture (2007) doi:10.1016/j.gaitpost.2007.04.011

Omega.http://www.omega.com/search/esearch.asp?start=0&perPage=10&summary=yes&sort=rank&search=STRAIN+GAUGE&submit=Search. Accessed: 1/20/08.

Perry, Jacquelin. Gait Analysis: Normal and Pathological Function New York: McGraw-Hill, 1992.

"Prosthetic Feet." University of Vienna. http://www.univie.ac.at/cga/courses/be524/feet/ Accessed 12/11/07.

Reisinger, Kim D. "Re: CIR responses to your questions." Email to the author. 15 Sept 2007.

"Rosette Strain Gauge." Efunda: Engineering Fundamentals. 2008. http://www.efunda.com/formulae/solid_mechanics/mat_mechanics/strain_gauge_rosette.cfm Accessed: 2/25/08.

"SACH w/ Molded Pyramid" Ohio Willow Wood. 2007. http://www.owwco.com/CategoryDetail.aspx?Key=63 Accessed: 10/1/07.

Sam, Michel, et al. "The 'Shape&Roll'Prosthetic Foot: I. Design and Development of Appropriate Technology for Low-Income Countries." Medicine, Conflict and Survival 24.4 (2004): 294-306

Saunders, Marnie M., et al. Finite Element Analysis as a Tool for Parametric Prosthetic Foot Design and Evaluation. Technique Development in the Solid Ankle Cushioned Heel (SACH) Foot. Computer Methods in Biomechanics and Biomedical Engineering. 6:1 (2003) 75-87

Serlin, David. "The Clean Room/Making the Jaipur Foot." Cabinet Magazine. Issue 4, Fall 2001. . http://www.cabinetmagazine.org/issues/4/jaipurfoot.php. Accessed: 10/9/07.

Stanton, Mary. "CIR Brings Prosthetic Services to Developing Nations." April 2006. http://www.oandp.com/resources/humanitarian/organization.asp?frmId=5BF96CEF-F32A-47B0-9248-C7BA8B1A292E. Accessed 9/14/07.

Stark, Gerald. "Perspectives on How and Why Feet are Prescribed." Journal of Prosthetics and Orthotics 17:4s (2005) 18-22

"Strain Gauge Rosettes: Selection, Application, and Data Reduction" Measurements Group: 2000. http://www.davidson.com.au/products/strain/mg/technology/technotes/tn515.pdf. Accessed: Feb. 13, 2008.

"Student manual for Strain gauge Technology." Vishay Measurements Group, Inc. pp. 17-23. 1992

Supan, Terry. "Clinical Perspectives on Prosthetic Ankle-Foot Designs." Journal of Prosthetics and Orthotics 17:4s (2005) 33-34

"Theory of Operation." National Instruments. SCXI-1520 User Manual.

Wheeler, Anthony J. Introduction to Engineering Experimentation. Second Edition. Pearson Prentice Hall. 2003.

Winter, David A.. The Biomechanics and Motor Control of Human Gait: Normal, Elderly, and Pathological. 2nd Edition. Waterloo, Ontario: University of Waterloo Press, 1991.

Appendix A

Measured Points For SR Base (in)

X	Y		X	Y
0	0		4	0.90625
0.0625	0.1875		4.5	0.783
0.125	0.1875		5	0.625
0.25	0.15625		5.5	0.557
0.375	0.15625		6	0.53125
0.5	0.15625		6.5	0.614
0.625	0.1875		7	0.71875
0.75	0.21875		7.5	0.78125
0.875	0.25		8	0.75
1	0.3125		8.5	0.437
1.0625	0.4375		8.6875	0
1.0625	0.75		8.5	-0.55
1	0.84375		8	-0.84375
0.875	0.90625		7.5	-1.017
0.5	0.9375		7	-1.09375
0.125	1		6.5	-1.155
0	1.03125		6	-1.1875
-0.09375	1.09375		5.5	-1.25
-0.15625	1.25		5	-1.3125
0.125	1.625		4.5	-1.339
0.25	1.625		4	-1.47063
0.5	1.625		3.5	-1.46875
1	1.625		3	-1.5
1.5	1.625		2.5	-1.588
2	1.5625		2	-1.5
2.5	1.46875		1.5	-1.227
3	1.34375		1	-0.96875
3.5	1.09375		0.5	-0.681

Appendix B

Bill of Materials and Exploded View of Test Set-ups

Bill of Materials		
Find Number	**Description**	**QTY**
1	Angle Block (15° and 20°)	2
2	M6 Threaded Rod	2
3	M6 Washer	4
4	M6 Nut	4
5	Metal Plate	2
6	Nail	6
7	M10 Bolt	1
8	M10 Washer	1
9	Prosthetic Foot Assembly	2
10	Monolimb	1
11	Adaptor	1
12	Set Screw	6

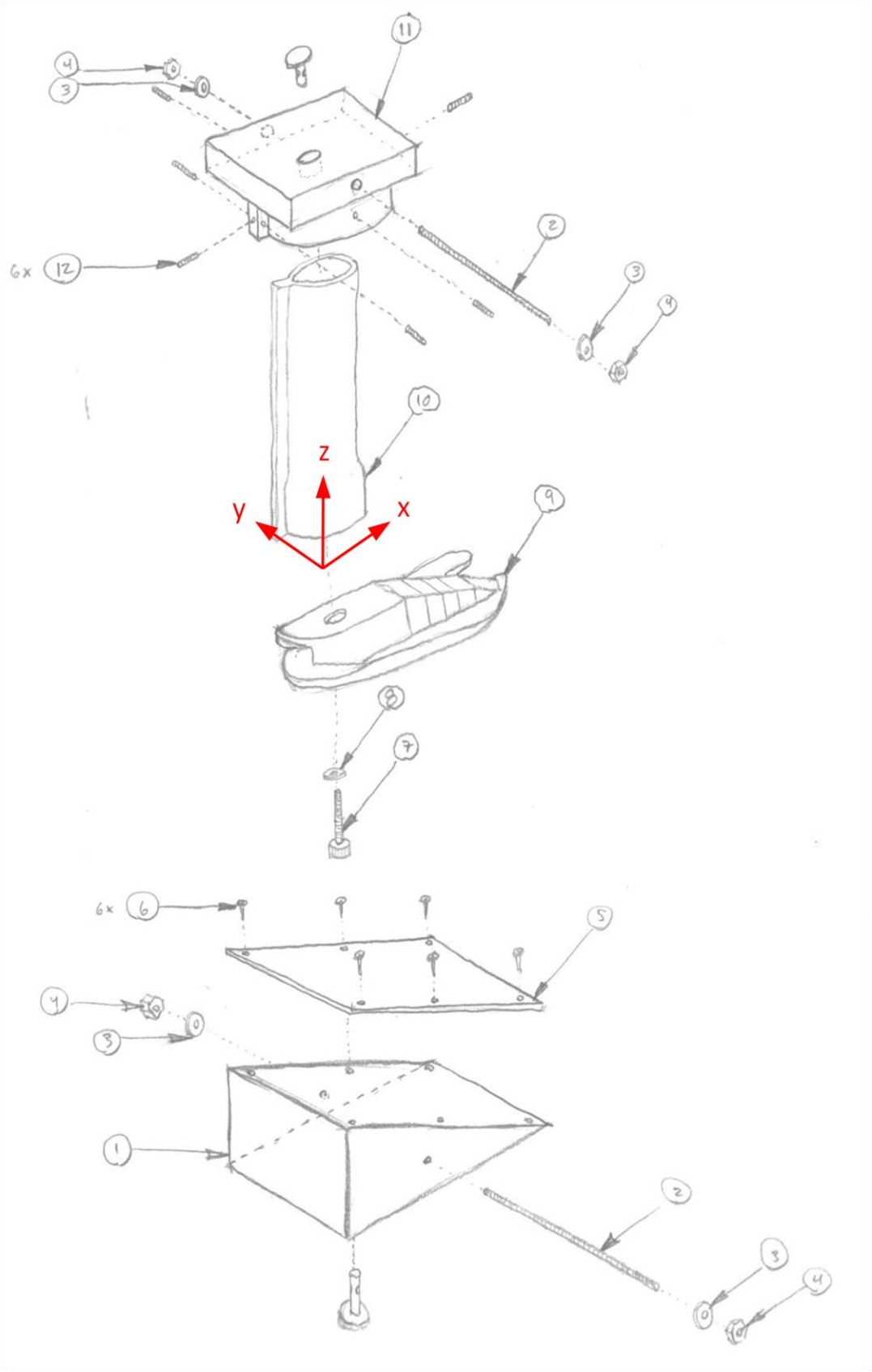
11
4
3
2
6x 12
3
4
10
z
y
x
9
8
7
6x 6
5
4
3
1
2
3
4

Appendix C

Calculations for the Approximate Deformation of Simple Midstance SR Assembly

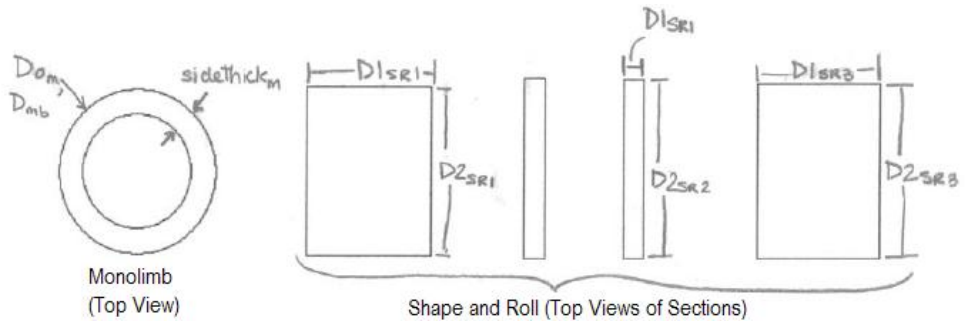

Force := 1300N

$E := 1500 \cdot 10^{6} Pa$

$Do_m := 0.05m$

$D_{mb} := 0.05m$

$sidethick_m := 0.005m$

$$Ac_m := \left(\frac{Do_m}{2}\right)^2 \cdot \pi - \left(\frac{Do_m}{2} - sidethick_m\right)^2 \cdot \pi$$

$Ac_m = 7.069 \times 10^{-4} m^2$

$$Ac_{mb} := \left(\frac{D_{mb}}{2}\right)^2 \cdot \pi$$

$Ac_{mb} = 1.963 \times 10^{-3} m^2$

$D1_{sr1} := 1.375in = 0.035\,m$

$D1_{sr2} := .0076m$

$D1_{sr3} := 1.25in = 0.032\,m$

$D2_{sr1} := 2.2in = 0.056\,m$

$D2_{sr2} := 2.2in = 0.056\,m$

$D2_{sr3} := 2.2in = 0.056\,m$

$Ac_{sr1} := D1_{sr1} \cdot D2_{sr1}$

$Ac_{sr1} = 1.952 \times 10^{-3} m^2$

$Ac_{sr2} := 2D1_{sr2} \cdot D2_{sr2}$

$Ac_{sr2} = 8.494 \times 10^{-4} m^2$

$Ac_{sr3} := D1_{sr3} \cdot D2_{sr3}$

$Ac_{sr3} = 1.774 \times 10^{-3} m^2$

$$Ac := \begin{pmatrix} Ac_m \\ Ac_{mb} \\ Ac_{sr1} \\ Ac_{sr2} \\ Ac_{sr3} \end{pmatrix}$$

$$\sigma := \frac{Force}{Ac} \qquad \sigma = \begin{pmatrix} 1.839 \times 10^{6} \\ 6.621 \times 10^{5} \\ 6.661 \times 10^{5} \\ 1.531 \times 10^{6} \\ 7.327 \times 10^{5} \end{pmatrix} Pa$$

$$\varepsilon := \frac{\sigma}{E} \qquad \varepsilon = \begin{pmatrix} 1.226 \times 10^{-3} \\ 4.414 \times 10^{-4} \\ 4.441 \times 10^{-4} \\ 1.02 \times 10^{-3} \\ 4.885 \times 10^{-4} \end{pmatrix}$$

$L_m := 0.224m$

$L_{mb} := 0.005m$

$L_{sr1} := 0.00635m$

$L_{sr2} := 0.0241m$

$L_{sr3} := 0.013m$

$\delta_m := \varepsilon_0 \cdot L_m \qquad \delta_m = 2.746 \times 10^{-4} m$

$\delta_{mb} := \varepsilon_1 \cdot L_{mb} \qquad \delta_{mb} = 2.207 \times 10^{-6} m$

$\delta_{sr1} := \varepsilon_2 \cdot L_{sr1} \qquad \delta_{sr1} = 2.82 \times 10^{-6} m$

$\delta_{sr2} := \varepsilon_3 \cdot L_{sr2} \qquad \delta_{sr2} = 2.459 \times 10^{-5} m$

$\delta_{sr3} := \varepsilon_4 \cdot L_{sr3} \qquad \delta_{sr3} = 6.35 \times 10^{-6} m$

$\delta_{monolimb} := \delta_m + \delta_{mb}$

$\delta_{monolimb} = 2.768 \times 10^{-4}\,m$

$\delta_{ShapeRoll} := \delta_{sr1} + \delta_{sr2} + \delta_{sr3}$

$\delta_{ShapeRoll} = 3.376 \times 10^{-5}\,m$

$\delta_{TOTAL} := \delta_{monolimb} + \delta_{ShapeRoll}$

$\delta_{TOTAL} = 3.106 \times 10^{-4}\,m$

$\delta_{TOTAL} = 0.311 \cdot mm$

$\delta_{monolimb} = 0.277 \cdot mm$

$\delta_{ShapeRoll} = 0.034 \cdot mm$

$error := \frac{(0.288mm - \delta_{TOTAL})}{0.288mm} \cdot 100$

$error = -7.851$

Appendix D

Raw Data From Coefficient of Friction Test

Foot	Orientation	Measured Angle
ICRC SACH Foot	Toe Down	25
		27
		25
		26
		27
	Avg:	26
	μ	0.4877
	Heel Down	22
		21
		21
		22
		20
	Avg:	21.2
	μ	0.3878

Foot	Orientation	Measured Angle
SR	Toe Down	18
		16
		16
		19
		19
	Avg:	17.6
	μ	0.3172
	Heel Down	17
		15
		16
		15
		15
	Avg:	15.6
	μ	0.2792

Foot	Orientation	Measured Angle
SR Cover	Toe Down	41
		40
		39
		38
		40
	Avg:	39.6
	μ	0.8273
	Heel Down	40
		41
		41
		39
		40
	Avg:	40.2
	μ	0.8451

Appendix E

Testing Procedure	Micro 2-20 psi	Ultra Low 28-85 psi	Super Low 70-350 psi	Low 350-1400 psi

SR Foot no Cover

Test Run 1: Heel-strike

Test Number	Percent Total Loading	Force Applied	Pressure Paper	Expected Load Area (cm^2)	Max Pressure (psi)	Pressure Paper Gradient
1	10%	130	*	0.5	179.26	Super Low Pressure
2	20%	260		0.5	358.53	Super Low Pressure
3	30%	390		1	268.90	Super Low Pressure
4	40%	520		1	358.53	Super Low Pressure
5	50%	650	*	2	224.08	Super Low Pressure
6	60%	780		2	268.90	Super Low Pressure
7	70%	910		2	313.71	Super Low Pressure
8	80%	1040		4	179.26	Super Low Pressure
9	90%	1170		4	201.67	Super Low Pressure
10	100%	1300	*	4	224.08	Super Low Pressure

SR Foot no Cover

Test Run 2: Mid-Stance

Test Number	Percent Total Loading	Force Applied	Pressure Paper	Expected Load Area (cm^2)	Max Pressure (psi)	Pressure Paper Gradient
1	10%	130	*	100	0.90	
2	20%	260		100	1.79	
3	30%	390		100	2.69	~~Micro Pressure~~
4	40%	520		100	3.59	~~Micro Pressure~~
5	50%	650	*	100	4.48	~~Micro Pressure~~
6	60%	780		100	5.38	~~Micro Pressure~~
7	70%	910		100	6.27	~~Micro Pressure~~
8	80%	1040		100	7.17	~~Micro Pressure~~
9	90%	1170		100	8.07	~~Micro Pressure~~
10	100%	1300	*	100	8.96	~~Micro Pressure~~

SR Foot no Cover

Test Run 3: Toe-off

Test Number	Percent Total Loading	Force Applied	Pressure Paper	Expected Load Area (cm^2)	Max Pressure	Pressure Paper Gradient
1	10%	130	*	0.25	358.53	Low Pressure
2	20%	260		0.25	717.06	Low Pressure
3	30%	390		0.5	537.79	Low Pressure
4	40%	520		1	358.53	Low Pressure
5	50%	650	*	2	224.08	Super Low Pressure
6	60%	780		2	268.90	Super Low Pressure
7	70%	910		3	209.14	Super Low Pressure
8	80%	1040		4	179.26	Super Low Pressure
9	90%	1170		4	201.67	Super Low Pressure
10	100%	1300	*	4	224.08	Super Low Pressure

SR Foot with Cover

Test Run 4: Toe-off

Test Number	Percent Total Loading	Force Applied	Pressure Paper	Expected Load Area (cm^2)	Max Pressure	Pressure Paper Gradient
1	10%	130	*	6	14.94	~~Micro Pressure~~
2	20%	260		6	29.88	Ultra Low Pressure
3	30%	390		6.5	41.37	Ultra Low Pressure
4	40%	520		6.5	55.16	Ultra Low Pressure
5	50%	650	*	7	64.02	Ultra Low Pressure
6	60%	780		7	76.83	Ultra Low Pressure
7	70%	910		7	89.63	Super Low Pressure
8	80%	1040		7.5	95.61	Super Low Pressure
9	90%	1170		7.5	107.56	Super Low Pressure
10	100%	1300	*	8	112.04	Super Low Pressure

SR Foot with Cover

Test Run 5: Midstance

Test Number	Percent Total Loading	Force Applied	Pressure Paper	Expected Load Area (cm^2)	Max Pressure	Pressure Paper Gradient
1	10%	130	*	120	0.75	~~Micro Pressure~~
2	20%	260		120	1.49	~~Micro Pressure~~
3	30%	390		120	2.24	~~Micro Pressure~~
4	40%	520		120	2.99	~~Micro Pressure~~
5	50%	650	*	120	3.73	~~Micro Pressure~~
6	60%	780		120	4.48	~~Micro Pressure~~
7	70%	910		120	5.23	~~Micro Pressure~~
8	80%	1040		120	5.98	~~Micro Pressure~~
9	90%	1170		120	6.72	~~Micro Pressure~~
10	100%	1300	*	120	7.47	~~Micro Pressure~~

SR Foot with Cover

Test Run 6: Heel-strike

Test Number	Percent Total Loading	Force Applied	Pressure Paper	Expected Load Area (cm^2)	Max Pressure	Pressure Paper Gradient
1	10%	130	*	4	22.41	Ultra Low
2	20%	260		4	44.82	Ultra Low
3	30%	390		4.5	59.75	Ultra Low
4	40%	520		4.5	79.67	Low Pressure
5	50%	650	*	4.5	99.59	Low Pressure
6	60%	780		4.5	119.51	Low Pressure
7	70%	910		5	125.48	Low Pressure
8	80%	1040		5	143.41	Low Pressure
9	90%	1170		5	161.34	Low Pressure
10	100%	1300	*	5	179.26	Low Pressure

SACH Foot

Test Run 7: Toe-off

Test Number	Percent Total Loading	Force Applied	Pressure Paper	Expected Load Area (cm^2)	Max Pressure	Pressure Paper Gradient
1	10%	130	*	5.5	16.30	~~Micro Pressure~~
2	20%	260		5.5	32.59	Ultra Low Pressure
3	30%	390		6	44.82	Ultra Low Pressure
4	40%	520		6	59.75	Ultra Low Pressure
5	50%	650	*	6.5	68.95	Ultra Low Pressure
6	60%	780		6.5	82.74	Ultra Low Pressure
7	70%	910		6.5	96.53	Super Low Pressure
8	80%	1040		7	102.44	Super Low Pressure
9	90%	1170		7	115.24	Super Low Pressure
10	100%	1300	*	7.5	119.51	Super Low Pressure

SACH Foot

Test Run 8: Midstance

Test Number	Percent Total Loading	Force Applied	Pressure Paper	Expected Load Area (cm^2)	Max Pressure	Pressure Paper Gradient
1	10%	130	*	110	0.81	~~Micro Pressure~~
2	20%	260		110	1.63	~~Micro Pressure~~
3	30%	390		110	2.44	~~Micro Pressure~~
4	40%	520		110	3.26	~~Micro Pressure~~
5	50%	650	*	110	4.07	~~Micro Pressure~~
6	60%	780		115	4.68	~~Micro Pressure~~
7	70%	910		115	5.46	~~Micro Pressure~~
8	80%	1040		115	6.24	~~Micro Pressure~~
9	90%	1170		115	7.01	~~Micro Pressure~~
10	100%	1300	*	115	7.79	~~Micro Pressure~~

SACH Foot

Test Run 9: Heel-strike

Test Number	Percent Total Loading	Force Applied	Pressure Paper	Expected Load Area (cm^2)	Max Pressure	Pressure Paper Gradient
1	10%	130	*	5	17.93	~~Micro Pressure~~
2	20%	260		5	35.85	Ultra Low
3	30%	390		5.5	48.89	Ultra Low
4	40%	520		5	71.71	Ultra Low
5	50%	650	*	6	74.69	Ultra Low
6	60%	780		6	89.63	Low Pressure
7	70%	910		7	89.63	Low Pressure
8	80%	1040		7	102.44	Low Pressure
9	90%	1170		8	100.84	Low Pressure
10	100%	1300	*	8	112.04	Low Pressure

Appendix F

Extension Data

SACH Extension				
Test Stance	Initial Extension (mm)	Final Extension (mm)	Load (N)	Compression (mm)
Midstance	-27.7	-39.54	1170	11.84
Toe-off	33.2	-7.64	910	40.84
Toe-off	0	-42.4	910	42.4
Heel-strike	0	-22.564	1300	22.564
Heel-strike	33	10.36	1300	22.64

SR Extension				
Test Stance	Initial Extension (mm)	Final Extension (mm)	Load (N)	Compression (mm)
Toe-off	0	-34.818	520	34.818
Toe-off	0	-32.9	520	32.9
Heel-strike	0	-11.228	910	11.228
Heel-strike	0	-10.35	911	10.35

Appendix G

FEA Results

SR Foot

Heel-strike

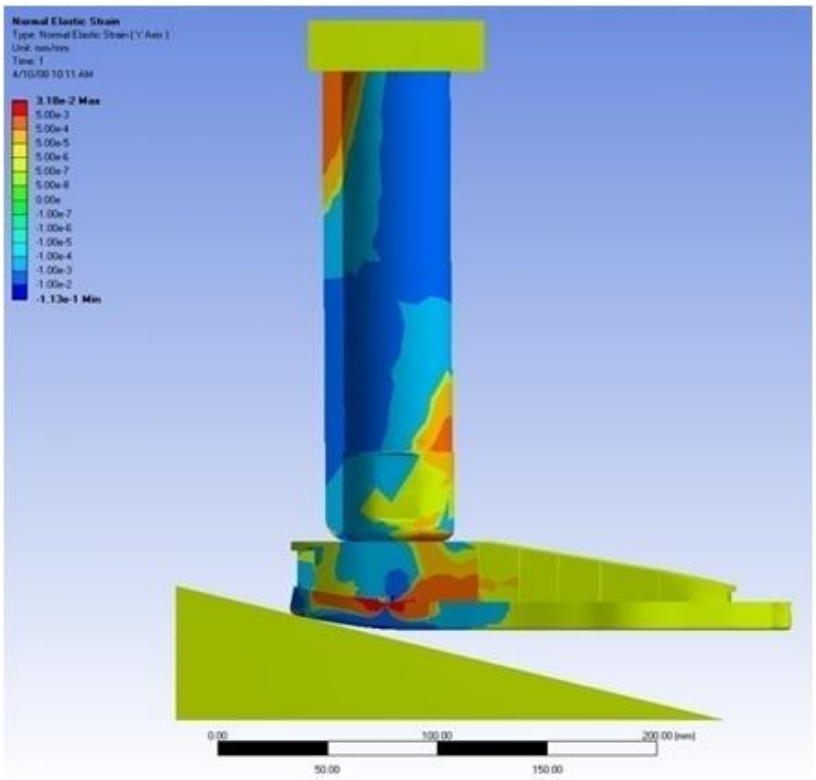

Figure 79: SR - Heel-strike- Normal Strain

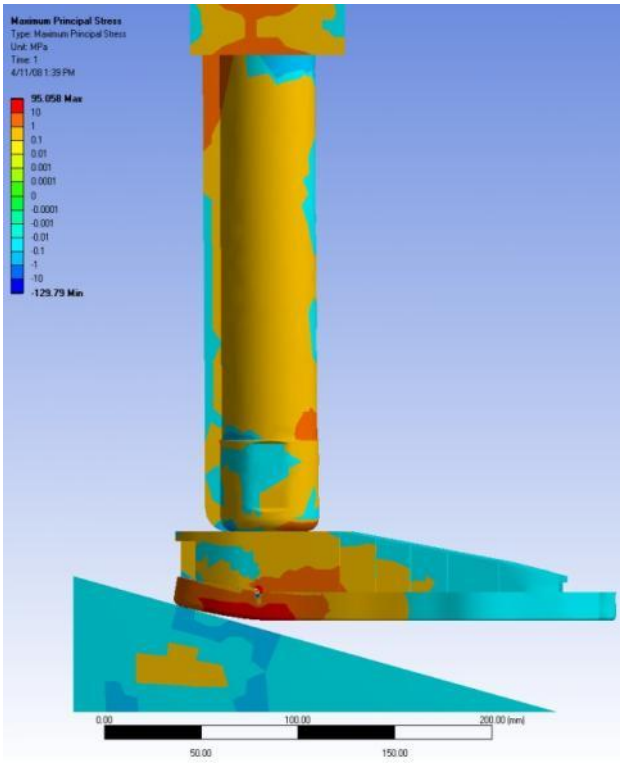

Figure 80: SR - Heel-strike - Maximum Principal Stresses

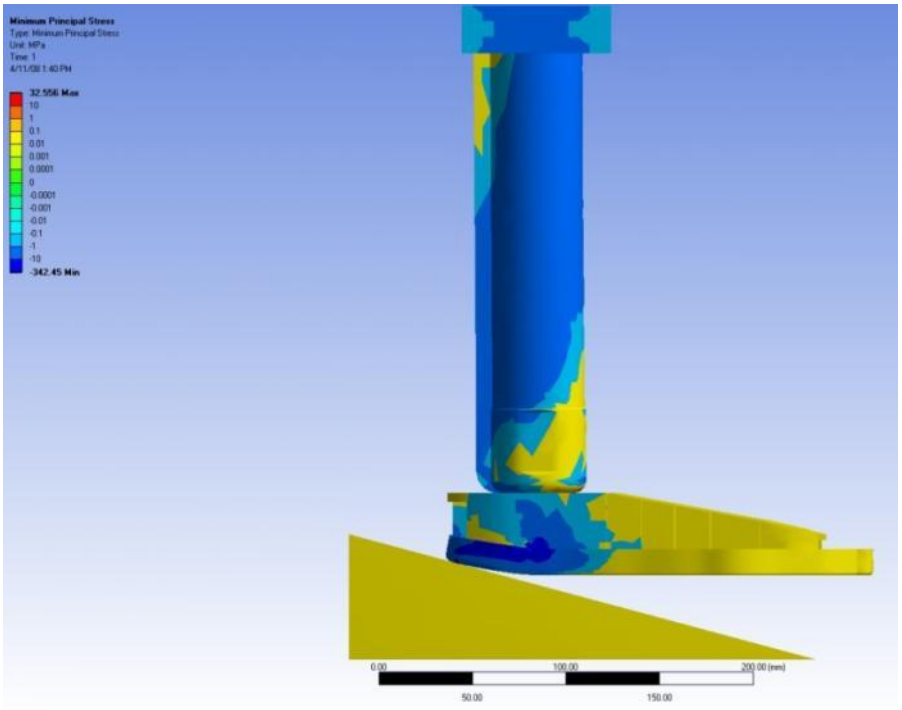

Figure 81: SR - Heel-strike - Minimum Principal Stresses

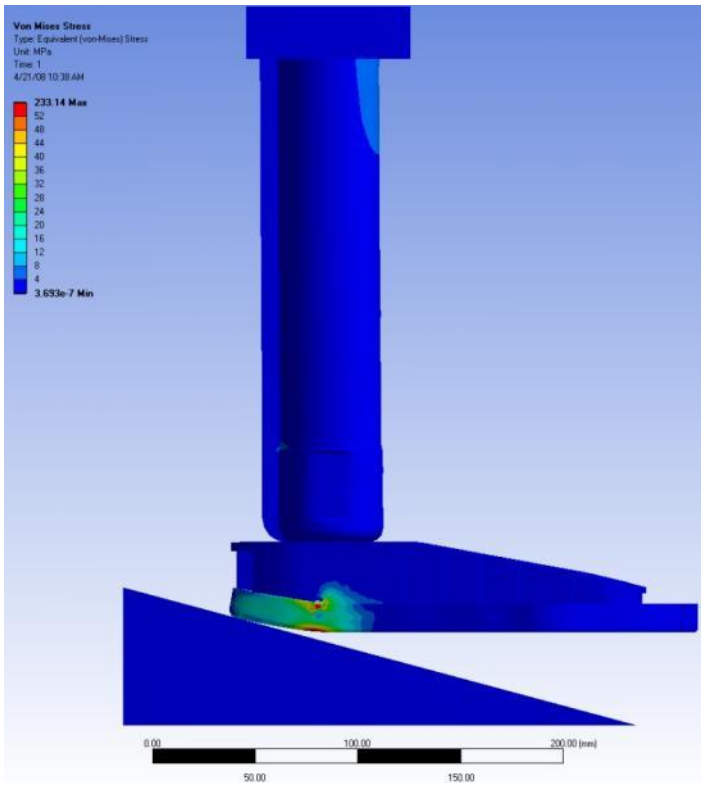

Figure 82: SR – Heel-strike - von Mises Stress

Midstance

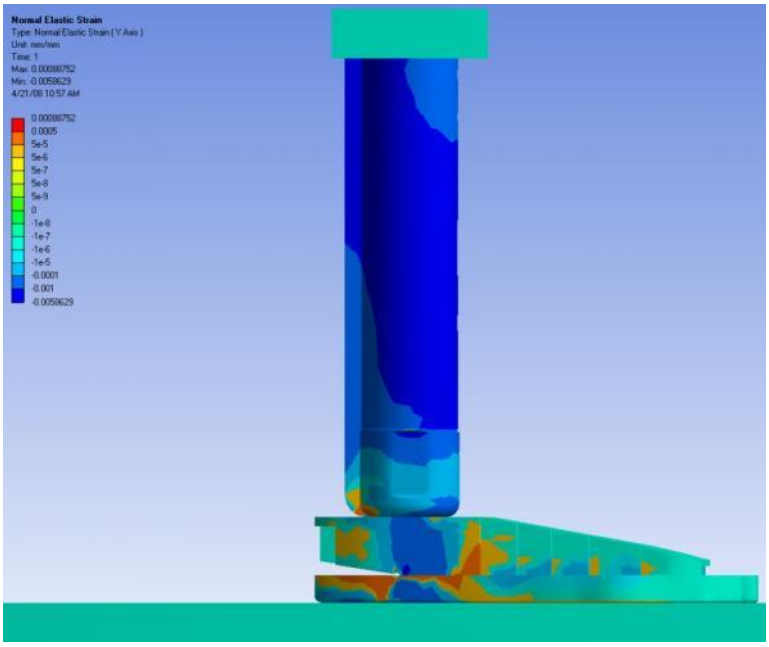

Figure 83: SR - Midstance - Normal Elastic Strain

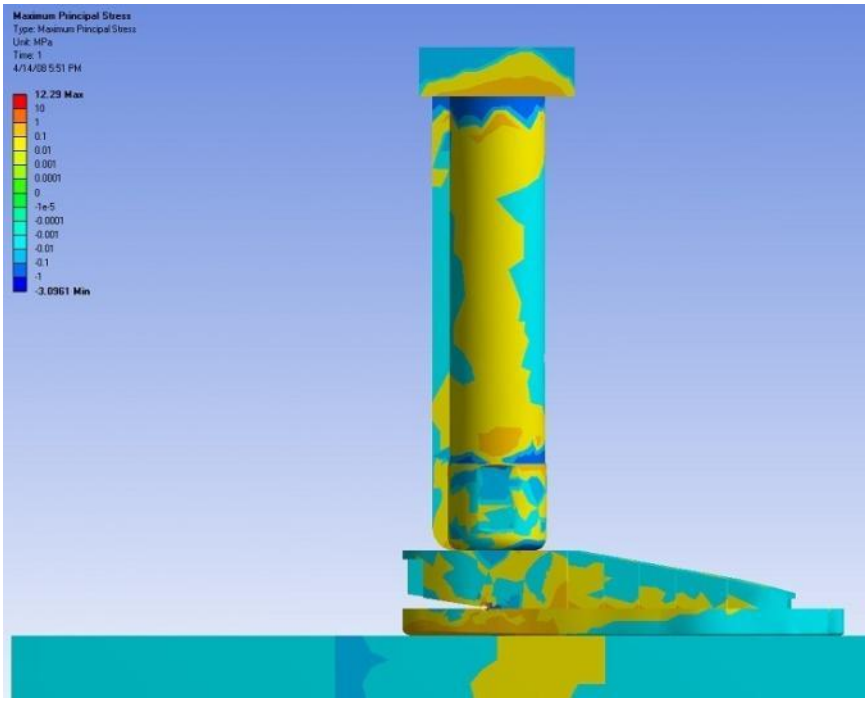

Figure 84: SR - Midstance - Maximum Principal Stress

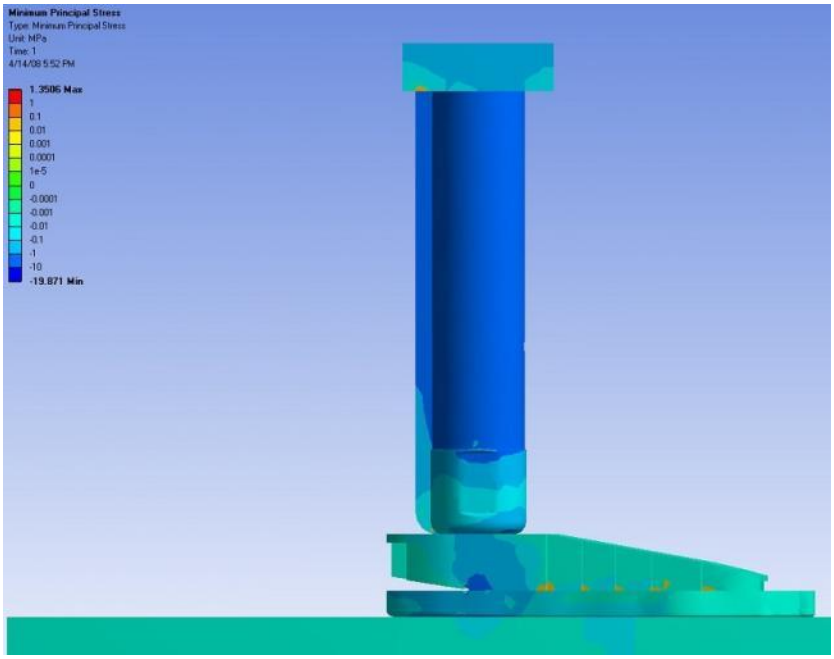

Figure 85: SR - Midstance - Minimum Principal Stress

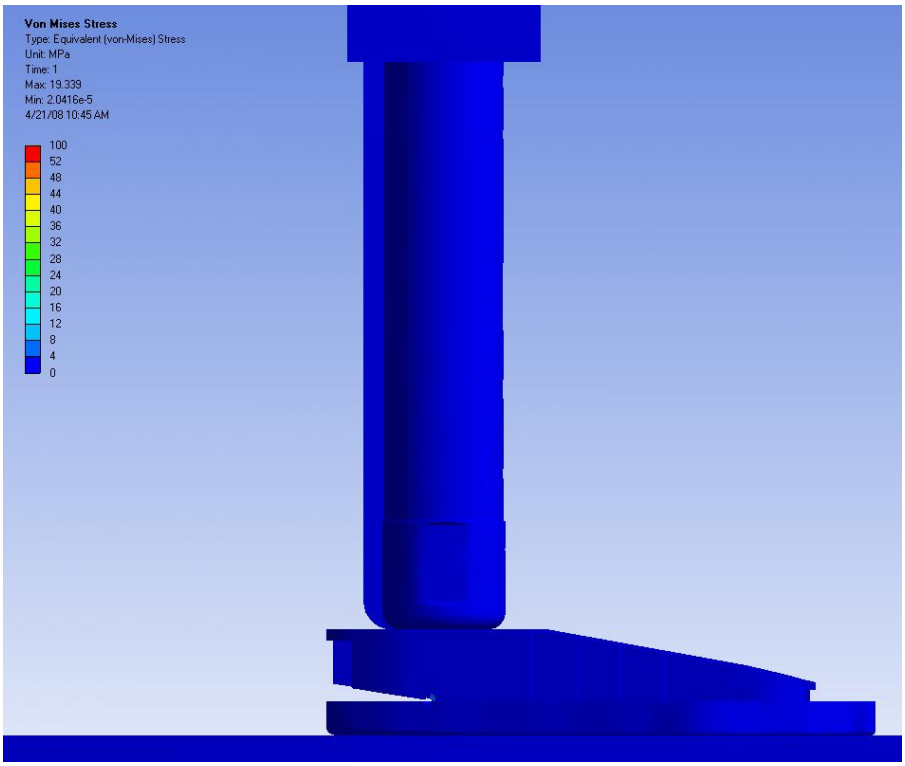

Figure 86: SR - Midstance - von Mises Stress

Toe-off

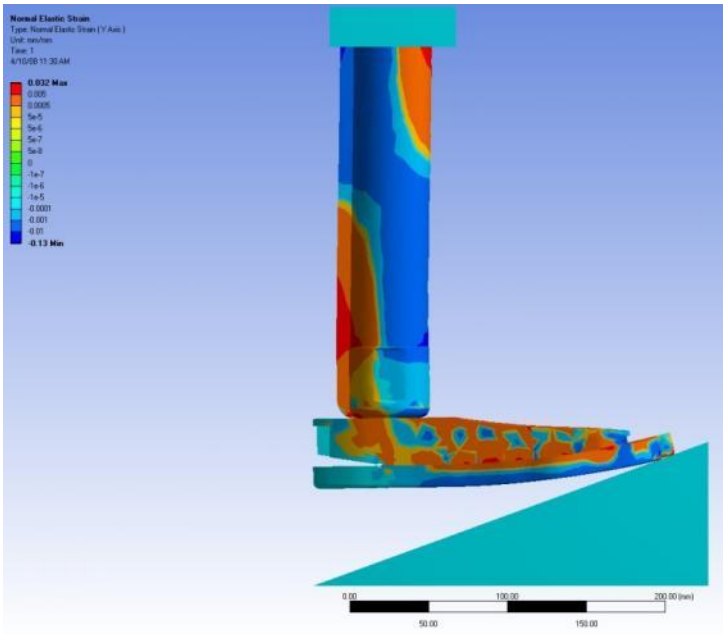

Figure 87: SR - Toe-off - Normal Strain

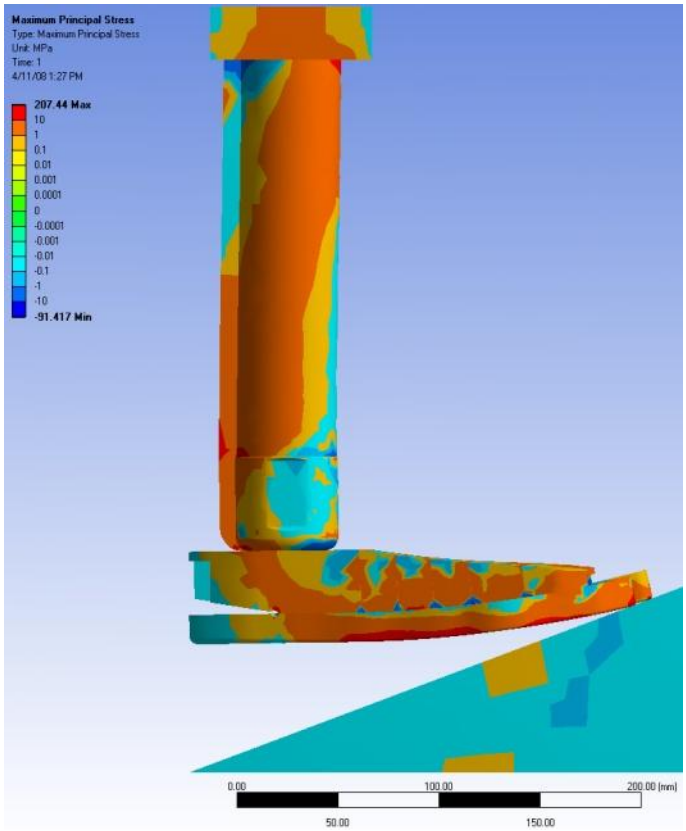

Figure 88: SR - Toe-off - Maximum Principal Stresses

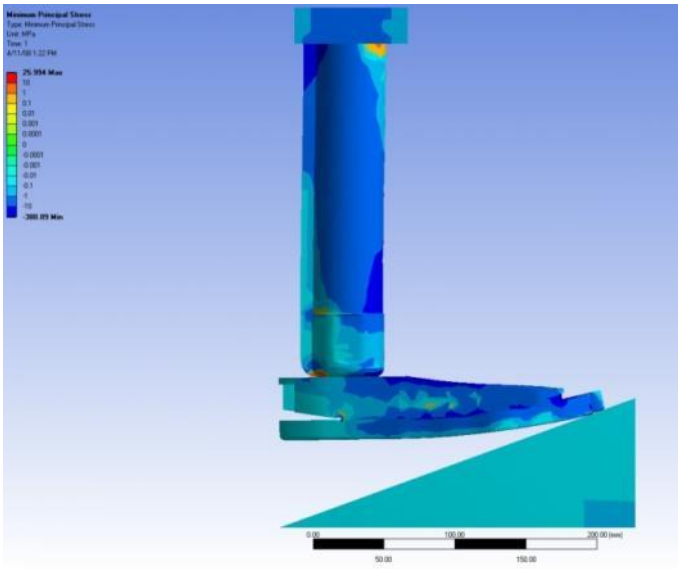

Figure 89: SR - Toe-off - Minimum Principal Stress

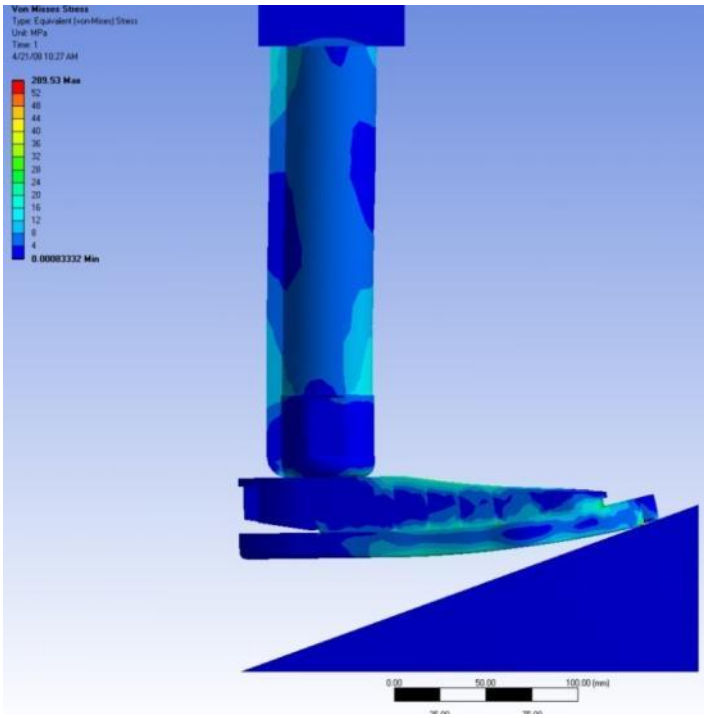

Figure 90: SR – Toe-off – von Mises Stress

ICRC SACH Foot

Heel-strike

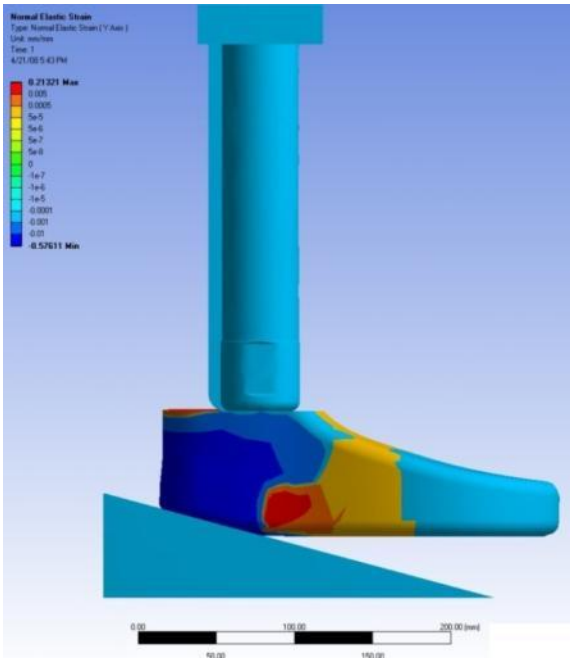

Figure 91: SACH - Heel-strike - Normal Elastic Strain

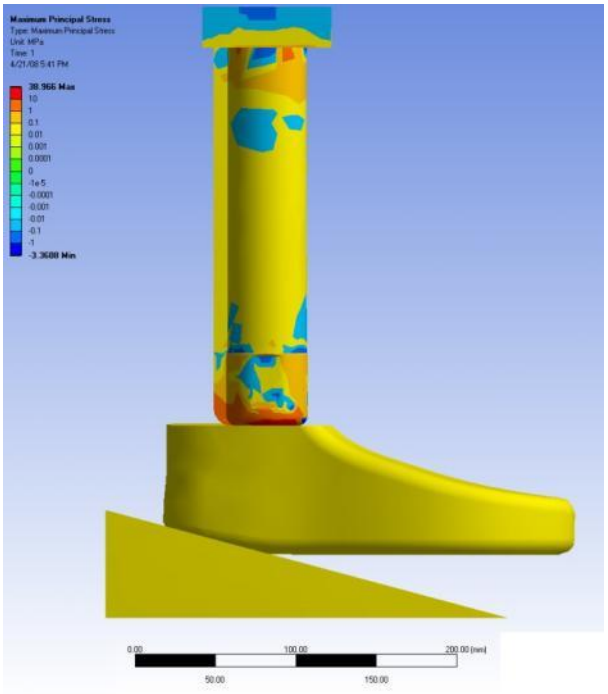

Figure 92: SACH - Heel-strike - Maximum Principal Stress

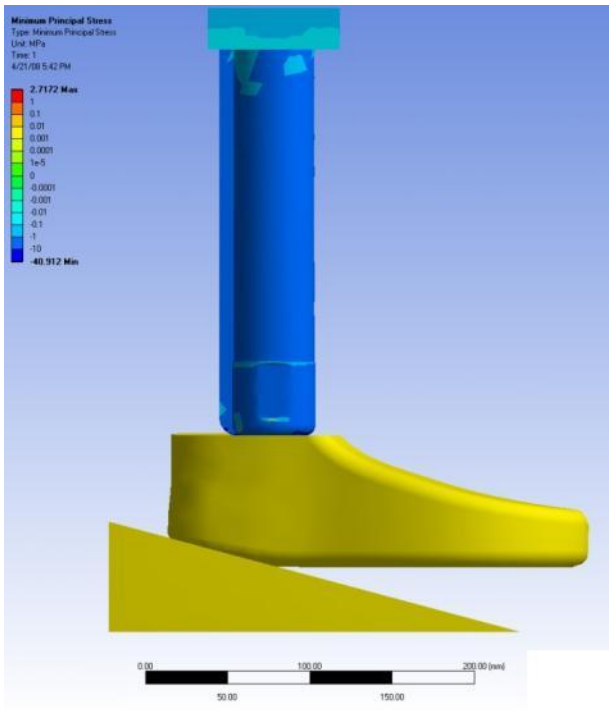

Figure 93: SACH - Heel-strike - Minimum Principal Stress

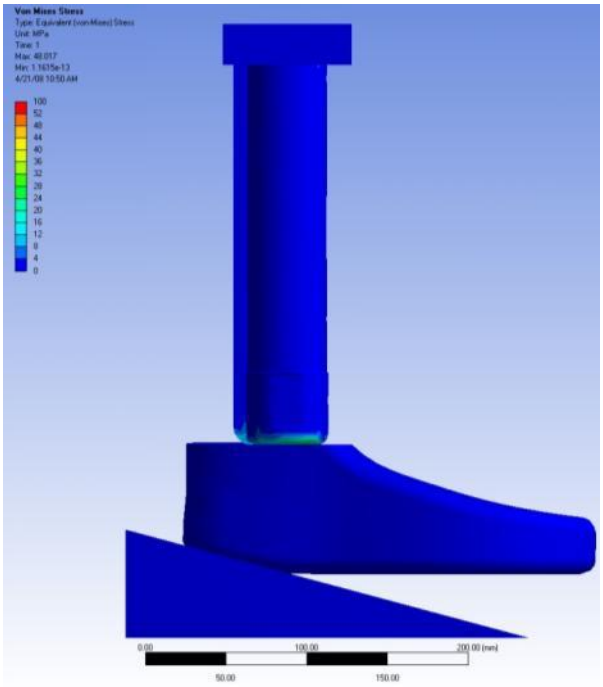

Figure 94: SACH - Heel-strike - von Mises Stress

Toe-off

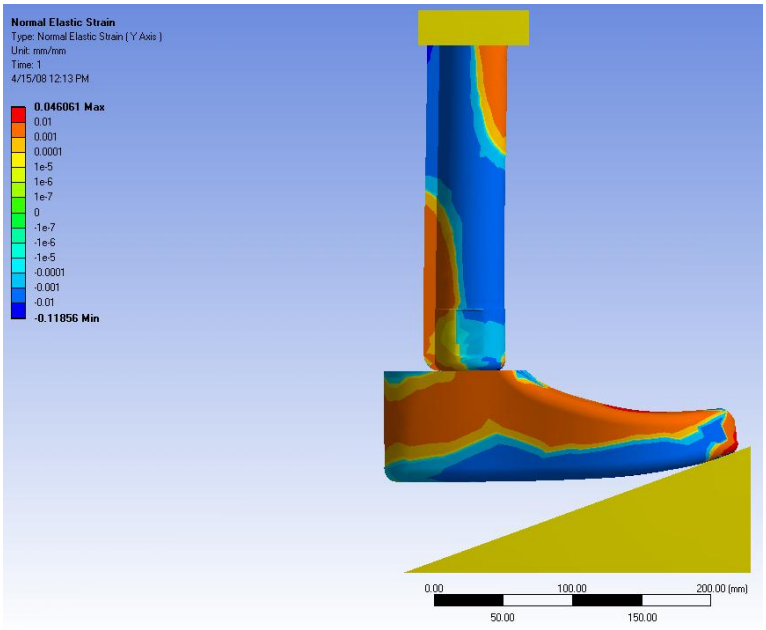

Figure 95: SACH - Toe-off - Normal Elastic Strain

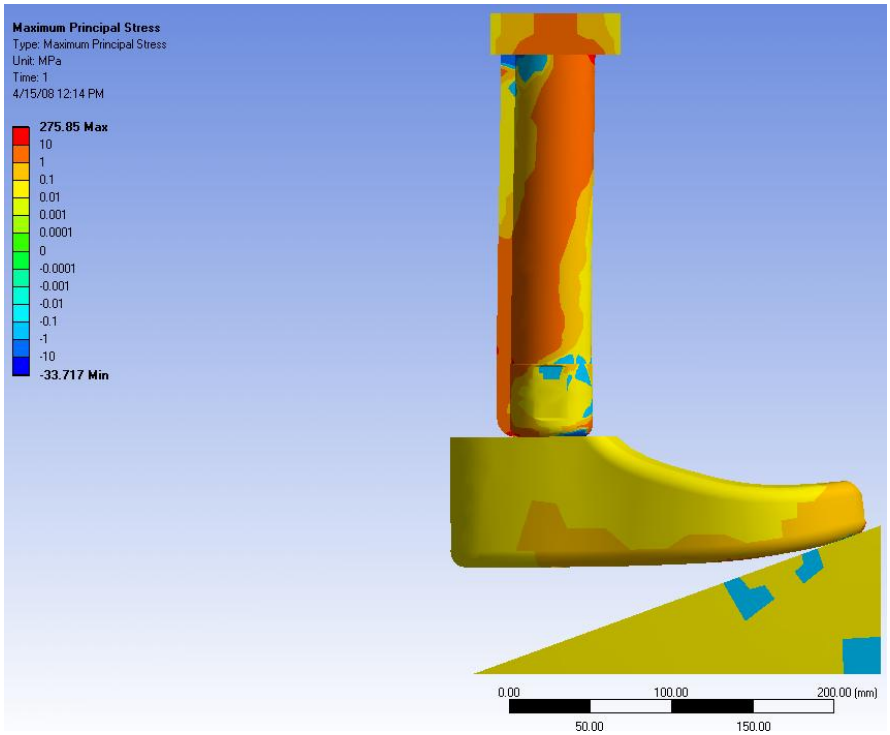

Figure 96: SACH - Toe-off - Maximum Principal Stress

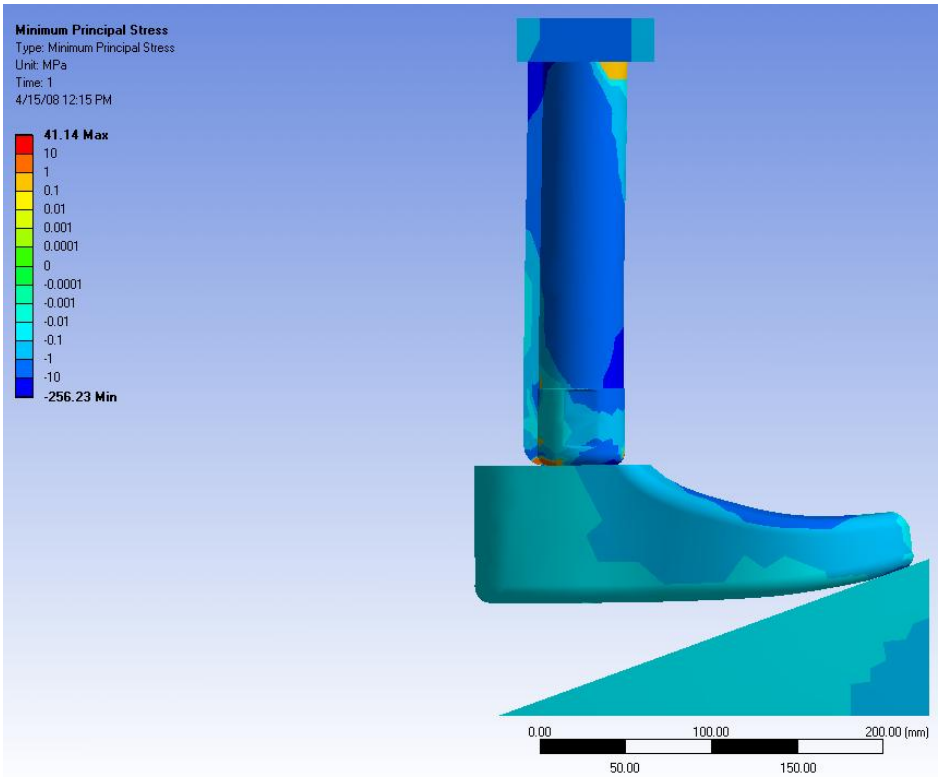

Figure 97: SACH - Toe-off - Minimum Principal Stress

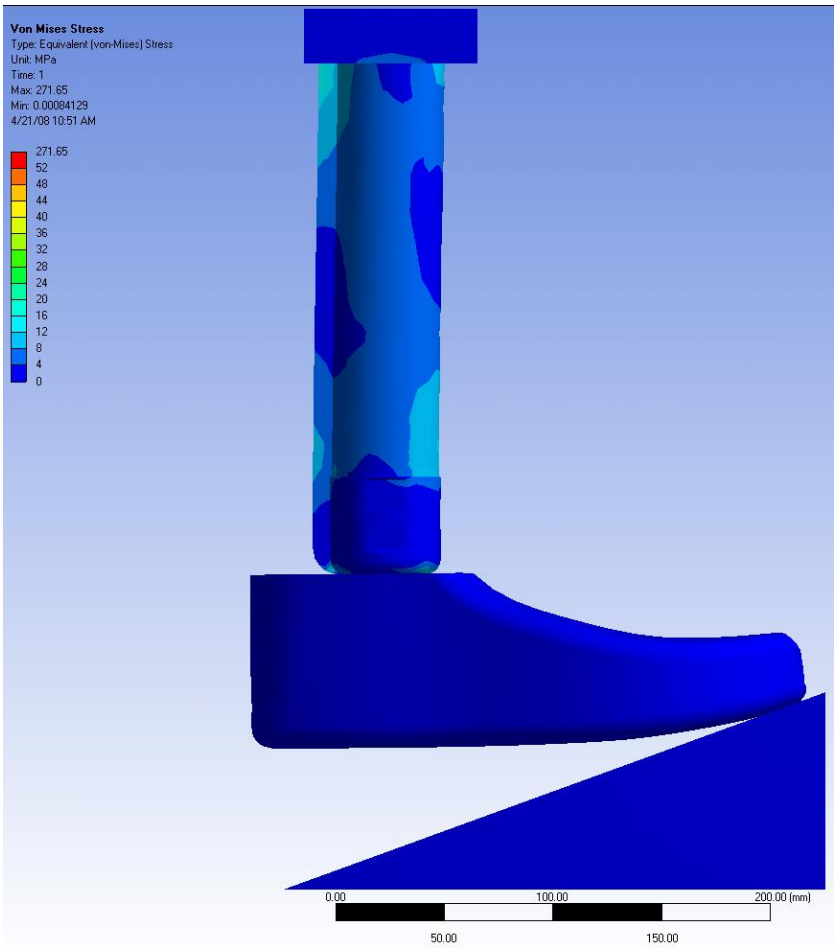

Figure 98: SACH - Toe-off - von Mises Stress